CONTRACT REPORT ARSCD-CR-79008

CONFIRMATION TESTS OF HOT AND COLD ARTILLERY SHELL DRAWING OPERATIONS

C. D. LAHOTI
P. S. RAGHUPATHI
T. L. SUBRAMANIAN
T. ALTAN

MAY 1979

US ARMY ARMAMENT RESEARCH AND DEVELOPMENT COMMAND
FIRE CONTROL AND SMALL CALIBER
WEAPON SYSTEMS LABORATORY
DOVER, NEW JERSEY

The views, opinions, and/or findings contained in this report are those of the author(s) and should not be construed as an official Department of the Army position, policy or decision, unless so designated by other documentation.

Destroy this report when no longer needed. Do not return to the originator.

UNCLASSIFIED

SECURITY CLASSIFICATION OF THIS PAGE (When Data Entered)

(19) REPORT DOCUMENTATION PAGE	READ INSTRUCTIONS BEFORE COMPLETING FORM
1. REPORT NUMBER: ARSCD-CR-79008, AD-E400 355	2. GOVT ACCESSION NO.: AD-E400 355
	3. RECIPIENT'S CATALOG NUMBER: (19) ARSCD, SBIE
4. TITLE (and Subtitle): (6) Confirmation Tests of Hot and Cold Artillery Shell Drawing Operations	5. TYPE OF REPORT & PERIOD COVERED: Final Technical Report May 17, 1978 - May 15, 1979
	6. PERFORMING ORG. REPORT NUMBER
7. AUTHOR(s): (10) C. D. Lahoti, P. S. Raghupathi, T. L. Subramanian, T. Altan	8. CONTRACT OR GRANT NUMBER(s): DAAK10-77-C-2007 (15) new
9. PERFORMING ORGANIZATION NAME AND ADDRESS: Battelle, Columbus Laboratories, 505 King Avenue, Columbus, Ohio 43201	10. PROGRAM ELEMENT, PROJECT, TASK AREA & WORK UNIT NUMBERS: Project #5776716
11. CONTROLLING OFFICE NAME AND ADDRESS: ARRADCOM, TSD, STINFO (DRDAR-TSS) (12) 169, Dover, NJ 07801	(11) 12. REPORT DATE: May 79; 13. NUMBER OF PAGES: 154
14. MONITORING AGENCY NAME & ADDRESS (if different from Controlling Office): ARRADCOM SC & SCWL, M&MT DIV (DRDAR-SCM-P), Dover, NJ 07801	15. SECURITY CLASS. (of this report): Unclassified
	15a. DECLASSIFICATION/DOWNGRADING SCHEDULE

16. DISTRIBUTION STATEMENT (of this Report)

Approved for public distribution; distribution unlimited.

17. DISTRIBUTION STATEMENT (of the abstract entered in Block 20, if different from Report)

(9) Final technical rept 17 May 78-15 May 79,

18. SUPPLEMENTARY NOTES

19. KEY WORDS (Continue on reverse side if necessary and identify by block number)

Hot & cold drawing, Artillery shell, Streamlined dies, Conical dies, Load-displacement curve, Dies in tandem, tapered punch

20. ABSTRACT (Continue on reverse side if necessary and identify by block number)

Mathematical models for optimization of hot and cold artillery shell drawing operations, developed under an earlier project, were expanded to simulate the state-of-the-art technology drawing process that uses multiple dies in tandem with a tapered punch. The computer program DRAWNG was developed based on this analysis.

Confirmation tests validated these mathematical models under production or near-production conditions. Conventional conical as well as computer-designed

→ over

DD FORM 1 JAN 73 1473 EDITION OF 1 NOV 65 IS OBSOLETE

UNCLASSIFIED 407 020

SECURITY CLASSIFICATION OF THIS PAGE (When Data Entered)

Cont

streamlined dies were also tested. A 4.2-inch M335 shell was used for the cold drawing tests, and a 155 mm M107 shell was used for the hot drawing tests.

The computer-designed streamlined dies produced good parts in all tests, and this operation appeared to be smoother than the conventional process. Although streamlined dies were 13% ~~percent~~ more efficient than conical dies during cold drawing, this difference was not measurably significant during hot drawing tests. In all cases, however, the computer program DRAWNG predicted the ram load versus ram displacement curve with acceptable accuracy and reliability.

41

SUMMARY

Mathematical models for optimization of hot and cold artillery shell drawing operations, developed under an earlier project (ref. 1), were expanded to simulate a process that uses multiple dies in tandem with punches having tapered profiles. The computer program DRAWNG, based on this analysis is designed for CDC computers in an interactive mode and uses a Tektronix Cathode Ray Tube (CRT) graphic display terminal as the input/output device. DRAWNG is capable of:

- Simulating the shell drawing process in discrete steps displayed on the CRT terminal
- Generating a ram load versus ram displacement diagram during the simulation, and
- Generating a product wall stress versus ram displacement diagram during the simulation.

DRAWNG reads billet, punch and die (both conical and streamlined) configurations, and then considers material flow stress as a function of strain, strain rate, and temperature. Friction at the tool-material interfaces is defined as a constant fraction (f) of the material flow stress. In addition, DRAWNG considers heat generation and heat transfer during the drawing operation. Thus, this system can be applied to both cold and hot drawing of artillery shells.

To validate these mathematical models, confirmation tests of the cold and hot drawing operations were conducted under production or near-production conditions. Conventional conical dies as well as computer-designed streamlined dies were used.

The cold drawing tests with conical dies were conducted with 4.2-inch M335 shells at Chamberlain Manufacturing Corporation's Waterloo, Iowa division under actual production conditions. The cold drawing tests with streamlined dies were conducted with the same shell in Chamberlain's R&D division under near-production conditions. The hot drawing tests with both conical and streamlined dies were conducted with 155-mm M107 shell at Chamberlain Manufacturing Corporation's Scranton, Pennsylvania division under actual production conditions. During these tests, all the pertinent dimensions of the shell before and after drawing were measured and the presses were instrumented to record ram displacement and ram pressure with respect to time.

In all the tests, the computer-designed streamlined dies produced parts, and the operation appeared smoother than the conventional process. In cold drawing, the streamlined dies were approximately 13 percent more efficient than the conical dies. This difference was not measurably significant during the hot drawing tests. However, in all the cases, the computer programs DRAWNG predicted the ram load-ram displacement curve with acceptable accuracy and reliability. All the important trends and features observed during the tests were reproduced in the predicted curves accurately and consistantly. Further, the computer programs DRAWNG were capable of predicting material failure in all the cases successfully.

FOREWORD

This contract, with Battelle's Columbus Laboratories, Columbus, Ohio, was on the "Confirmation Testings of the Drawing Operations." Technical supervision of this contract was provided by Mr. Fee M. Lee of the Materials Technology Branch, Materials & Manufacturing Technology Division, U.S. Army Armament Research and Development Command, Dover, New Jersey, 07801.

Battelle's Columbus Laboratories conducted this study in its Metalworking Section, under the direction of Mr. T. G. Byrer, Section Manager. Dr. G. D. Lahoti was the principal investigator of the program and the technical work was directed by Dr. T. Altan, Senior Research Leader. Other members of the Battelle staff were: Drs. P. S. Raghupathi, T. L. Subramanian, and N. Akgerman; and Messrs. Willis Sunderland and Frank Syler who participated in the confirmation tests.

Confirmation tests were performed at Chamberlain Manufacturing Corporation's Waterloo, Iowa, and Scranton, Pennsylvania Divisions, under the supervision of Mr. Leverne Sidler, Engineering Manager. Mr. Charles Nielsen, Senior Process Engineer at Chamberlain's R & D Division, and Mr. Jim Kane, Senior Process Engineer at the Scranton Division, were the principal investigators. Conclusions and recommendations from Chamberlain's report on the confirmation tests are contained in Appendix D.

TABLE OF CONTENTS

TABLE OF CONTENTS
(Continued)

FIGURES

FIGURES
(Continued)

FIGURES
(Continued)

FIGURES
(Continued)

FIGURES
(Continued)

FIGURES
(Continued)

TABLES

INTRODUCTION

The mathematical models and the computer programs capable of optimizing the shell drawing process for actual artillery shells and cartridge cases were developed under an earlier project (ref. 1). These mathematical models were based on the analysis of plastic deformations and included the effects of the various process variables (such as punch speed, billet temperature, and lubrication), the properties of shell, die, and punch materials, and the die configuration (both conical and streamlined). These models were computerized so that they can be used to analyze the mechanics of the process and predict potential material failure (such as punch-through), and optimize the die configuration and process variables.

The scope of work under the present contract, which was originally on the billet separation technology, was redirected in May, 1978 to conduct confirmation testing of the drawing operations in order to verify these computerized mathematical models developed earlier. The purpose of this redirection was to enhance the value of the mathematical models by substantiating them with confirmation tests conducted under production or near-production conditions. In addition, the redirected scope of work included expansion of the drawing model to simulate the tandem drawing operation with a tapered punch.

Under the redirected scope of work, the mathematical model of the shell drawing operation was expanded to simulate shell drawing through multiple dies in tandem, with a tapered punch. Graphical display capabilities were also included during computerization of these math models. The confirmation tests of the shell drawing operation at room temperature were conducted with 106.68mm (4.2-inch) M335 shell at Chamberlain Manufacturing Corporation's Waterloo, Iowa division under production and near-production conditions. The confirmation tests at hot forging temperatures were conducted with 155 mm M107 shell at Chamberlain Manufacturing Corporation's Scranton, Pennsylvania division under production conditions. In both cases, tests were conducted using conventional conical and computer-designed streamlined dies. Finally, the evaluation of the mathematical models with the test results was conducted at Battelle.

Although tested for drawing of large caliber shells, these programs can be also applied to the drawing of small caliber shells from either steel

or aluminum. These programs are expected to:

a. reduce the empirical knowledge and long years of experience required in setting up drawing operations, and

b. predict more accurately process conditions and die design for optimum operations.

PURPOSE AND OBJECTIVES

The purpose of this work was to verify the computerized mathematical models of the drawing operations by conducting confirmation tests. Specific objectives were:

a. to expand existing mathematical models of the drawing operation to include tandem drawing with tapered punch in order to determine the optimum combination of process variables, and

b. to substantiate all mathematical modeling work on shell-drawing processes by confirmation tests conducted under production or near-production conditions.

BACKGROUND

Cold Drawing

Smaller caliber shells (up to 105 mm) can be cold drawn while larger shells (155 mm and up) must be hot drawn. Initially the shell is at constant temperature and has uniform flow stress. However, plastic deformation hardens the shell material; therefore, intermediate annealing is often necessary between the initial and the final draw. Prior to cold drawing, the shell body is pickle-cleaned, phosphated and lubricated with soap. Normally, the billet is pushed through either a single conical or through two conical dies in tandem. When there are two dies, the second one is often used to keep the punch straight; therefore, reduction through it is very small. Although reductions in area per draw depend upon shell material and available equipment capacity, reductions of up to 40 percent are fairly common in a single cold drawing operation. Cold drawing produces shells with good surface finish and dimensional accuracy, and product eccentricity is generally better than that of the incoming cup. Since material yield strength increases considerably due to

cold drawing, low-to-medium carbon steels can often meet the strength requirements. But cold drawing produces undesirable residual stresses, in which stress relieving is almost essential.

Cold drawing dies are made from hardened tool steel (R_C 60-62), or other hard-tool materials, such as titanium carbide. Although die wear normally is not a serious problem, punch breakage commonly occurs due to poor lubrication, misalignment and other factors. Cold drawing equipment is typically less massive due to the small workpiece size. A typical cold drawing press for a 105 mm shell is rated at 1.78 MN (200 tons) and has a stroke of 1.02 m (40 inches).

Hot Drawing

In hot drawing, the billet is normally heated in a furnace to temperatures between 1093°C (2000°F) and 1149°C (2100°F) and then cabbaged and pierced. The workpiece temperature is usually between 1038°C (1900°F) and 1093°C (2000°F) prior to actual drawing. Hot drawing is done at one station by two or three dies in tandem. These dies, however, are spaced far enough apart so that the shell is only drawn through one die at a time. This is necessary to avoid punch through, since hot drawn shells usually have a taper on the inside wall and the reduction in area increases with increasing punch movement. Normally, no lubrication is used during hot drawing since scale caused by heating provides adequate separation to avoid metal-to-metal contact. The hot drawing punch is externally cooled by dipping it into a coolant after the operation. Therefore, modern hot drawing presses are often equipped with two shuttle punches, water-cooled internally, to increase the production rate.

The flow stress of the deforming materials under hot drawing conditions is a function of strain rate and temperature. The strain rate is directly proportional to the drawing speed (one modern press is rated at 0.466 m/s (1100 inch/min)). The temperature in the shell wall is influenced by the preheating conditions, heat generation due to plastic deformation, and heat transfer to colder tooling.

Hot drawing dies are usually fabricated from hot-work tool steels, with the contact surface being overlay-welded with super alloys to increase die life. These dies are held in steel die holders. Normally, when working with carbon steels, the die wear is not a serious concern, and die lives of

up to 50,000 shells have been reported. Although tonnage is not necessarily large, the press frame must be big enough to accommodate a large stroke. Therefore, hot drawing equipment is typically massive. For example, a hot drawing press uses hydraulic drive and is rated at 3.65 MN (400 tons) with a stroke length of 3.05 m (120 inches).

MATHEMATICAL MODELING OF TANDEM DRAWING WITH A TAPERED PUNCH

The mathematical models developed earlier at Battelle (ref. 1) were valid only for drawing through a single conical or streamlined die with a straight punch. Actual shell drawing operations, however, very often use more than one drawing die in tandem. Further, in these operations, the front portion of the punch is invariably tapered, as shown in figure 1. Therefore, these existing mathematical models were modified to include drawing through tandem dies with a tapered punch.

Stress Analysis

The present model simulates the actual drawing process by dividing the punch movement into a finite number of discrete steps. The slab method (ref. 2) of analysis was used to calculate stresses and drawing loads at each step. This analysis is valid for both conical and streamlined dies, since a complex die profile can be approximated by a series of straight lines.

Figure 2 shows a segment of the shell between the die and the punch, where the die is stationary and the punch is moving to the right. The operation consists of drawing a tube of outside radius R_o and inside radius R_i by a punch through a die to a tube of outside radius r_o and inside radius r_i. The details of the analysis of the stresses and the loads in this operation are given in appendix A.

In calculating the stresses, the flow stress of each element is considered as a function of strain, strain rate, and temperature. The strain in an element is the cumulative strain, and strain rate is calculated from a velocity field developed during earlier studies (ref. 1). The temperature of an element will depend upon the heat generated from plastic deformation, and friction at the tool-material interfaces, and the heat conduction to the colder

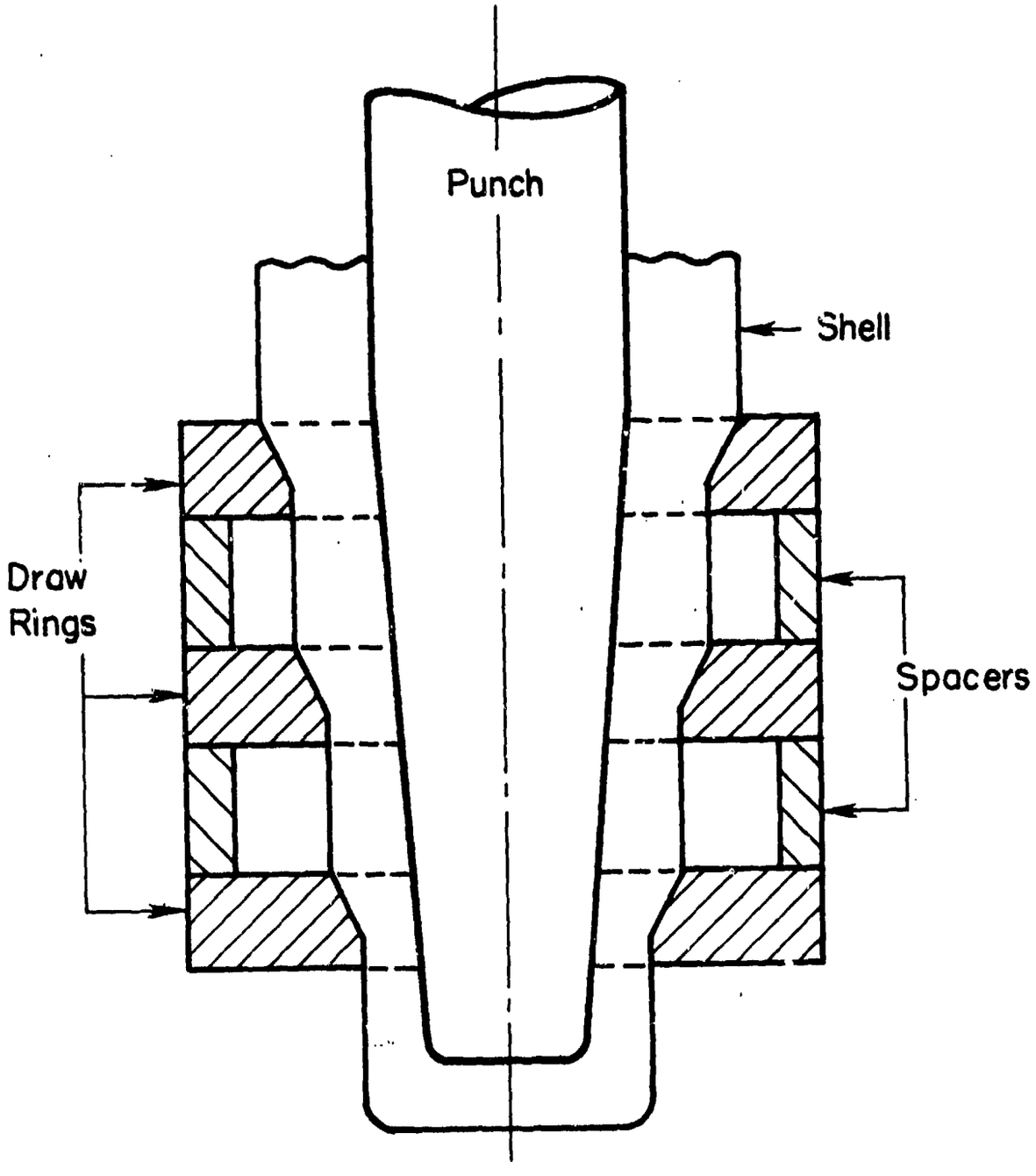

Figure 1. Shell drawing with dies in tandem and with a tapered punch.

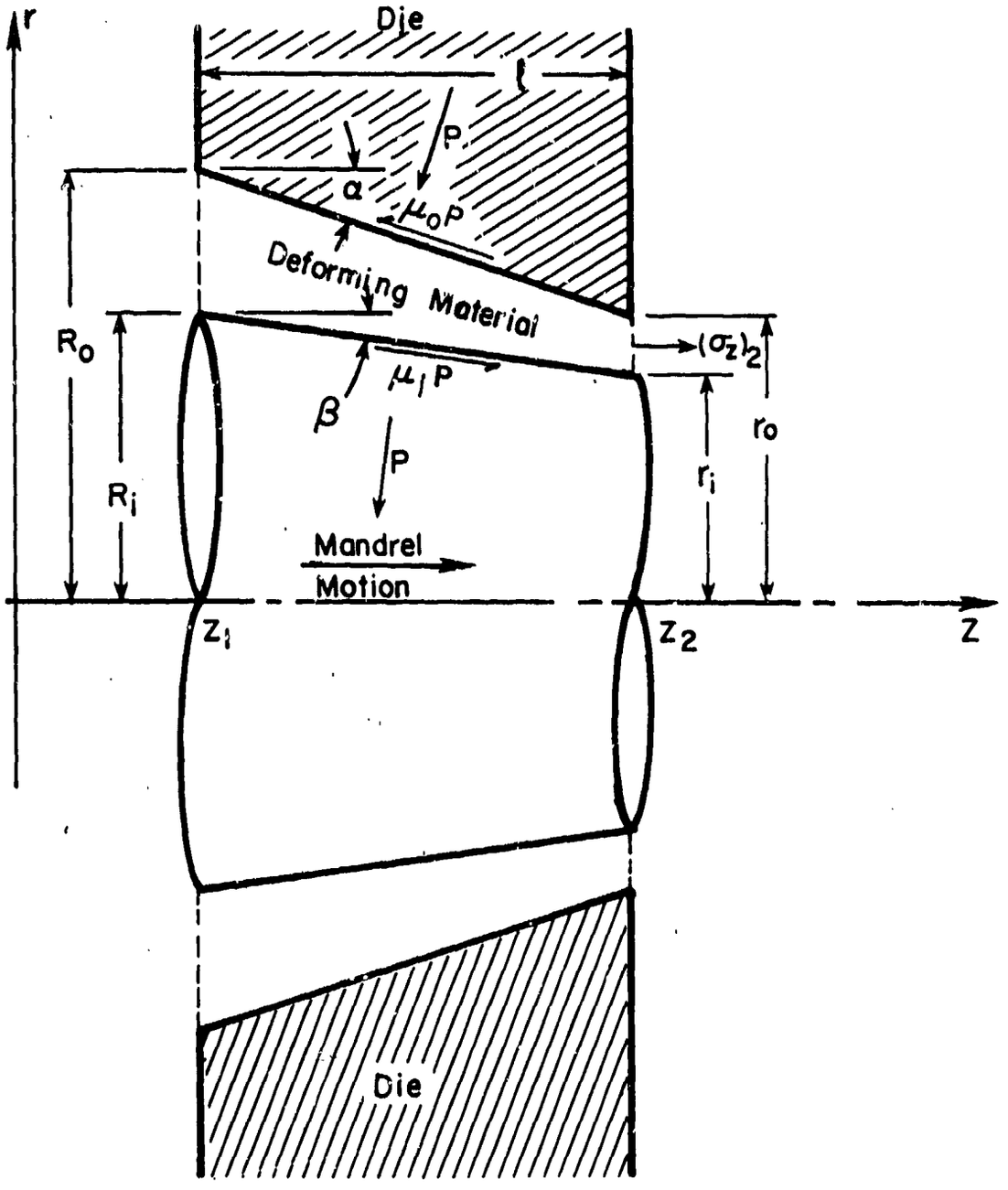

Figure 2. Drawing through conical die with a tapered punch.

dies and punch. Expressions for strain, strain rate and temperature of an element inside a die are also given in appendix A.

Computer Model

Based on this stress analysis, a system of computer programs, named DRAWNG, was developed to simulate the drawing operation for artillery shells through multiple dies in tandem that employs a tapered punch. These computer programs are coded in Fortran IV and are applicable to both the cold and hot drawing of shells. A functional flow chart of DRAWNG is given in figure 3. In its present form, DRAWNG is operational on a CDC system in interactive mode using a Tektronix graphics terminal. The die, billet and punch geometry are inputed to the program. This input can be read either through a data file prestored in the computer as a cataloged file or through the keyboard. A detailed description of the computer programs DRAWNG and instructions for its use, preparation of input, and an example output are included in appendix B.

DRAWNG simulates the tandem drawing operation on a real-time basis, and the step-by-step results are displayed on the computer's graphic display terminal, as shown in figure 4. On the top one-third of the screen, first the title is printed, and then the dies are drawn showing specified spacings between them, and the billet and punch are positioned for beginning of the simulation. Once the simulation begins, the step-by-step movement of the punch and the billet is shown on the top one-third of the screen. At the same time, the total ram load versus punch displacement and wall stress versus punch displacement are shown on the left half and right half of the lower two-thirds of the screen, respectively. During the simulation, the computer programs calculate the correct flow stress in the deformation zone corresponding to local strain, strain rate, and temperature, and utilize appropriate equations for stresses, depending upon whether the element is free, or within a die, or in between two dies. In addition, the tensile strength of the product is plotted on the wall stress-versus-displacement diagram to show whether punch-through is predicted at any stage of the drawing operation. At the end of simulation, the computer program provides messages which enable the user to enlarge any of the three diagrams on the screen, as shown in figures 5 through 7. If further details are needed, the user can transfer various outputs stored on tapes to a line printer or to a similar output device.

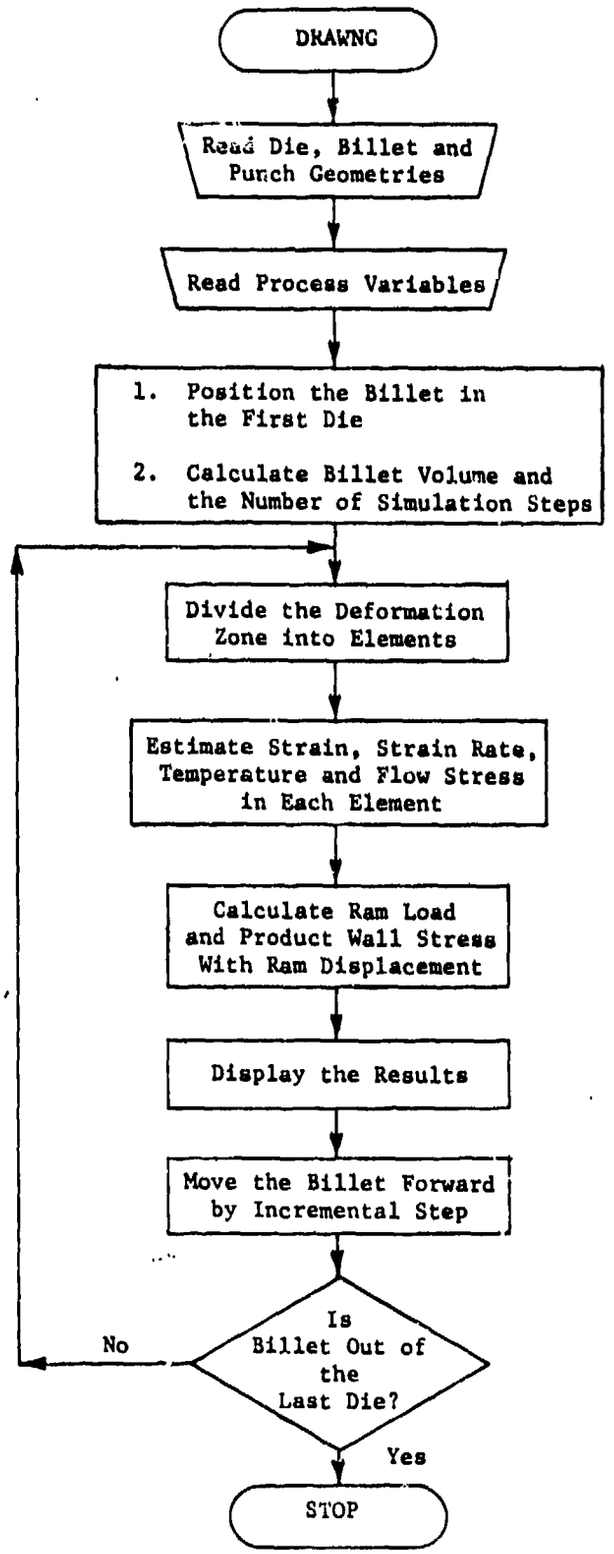

Figure 3. Functional flow chart of the computer program DRAWNG.

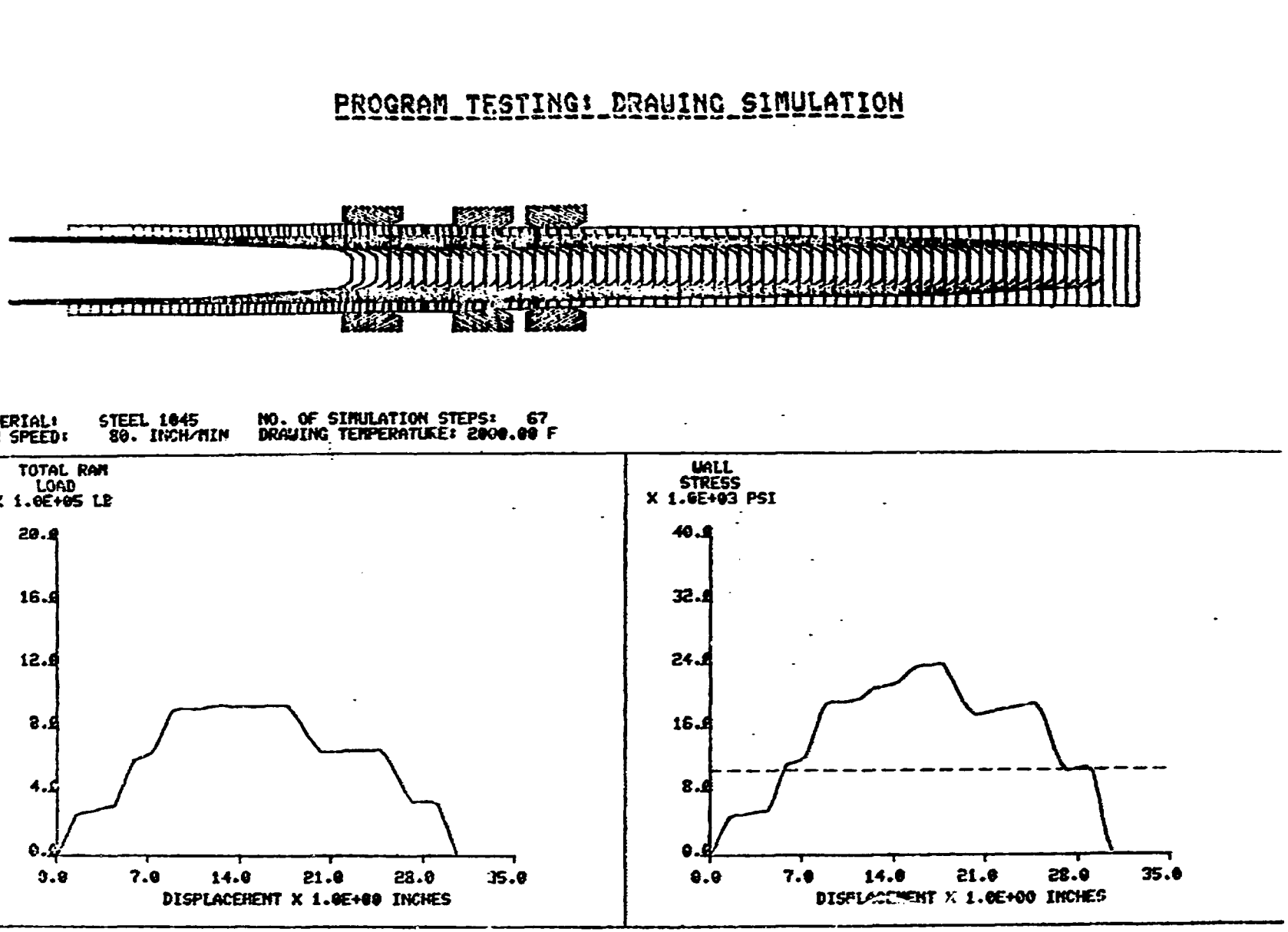

Figure 4. Simulation of tandem drawing as displayed on a CRT screen.

PROGRAM TESTING: DRAWING SIMULATION

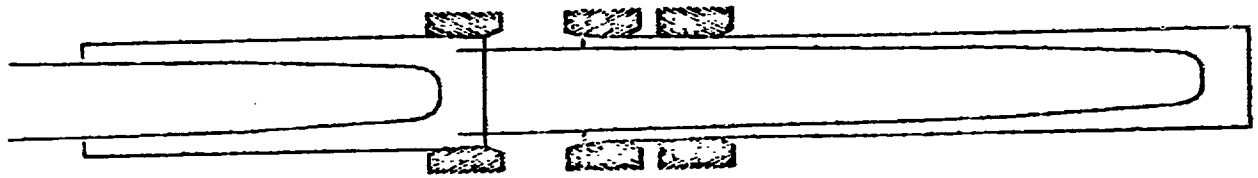

AT THE END OF SIMULATION STEP 50

MATERIAL: STEEL 1045 NO. OF SIMULATION STEPS: 67
RAM SPEED: 80. INCH/MIN DRAWING TEMPERATURE: 2000.00 F

TO CONTINUE, TYPE ANY CHARACTER AND STRIKE THE RETURN KEY

Figure 5. Die and punch geometries on a full screen.

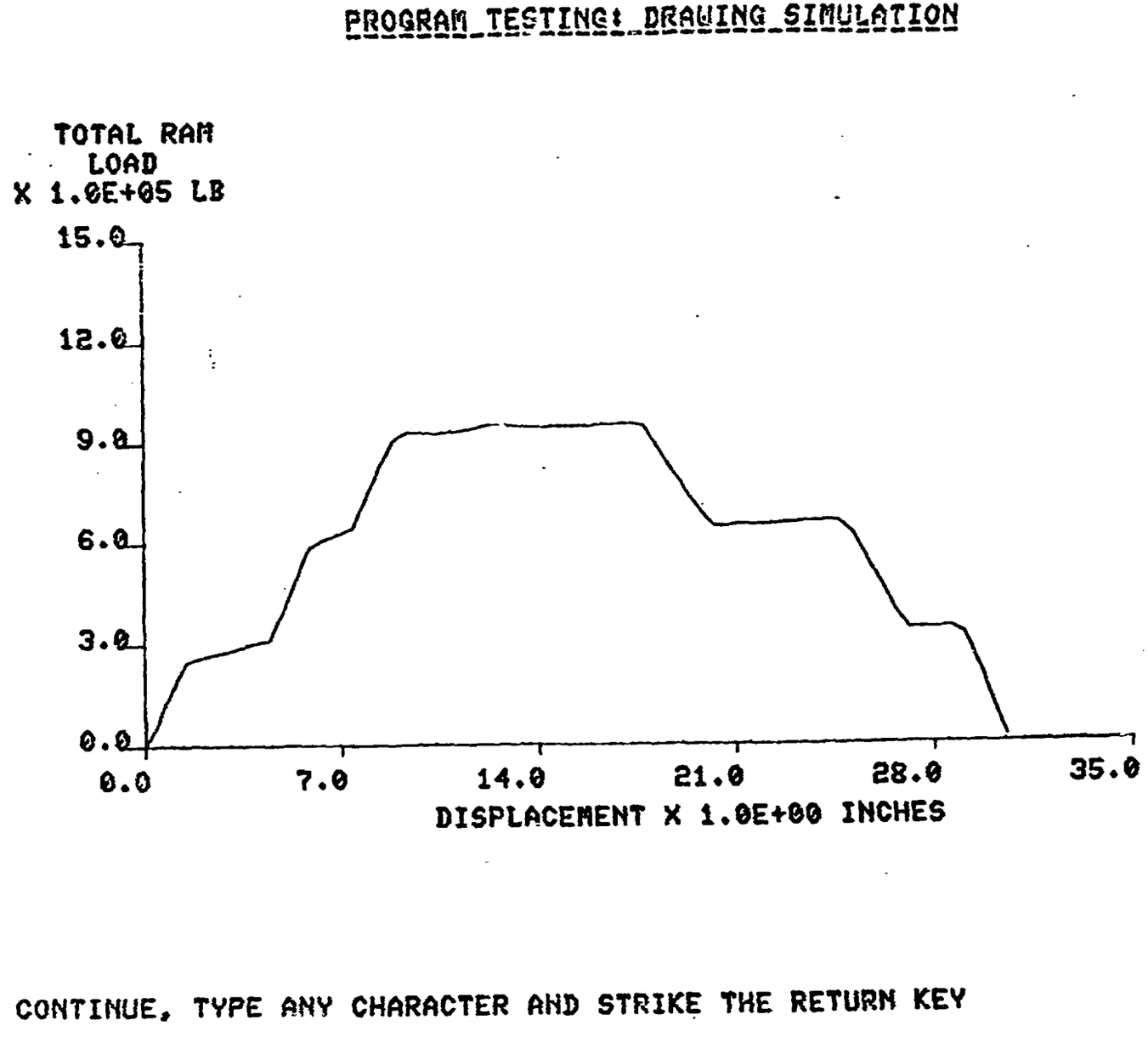

Figure 6. Load-displacement plot on a full screen.

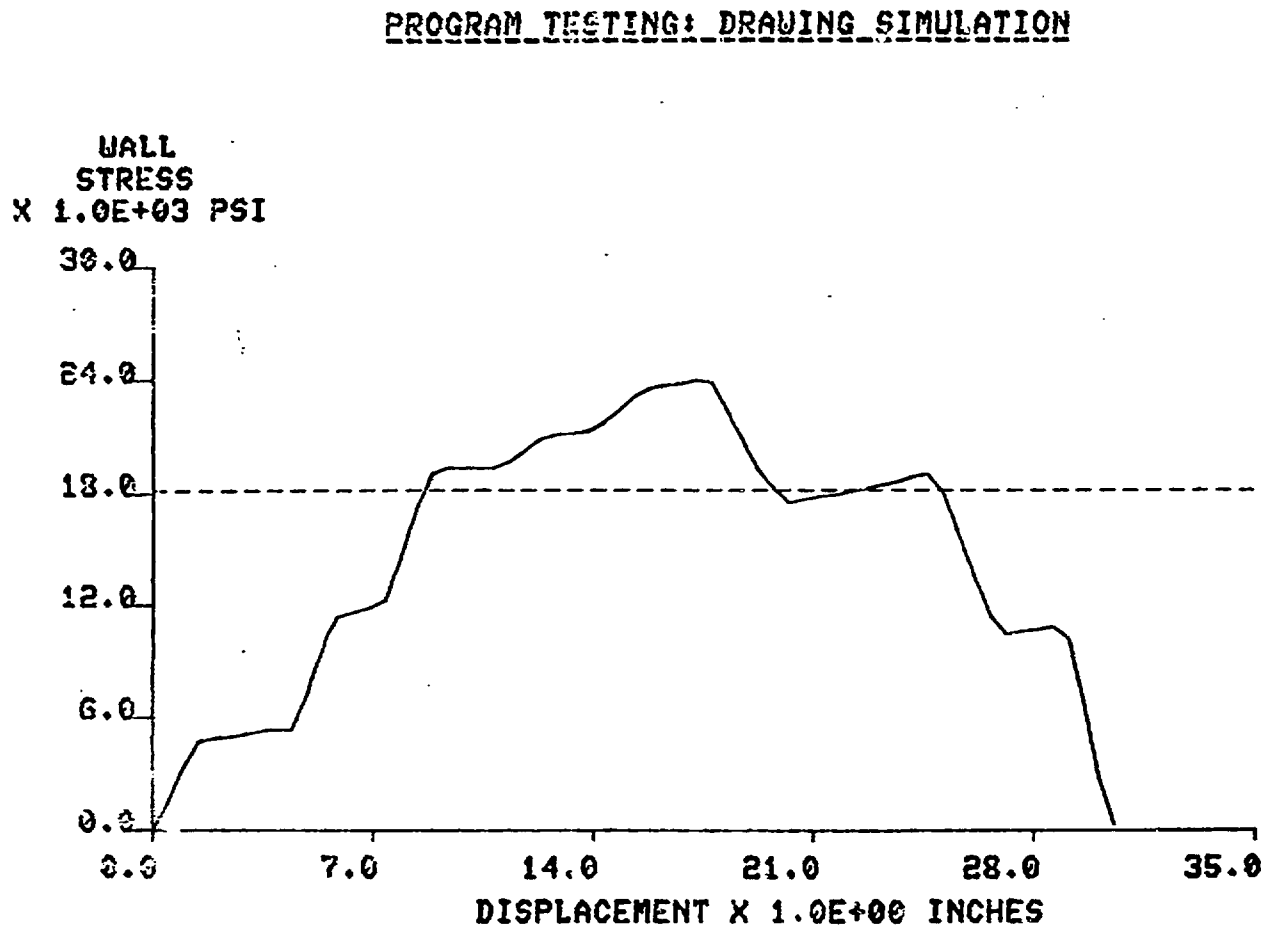

Figure 7. Wall stress-ram displacement plot on a full screen.

Thus the computer program DRAWNG is capable of predicting:

(a) The load-stroke curves

(b) The failure due to punch-through, and

(c) The effect of process variables on the total ram load and punch-head load.

DRAWNG is entirely user-oriented and can therefore be used readily by engineers and technicians who have little, if any, computer programming background and training.

CONFIRMATION TESTINGS OF THE SHELL DRAWING OPERATIONS

Confirmation tests of the shell drawing operation were conducted under production or near-production conditions to evaluate the accuracy of the predictions. These tests were conducted at two different shell manufacturing plants. The cold drawing tests (at room temperature) were performed at Chamberlain Manufacturing Corporation's Waterloo, Iowa division under either production or near-production conditions. Hot-drawing tests (at hot-working temperatures) were conducted at Chamberlain Manufacturing Corporation's Scranton, Pennsylvania division under actual production conditions. In both cases, the tests were conducted with standard army shells which are under current production, and except for the drawing dies, the existing tooling (punch, die holder, etc.) were used. The tests were first conducted using conventional conical dies, and later they were repeated using the optimally designed streamlined dies with double-curvature profiles (designed based on prior mathematical modeling work on drawing of shells (ref. 1)). All the tests were designed by Battelle and were planned jointly by Battelle and the Chamberlain Corporation at each of the two locations.

Cold Drawing

Selected Shell and Process

The 4.2-inch M335 standard army shell was selected for these tests. Currently, this shell is in production in Chamberlain's Waterloo division. The material used was AISI 1030 as per specification ASTM 273. This shell is accomplished in two cold double draws, with intermediate annealing and rough machining. Prior to each cold drawing operation, both inside and outside of the preform

is pickle-cleaned, phosphated and lubricated with a commercial soap. In the present investigation, the final double draw operation was selected. Drawing No. 7000-90, Sheets 5 and 6 given in figures 8 and figure 9 show the shell before and after the final double draw.

Equipment and Instrumentation

Confirmation tests of the cold drawing operation with conventional dies were conducted under an actual production environment at Chamberlain Corporation's Waterloo, Iowa division. For this purpose, the final double draw operation of 4.2-inch M335 shell on a Bliss production hydraulic press was selected, figure 10. The press is rated at 1.78 MN (200 tons), and has a 1.02 m (40-inch) stroke. The nominal ram speed is 68 mm/s (160 inch/min), and the ram diameter is 368.3 mm (14.5 inch). To measure ram load, the hydraulic line was tapped with a pressure transducer (Gilmore 500 S). Its conditioned output, amplified by a power supply, was then connected to the left-hand channel of a two-channel brush recorder (Gould). Pressure calibration was kept at 10.34 MN/m^2 (1500 psi) for the full width of the chart. Ram displacement was measured simultaneously with the ram pressure, with a potentiometer-type displacement transducer. The displacement transducer housing was bolted to the lower frame of the press, and its cable was hooked to the slider of the press ram. The amplified output of the displacement transducer was concected to the right-hand channel of the brush recorder. This displacement calibration was fixed at 1.27 m (50 inch) for the full width of the chart. Chart speed during the tests was kept at 5 mm/s (11.8 in./min).

Confirmation tests of the cold drawing operation with streamlined dies were conducted under near-production conditions in Chamberlain Corporation's Research and Development division at Waterloo, Iowa. These tests were performed on a Verson hydraulic press rated at 5.34 MN (600 tons) with a maximum ram displacement of 1.676 m (66 inch). This press has a nominal ram speed of 91.4 mm/s (216 inch/min) and ram diameter of 0.60 m (23-5/8 inch) (ram area = 0.283 sq m (438 sq in.)). The press was instrumented with a pressure transducer and a displacement transducer, and the ram pressure and the ram displacements were recorded simultaneously on two separate channels of the two-channel brush recorder. Chart calibrations for pressure and displacements were 5.17 MN/m^2 (750 psi) and 1.27 m (50 inch) for the full width of the chart, respectively. Again, chart speed during these tests was kept at 5 mm/s (11.8 in./min).

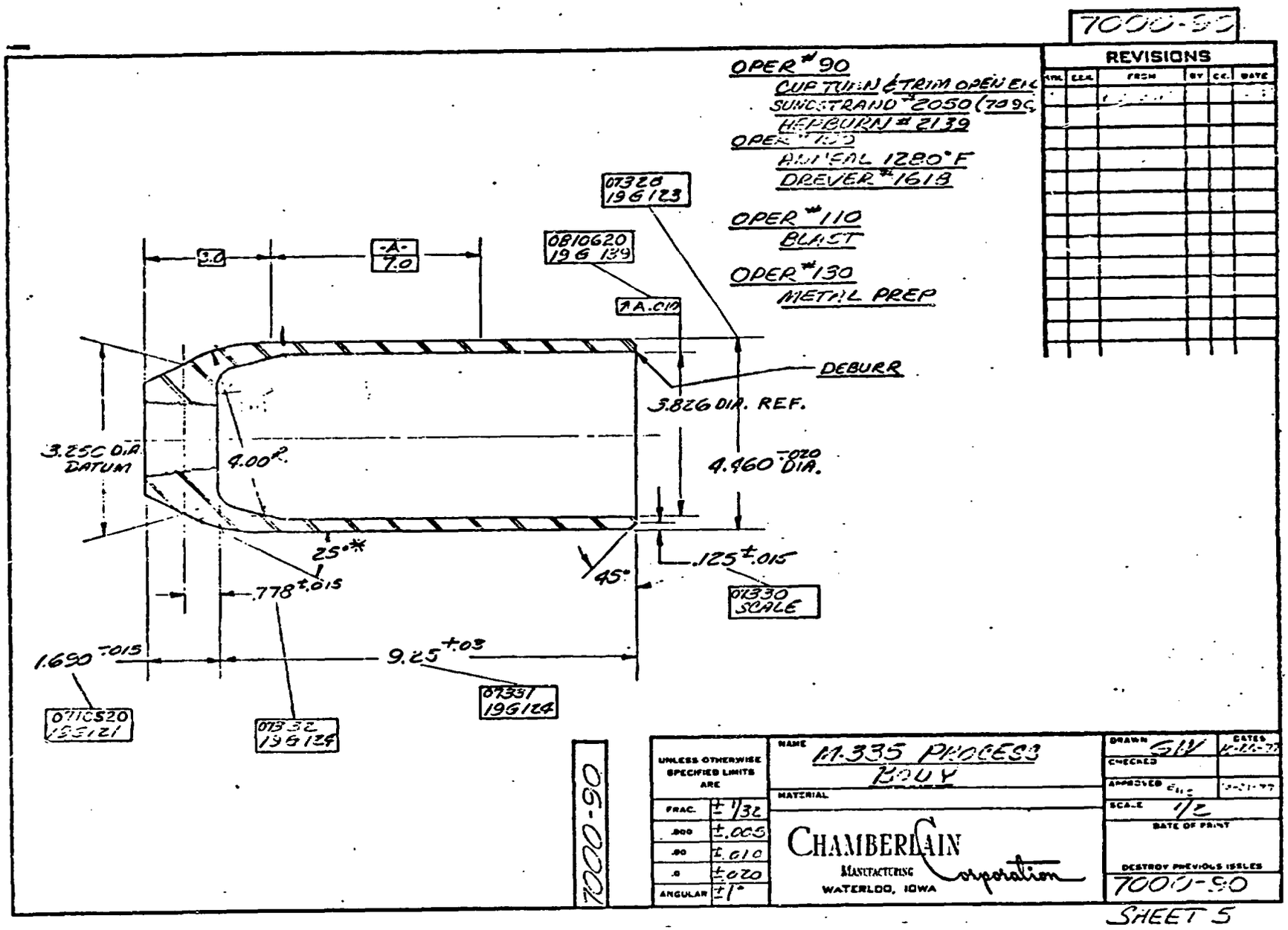

Figure a). Body of M335 shell prior to final double-drawing operation.

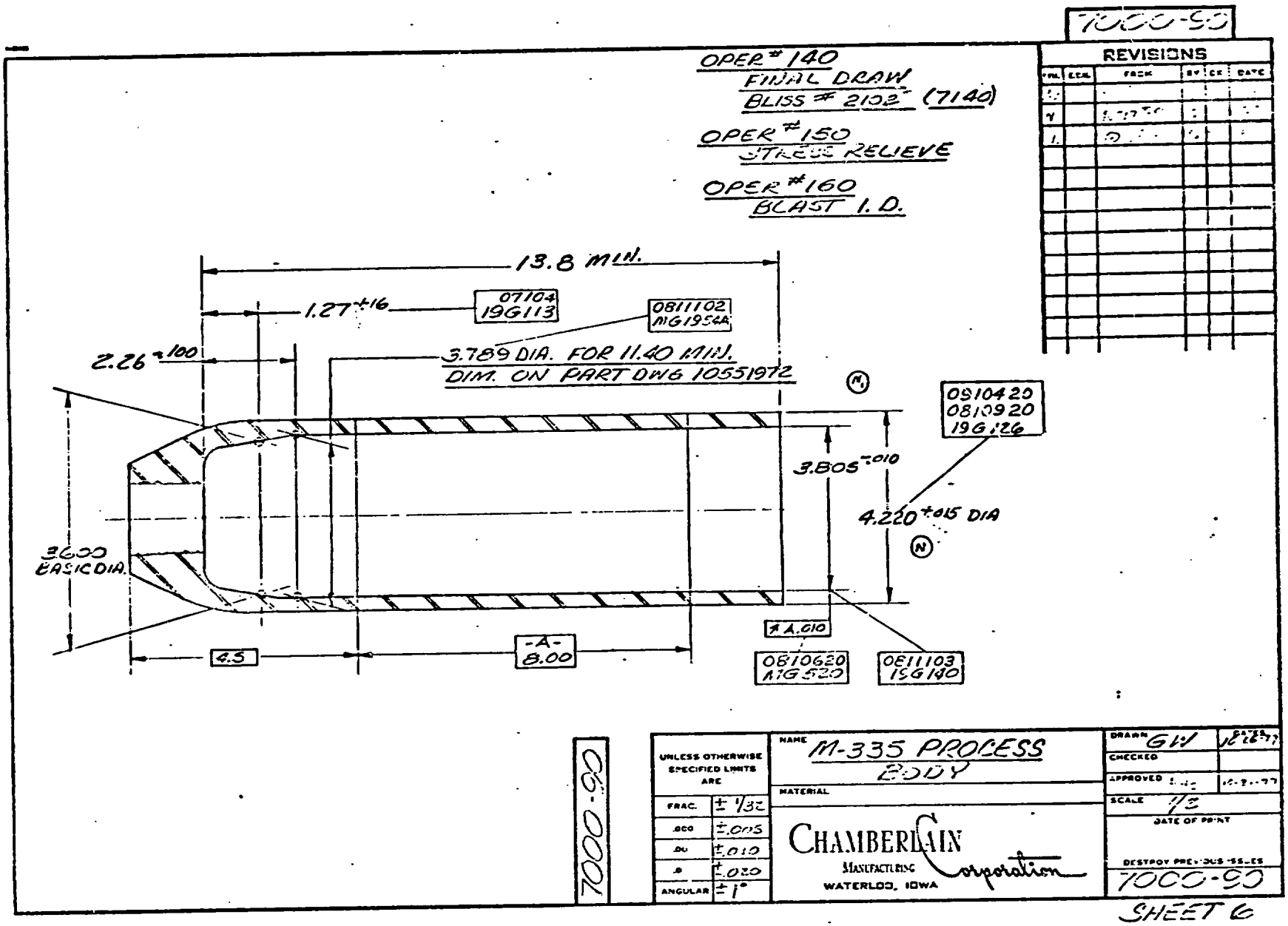

Figure 8(b). Body of M335 shell after the final double-drawing operation.

Figure 9. M335 Projectile bodies before and after final double cold drawing operation.

All dimensions are in inches. (1 inch = 25.4 mm.)

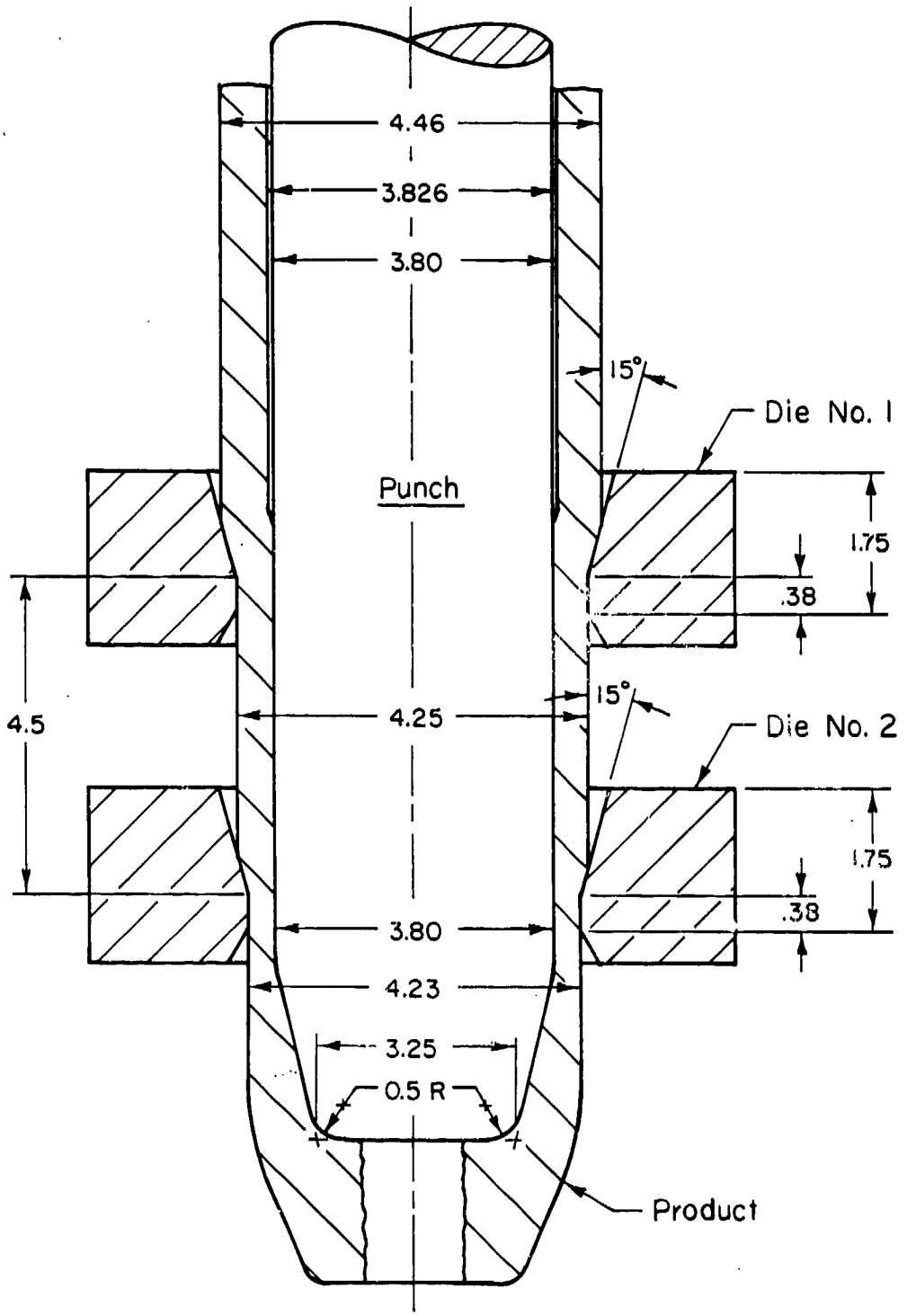

Figure 10. Schematic representation of final double draw of M335 shell under current production conditions.

Dies and Punch

The general practice in the industry is to use a conical shape at the entrance of the drawing dies. These dies are easy to machine and therefore when worn can be remachined to replace dies with the larger openings in a tandem arrangement. However, the mathematical models of the drawing operation, developed earlier (ref. 1), indicate that the dies with streamlined profiles are more efficient and help to reduce the probability of punch-through. Therefore, in the present investigation, tests were conducted with both conventional conical and streamlined die designs to evaluate the mathematical models of the shell drawing operation.

Conical dies, used under actual conditions, have an entrance angle of 15 degrees, as shown in figure 10. These dies were press fitted in a die block, which was assembled in the tool assembly, as shown in figure 11. The cold drawing punch, which fits into the interior of the preform shape, is also shown in figure 10. All these dies and toolings are used currently at Chamberlain's Waterloo division in production of M335 shell.

Two sets of streamlined dies were also designed using the computer program CDVEL, developed earlier at Battelle (ref. 1). One set of dies was designed with a double-curvature profile and the other set was designed with a polynomial profile. For the reasons of simplicity, the double-curvature dies were selected for confirmation testing.

As shown in figure 12, two double-curvature dies were designed, one for the first draw of the final double draw and the other for the combined reduction of the final double draw. Based on the die design, a simple computer program was developed for NC machining of the templates at Battelle. The actual dies were machined by Chamberlain Corporation using these templates. The details of the streamlined die design and machining of the templates are included in appendix C. The important portions of the outputs from the computer program CDVEL for these dies and the computer program for NC machining of templates are also included in appendix C.

Tests with Conventional Conical Dies

The tests with conventional conical dies were conducted during a production run at the Chamberlain's Waterloo plant on November 30, 1978. The 1.78-MN (200-ton) Bliss production hydraulic press was instrumented to record

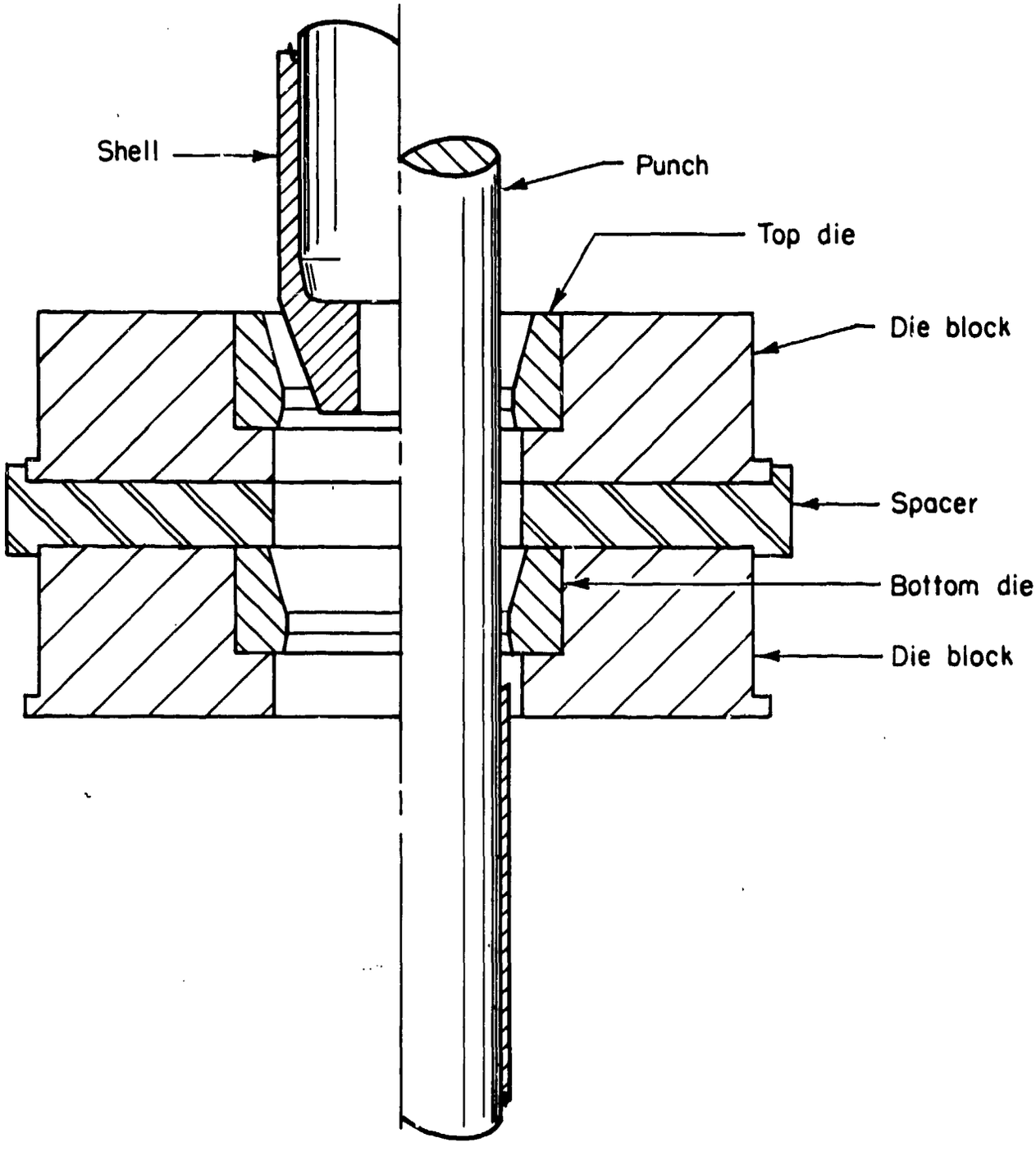

Figure 11. Tool assembly for cold drawing (final double draw) of M335 shell under production conditions.

(All dimensions are in mm; dimensions in parentheses are in inches.)

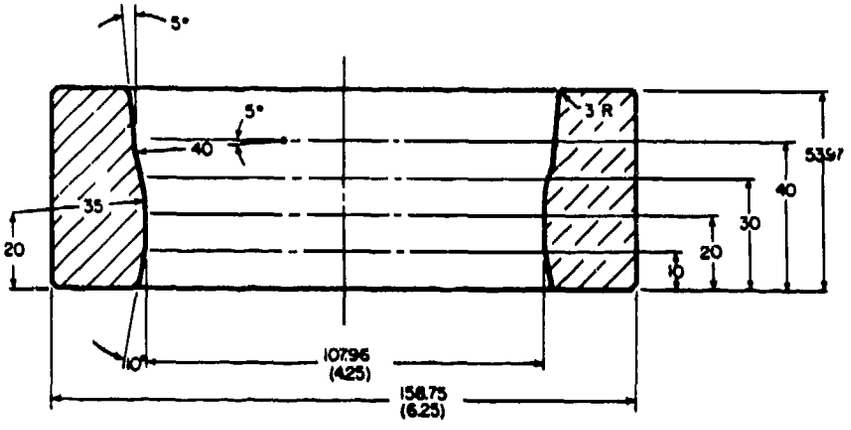

(a) Die No. CDS2—For first die of final double draw

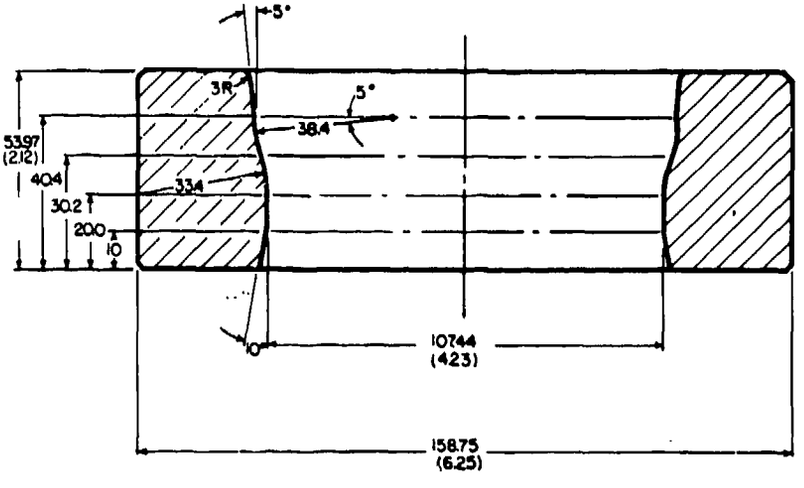

(b) Die No. CDS23--For combined reduction of final double draw

Figure 12. Streamlined dies with double curvature profile for cold drawing of M335 shell.

ram pressure and ram displacement on a two-channel brush recorder. Twenty-five preforms were taken out randomly from the production line at various intervals, and all the important preform dimensions and eccentricity were measured. For the selected shells, the ram pressure and ram displacement were recorded on the two-channel brush recorder. A typical recording is shown in figure 13.

Typically, the shell is loaded and the punch is inserted. Once the punch touches the bottom of the preform, the pressure starts to build up while the press ram dwells. As soon as the break-through pressure for the first die is developed, the shell begins to draw, and soon a steady state is reached until the shell bottom touches the second die. At this time, the pressure again begins to build up but no noticeable dwelling of the press occurs. However, a noticeable break-through peak is observed. As soon as the shell exits from the first die, the pressure instantaneously drops considerably and the shell is drawn through the second die only until the end of drawing, then is ejected by the ejector.

After drawing, all important dimensions and the eccentricity of the selected shells were measured. These various preform and product dimensions are given in table 1. The locations of various measurements in table 1 are shown in figure 14. A few preforms and six drawn shells were selected for further detailed investigation and determination of the properties of drawn shells. Note that the eccentricity of the drawn shell was almost always better than that of the preform. Table 2 shows the recorded displacement and the peak ram load for the selected cases during these tests. The maximum and minimum recorded peak ram loads were 0.804 MN (90.41 tons) and 0.738 MN (82.98 tons), respectively. Average peak ram load was 0.771 MN (86.69 tons). Thus, the maximum variation in the measured peak load was within ± 4.3 percent.

Tests with Streamlined Dies

The tests with streamlined dies of double-curvature profile were conducted under near-production conditions at the Chamberlain's Research and Development division on February 15, 1979. The 5.34-MN (600-ton) Verson hydraulic press was instrumented to record ram pressure and ram displacement on a two-channel brush recorder. Sixty lubricated preforms were removed from the production line at the adjacent Waterloo division of Chamberlain Corporation. All important dimensions and the eccentricity of these selected preforms were measured, as given in table 3.

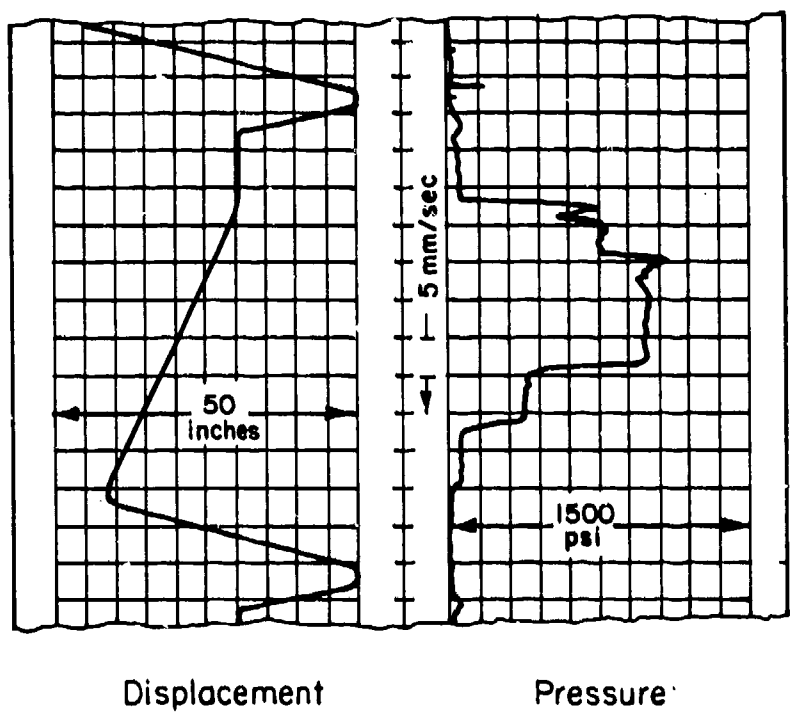

Figure 13. Typical ram displacement and ram pressure recordings during cold drawing (final double draw) of M335 shell using conventional conical dies.
(1 inch = 25.4 mm; 1 psi = 6,895 kN/m^2.)

Table 1. Dimensions of preform and product from cold drawing tests with conventional conical dies (1 inch = 25.4 mm)

Specimen No.	Interval Size	Preform Dimensions, inch(+)							Product Dimensions, inch(+)						
		OD Measurement			ID	Overall Length	Eccentricity		OD Measurement			ID	Overall Length	Eccentricity	
		Rotation, degrees	Forward	Rear			Forward	Rear	Rotation, degrees	Forward	Rear			Forward	Rear
C-1(*)	—	0 90	4.448 4.448	4.465 4.465	3.823	11.729	.004	.006	0 90	4.225 4.224	4.231 4.2315	3.8005	16.150	.004	.005
C-2	25	0 90	4.4665 4.462	4.469 4.467	3.824	11.744	.008	.011	0 90	4.222 4.2265	4.233 4.2295	3.800	16.150	.004	.007
C-3	20	0 90	4.469 4.460	4.467 4.4565	3.8235	11.746	.007	.009	0 90	4.227 4.222	4.231 4.230	3.7995	16.100	.004	.006
C-4	100	0 90	4.462 4.4635	4.466 4.471	3.8245	11.732	.004	.004	0 90	4.2255 4.230	4.231 4.231	3.800	16.148	.003	.003
C-5(*)	25	0 90	4.464 4.464	4.466 4.465	3.825	11.720	.007	.004	0 90	4.224 4.2245	4.231 4.231	3.800	16.160	.004	.005
C-6	15	0 90	4.458 4.4615	4.465 4.466	3.8245	11.736	.006	.007	0 90	4.2245 4.224	4.231 4.231	3.8005	16.150	.004	.005
C-7	15	0 90	4.4635 4.463	4.4675 4.4645	3.8245	11.715	.011	.009	0 90	4.2245 4.2265	4.231 4.231	3.8005	16.115	.006	.004
C-8	15	0 90	4.464 4.461	4.465 4.464	3.824	11.732	.008	.006	0 90	4.225 4.224	4.230 4.231	3.801	16.100	.007	.003
C-9	10	0 90	4.464 4.462	4.467 4.464	3.8245	11.740	.006	.005	0 90	4.225 4.224	4.231 4.2315	3.8005	16.200	.004	.003
C-10(*)	15	0 90	4.457 4.463	4.453 4.469	3.8245	11.745	.008	.010	0 90	4.222 4.222	4.2315 4.2315	3.800	16.100	.005	.004
C-11	15	0 90	4.461 4.458	4.456 4.462	3.824	11.736	.007	.010	0 90	4.2235 4.223	4.231 4.231	3.800	16.065	.003	.007
C-12	15	0 90	4.4575 4.464	4.456 4.465	3.825	11.715	.006	.010	0 90	4.223 4.2235	4.231 4.232	3.800	16.030	.004	.005
C-13	15	0 90	4.470 4.467	4.4665 4.463	3.8235	11.748	.006	.007	0 90	4.225 4.223	4.234 4.230	3.7995	16.125	.004	.004

Table 1. (Continued)

Specimen No.	Interval Size	Preform Dimensions, inch(+) OD Measurement Rotation, degrees	Forward	Rear	ID	Overall Length	Eccentricity Forward	Rear	Product Dimensions, inch(+) OD Measurement Rotation, degrees	Forward	Rear	ID	Overall Length	Eccentricity Forward	Rear
C-14	15	0 90	4.464 4.465	4.461 4.465	3.8245	11.727	.009	.009	0 90	4.224 4.223	4.231 4.232	3.800	16.155	.006	.005
C-15(*)	15	0 90	4.465 4.463	4.461 4.463	3.824	11.740	.006	.007	0 90	4.225 4.222	4.232 4.232	3.8005	16.100	.005	.005
C-16	15	0 90	4.467 4.465	4.455 4.460	3.8235	11.749	.006	.008	0 90	4.2255 4.222	4.232 4.2315	3.8005	16.050	.004	.005
C-17	30	0 90	4.473 4.467	4.468 4.4625	3.824	11.730	.006	.009	0 90	4.2245 4.2245	4.232 4.230	3.799	16.225	.002	.008
C-18	15	0 90	4.4565 4.459	4.456 4.463	3.8225	11.748	.005	.008	0 90	4.225 4.223	4.2295 4.2325	3.800	16.025	.003	.006
C-19	15	0 90	4.4595 4.4525	4.461 4.455	3.824	11.740	.009	.009	0 90	4.2265 4.2285	4.231 4.231	3.800	15.930	.006	.005
C-20(*)	15	0 90	4.470 4.467	4.464 4.460	3.824	11.741	.006	.004	0 90	4.227 4.226	4.232 4.232	3.800	16.280	.005	.005
C-21	15	0 90	4.467 4.467	4.463 4.464	3.823	11.744	.004	.005	0 90	4.226 4.225	4.2315 4.232	3.800	16.240	.002	.005
C-22	15	0 90	4.467 4.4665	4.4655 4.467	3.824	11.723	.003	.004	0 90	4.225 4.225	4.232 4.2315	3.801	16.210	.003	.004
C-23	15	0 90	4.465 4.4635	4.465 4.471	3.8235	11.721	.003	.005	0 90	4.225 4.225	4.231 4.233	3.8005	16.320	.002	.005
C-24	15	0 90	4.4595 4.4595	4.468 4.471	3.824	11.747	.007	.007	0 90	4.226 4.225	4.2315 4.232	3.800	16.180	.004	.004
C-25(*)	15	0 90	4.466 4.466	4.467 4.470	3.823	11.742	.003	.005	0 90	4.225 4.225	4.2325 4.2315	3.8005	16.320	.003	.003

(+) Preform and product measurement locations are given in Figure 4.

(*) Selected for tensile testing.

All dimensions are in inches. (1 inch = 25.4 mm.)

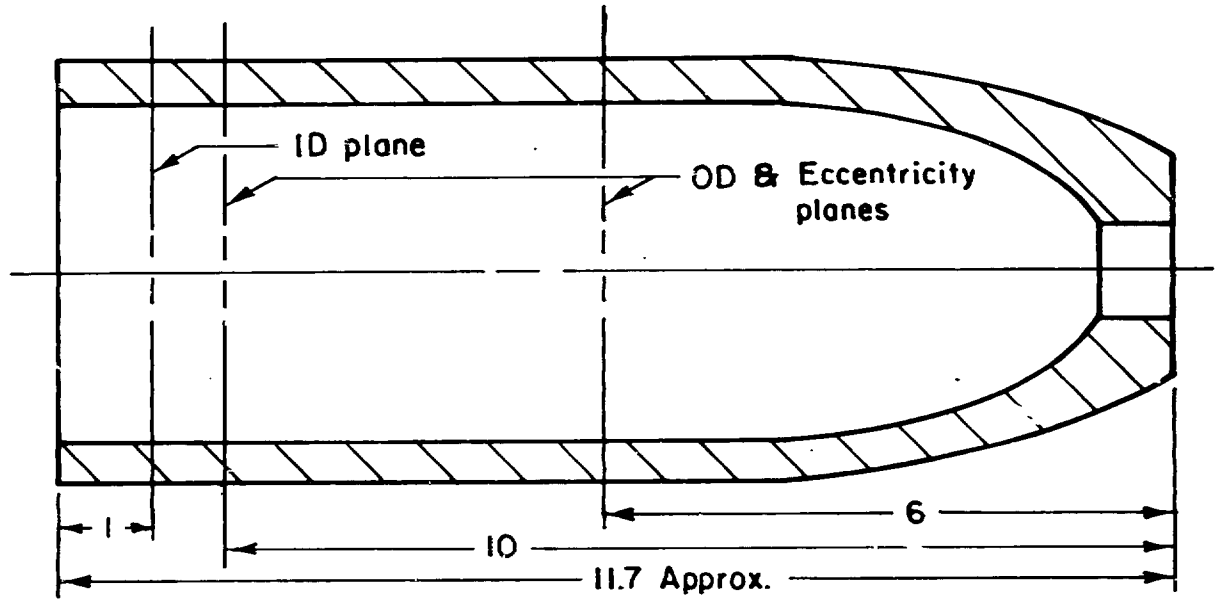

Preform

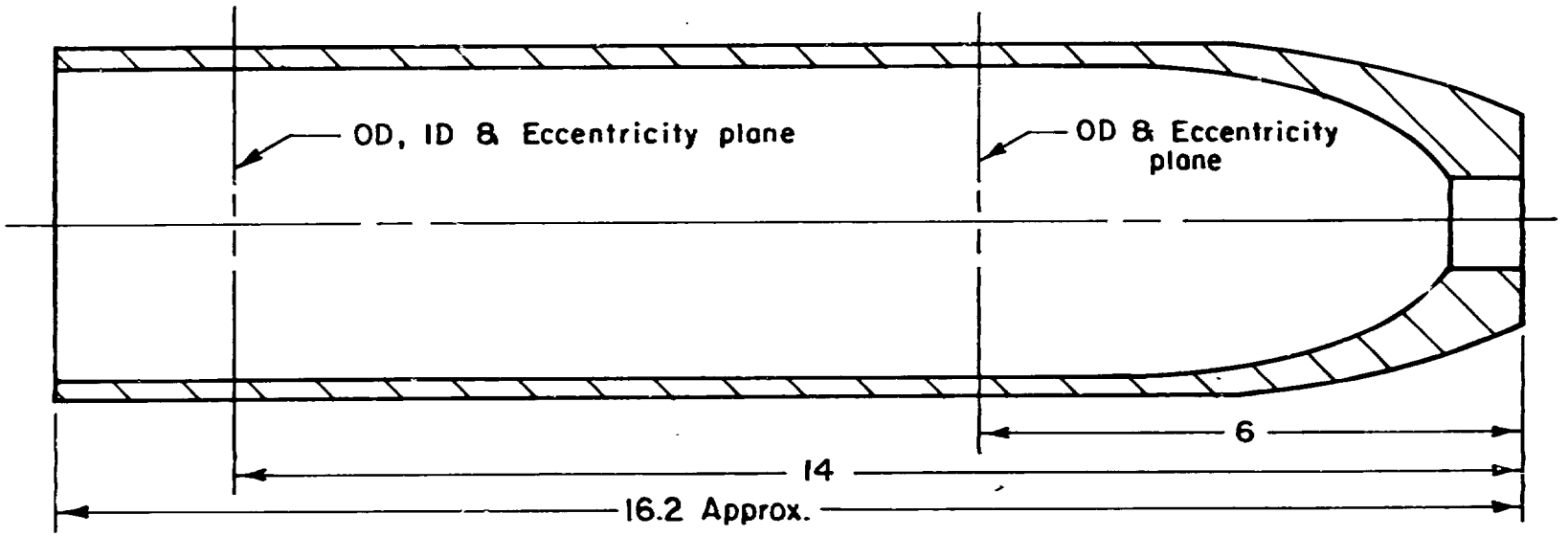

Product

Figure 14. Location of dimensional measurements on M335 shell preform and product.

Table 2. Recorded ram displacement and peak ram load for cold drawing of M335 shell through conventional conical dies.

Specimen No.	Ram Displacement, mm (inch)	Peak Ram Load, MN (tons)
C-1	447 (17.6)	0.771 (86.69)
C-2	447 (17.6)	0.771 (86.69)
C-3	447 (17.6)	0.804 (90.41)
C-4	447 (17.6)	0.793 (89.17)
C-5	447 (17.6)	0.782 (87.93)
C-6	447 (17.6)	0.760 (85.45)
C-7	447 (17.6)	0.782 (87.93)
C-8	447 (17.6)	0.782 (87.93)
C-9	447 (17.6)	0.771 (86.69)
C-10	447 (17.6)	0.760 (85.45)
C-11	447 (17.6)	0.760 (85.45)
C-12	447 (17.6)	0.749 (84.22)
C-13	447 (17.6)	0.771 (86.69)
C-14	447 (17.6)	0.771 (86.69)
C-15	447 (17.6)	0.771 (86.69)
C-16	447 (17.6)	0.793 (89.17)
C-17	447 (17.6)	0.782 (87.93)
C-18	447 (17.6)	0.738 (82.98)
C-19	447 (17.6)	0.738 (82.98)
C-20	447 (17.6)	0.771 (86.69)
C-21	447 (17.6)	0.751 (84.45)
C-22	447 (17.6)	0.782 (87.93)
C-23	447 (17.6)	0.771 (86.69)
C-24	447 (17.6)	0.771 (86.69)
C-25	447 (17.6)	0.771 (86.69)

Table 3. Dimensions of the preform and the product from cold drawing tests with streamlined dies (1 inch = 25.4 mm).

Specimen No.	Die No.	Preform Dimensions, inch(+)							Product Dimension, inch(+)						
		OD Measurement			ID	Overall Length	Eccentricity		OD Measurement			ID	Overall Length	Eccentricity	
		Rotation, degrees	Forward	Rear			Forward	Rear	Rotation, degrees	Forward	Rear			Forward	Rear
S-2	CDS-23	0 90	4.464 4.4645	4.4595 4.4605	3.825	11.714	.002	.003	0 90	4.238 4.239	4.239 4.239	3.797	15.544	.003	.002
S-4	Ditto	0 90	4.466 4.466	4.461 4.462	3.825	11.721	.004	.002	0 90	4.239 4.239	4.2395 4.239	3.798	15.584	.002	.003
S-6	"	0 90	4.4605 4.461	4.4595 4.463	3.825	11.718	.003	.002	0 90	4.2385 4.2385	4.239 4.239	3.798	15.434	.003	.003
S-8	"	0 90	4.4655 4.4655	4.4615 4.4605	3.826	11.712	.004	.002	0 90	4.239 4.2385	4.2395 4.239	3.798	15.550	.002	.002
S-10	"	0 90	4.465 4.465	4.456 4.458	3.8255	11.700	.004	.002	0 90	4.2385 4.238	4.2385 4.2385	3.798	15.500	.004	.005
S-12	"	0 90	4.465 4.465	4.459 4.459	3.825	11.720	.005	.002	0 90	4.238 4.2385	4.2385 4.239	3.8015	15.596	.002	.003
S-14	"	0 90	4.467 4.465	4.461 4.460	3.825	11.722	.003	.002	0 90	4.239 4.239	4.239 4.2385	3.8015	15.575	.002	.003
S-16	"	0 90	4.4655 4.464	4.459 4.4595	3.824	11.721	.003	.002	0 90	4.239 4.238	4.239 4.239	3.801	15.533	.003	.002
S-18	"	0 90	4.464 4.467	4.4575 4.4595	3.8255	11.702	.005	.003	0 90	4.239 4.2385	4.239 4.2395	3.801	15.582	.003	.003
S-20	"	0 90	4.4625 4.463	4.4565 4.459	3.825	11.720	.002	.003	0 90	4.239 4.239	4.240 4.239	3.801	15.570	.003	.003

Table 3 (Continued).

Specimen No.	Die No.	Preform Dimnesions, inch(+) OD Measurement Rotation, degrees	Forward	Rear	ID	Overall Length	Eccentricity Forward	Eccentricity Rear	Product Dimensions, inch(+) OD Measurement Rotation, degrees	Forward	Rear	ID	Overall Length	Eccentricity Forward	Eccentricity Rear
S-21	CDS2 + CDS25	0	4.464	4.460	3.824	11.708	.004	.002	0	4.2335	4.239	3.800	15.625	.004	.003
		90	4.465	4.462					90	4.236	4.240				
S-22	Litto	0	4.465	4.460	3.825	11.713	.006	.003	0	4.2365	4.239	3.800	15.575	.004	.008
		90	4.462	4.459					90	4.234	4.239				
S-23	"	0	4.465	4.461	3.8255	11.710	.005	.002	0	4.234	4.2385	3.8005	15.755	.004	.004
		90	4.464	4.461					90	4.2335	4.2395				
S-24	"	0	4.464	4.462	3.825	11.713	.006	.003	0	4.234	4.239	3.801	15.725	.005	.008
		90	4.464	4.460						4.234	4.240				
S-25	"	0	4.466	4.4615	3.825	11.714	.007	.004	0	4.238	4.239	3.801	15.565	.004	.006
		90	4.462	4.452					90	4.231	4.240				
S-26	"	0	4.465	4.459	3.825	11.710	.003	.002	0	4.235	4.240	3.801	15.707	.004	.004
		90	4.4645	4.457					90	4.234	4.240				
S-27	"	0	4.4645	4.460	3.825	11.712	.003	.002	0	4.236	4.239	3.801	15.678	.006	.005
		90	4.4635	4.461					90	4.2335	4.239				
S-28	"	0	4.462	4.4565	3.8255	11.718	.004	.002	0	4.232	4.240	3.8005	15.595	.003	.005
		90	4.465	4.4575					90	4.237	4.240				
S-29	"	0	4.4645	4.459	3.825	11.701	.003	.002	0	4.2365	4.239	3.8015	15.633	.004	.004
		90	4.4665	4.4605					90	4.2325	4.240				
S-30	"	0	4.4645	4.459	3.8255	11.705	.003	.003	0	4.234	4.239	3.8005	15.675	.003	.002
		90	4.465	4.4615					90	4.235	4.240				
S-31	"	0	4.4635	4.4575	3.825	11.722	.003	.002	0	4.235	4.2395	3.8005	15.700	.003	.004
		90	4.4625	4.457					90	4.234	4.240				

(+) Preform and product measurement locations are given in Figure 4.

The tests were conducted using a single streamlined die (CDS23) producing the total required deformation and with two streamlined dies in tandem (CDS2 & CDS23) separated by a 64.8-mm (2.55-inch) spacer, as in the case of tests with conventional conical dies. The first twenty preforms were drawn through the single die, CDS 23; the next forty preforms were drawn through two dies (CDS2 and CDS23) in tandem. All measurements were made on the first twenty pieces, and then measurements were taken on eleven of the next forty pieces. Load and displacements were recorded for all the sixty pieces. Figure 15 shows typical ram pressure and ram displacement recordings for drawing through a single streamlined die (CDS23) and for drawing through two streamlined dies (CDS2 and CDS23). The measured peak load for the selected cases are given in table 4. Note that deformation through these dies required lower forces compared to those required by the conical dies. Further, the breakthrough peak was typically absent here due to more uniform deformation. Billet temperature after deformation was approximately 93.3°C (200°F) as compared to 104.4°C (220°F) in conventional drawing, also indicating a less severe deformation through streamlined dies.

Important dimensions and eccentricity of drawn shells were measured for the selected shells and are included in table 3. Dimensional accuracy through these dies is as good as through the conventional conical dies. Several drawn shells were set aside for further measurements and determination of their properties. Two shells, one each drawn through the conical and the streamlined dies, were sectioned to measure their hardness distribution. Shell drawn through streamlined dies warped less than those drawn through conical dies, indicating the presence of lower residual stresses in the former case.

Hot Drawing

Selected Shell and Process

The 155 mm M107, high explosive standard army shell was selected for these tests. Currently, this shell is in production at Chamberlain's Scranton division. The M107 is fired from all 155 mm howitzers except from the XM198 at high propelling charge zone.

The body of this shell is manufactured from AISI 1046 steel per Mil-P-14824 A (Amendment 1). The M107 is hot forged at approximately

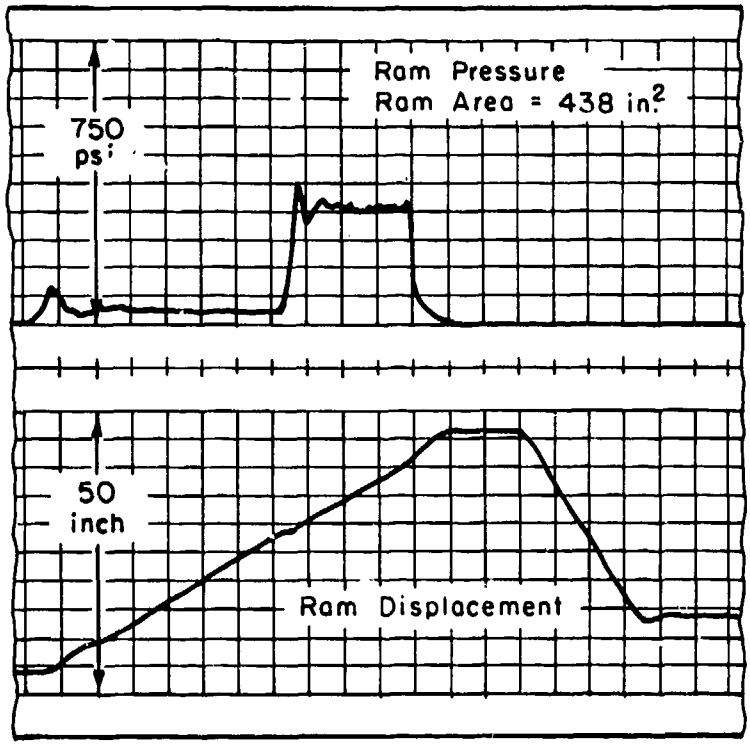

(a) Single streamlined die (CDS23)

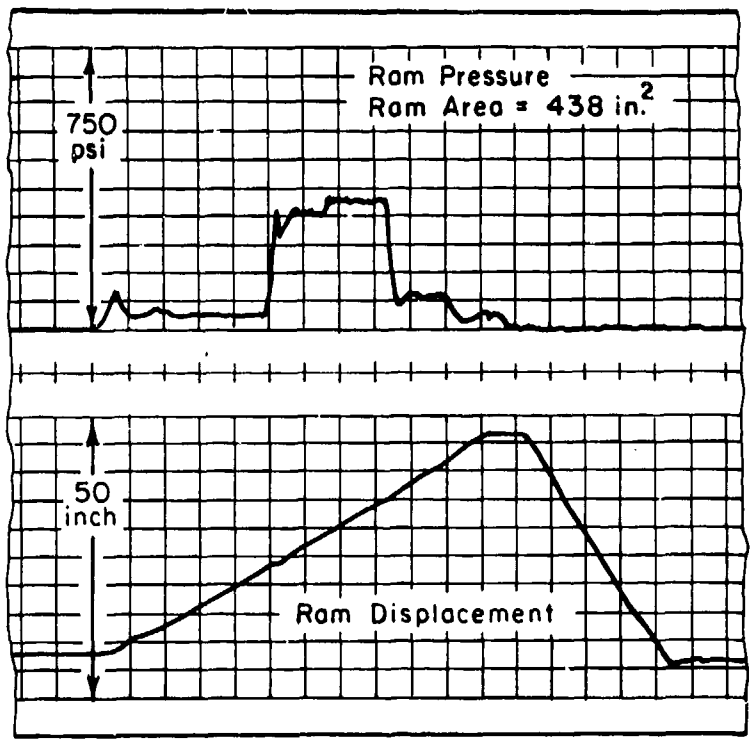

(b) Double streamlined dies (CDS2 + CDS23)

Figure 15. Typical ram pressure and ram displacement recordings during cold drawing of M335 shell using streamlined dies. (1 inch = 25.4 mm; 1 psi = 6.895 kN/m^2.)

Table 4. Recorded ram displacement and peak ram load for cold drawing of M335 shell through streamlined dies.

Specimen No.	Die No.	Ram Displacement, mm (inch)	Peak Ram Load, MN (ton)
S-2	CDS 23	381 (15.0)	0.702 (78.90)
S-4	Ditto	381 (15.0)	0.717 (80.55)
S-6	"	381 (15.0)	0.658 (73.97)
S-8	"	381 (15.0)	0.731 (82.19)
S-10	"	381 (15.0)	0.702 (78.90)
S-12	"	381 (15.0)	0.717 (80.55)
S-14	"	381 (15.0)	0.702 (78.90)
S-16	"	381 (15.0)	0.667 (74.96)
S-18	"	381 (15.0)	0.687 (77.26)
S-20	"	381 (15.0)	0.673 (75.61)
S-21	CDS2 + CDS 23	546 (21.5)	0.731 (82.19)
S-22	Ditto	546 (21.5)	0.702 (78.90)
S-23	"	546 (21.5)	0.687 (77.26)
S-24	"	546 (21.5)	0.702 (78.90)
S-25	"	546 (21.5)	0.702 (78.90)
S-26	"	546 (21.5)	0.702 (78.90)
S-27	"	546 (21.5)	0.687 (77.26)
S-28	"	546 (21.5)	0.687 (77.26)
S-29	"	546 (21.5)	0.687 (77.26)
S-30	"	546 (21.5)	0.702 (78.90)
S-31	"	546 (21.5)	0.673 (75.61)

1093°C (2000°F), well over the critical transformation temperature of the material. Complete forging is accomplished in three steps, namely, cabbaging, piercing and drawing. Cabbaging and piercing operations can be accomplished in two separate presses or in a single press, depending on the equipment. The drawing operation is usually conducted in a long stroke high-speed hydraulic press with two or three rings. The projectile shapes before and after hot drawing are shown in figures 16(a) and (b), and in figure 17.

Equipment and Instrumentation

Confirmation tests of hot drawing operations with both conventional conical and streamlined dies were conducted under actual production conditions at Chamberlain Corporation's Scranton, Pennsylvania division. These tests were conducted on the No. 1 Bliss press line which consists of a vertical hydraulic press. It has a load capacity of 3.56 MN (400 tons), a stroke of 3.05 m (120 inch), a nominal press speed of 0.466 m/s (1100 inch/minute), and a ram diameter of 0.511 m (20.125 inch).

To measure ram load during the drawing operation, the hydraulic line of the press was tapped with a pressure transducer, and its conditioned output (5 V for 34.48 MN/m^2 (5000 psi)) was connected to one of the two channels of a strip recorder (Honeywell). The second channel of the recorder was connected to the output from a displacement transducer to measure the ram displacement. The housing of the displacement transducer was bolted to a plate on the shop floor, and its cable was hooked to the press ram slider. The full width of chart was calibrated to record the last 2.54 m (100 inch) of the press stroke and 17.24 MN/m^2 (2500 psi) pressure. During the tests, the chart speed was kept at 25.4 mm/s (1 inch/sec).

In addition to the above, the temperatures of the incoming billet (after cabbaging and piercing) and of the product were measured with an infrared digital pyrometer. The temperatures of the dies were measured periodically with a contact pyrometer.

Dies and Punch

A schematic representation of the hot drawing operation is shown in figure 18. As in the case of cold drawing of shells, the general practice in industry for hot drawing of shells is to use dies with a conical entrance. The general configuration of the three dies used for hot drawing of 155 mm M107 shell

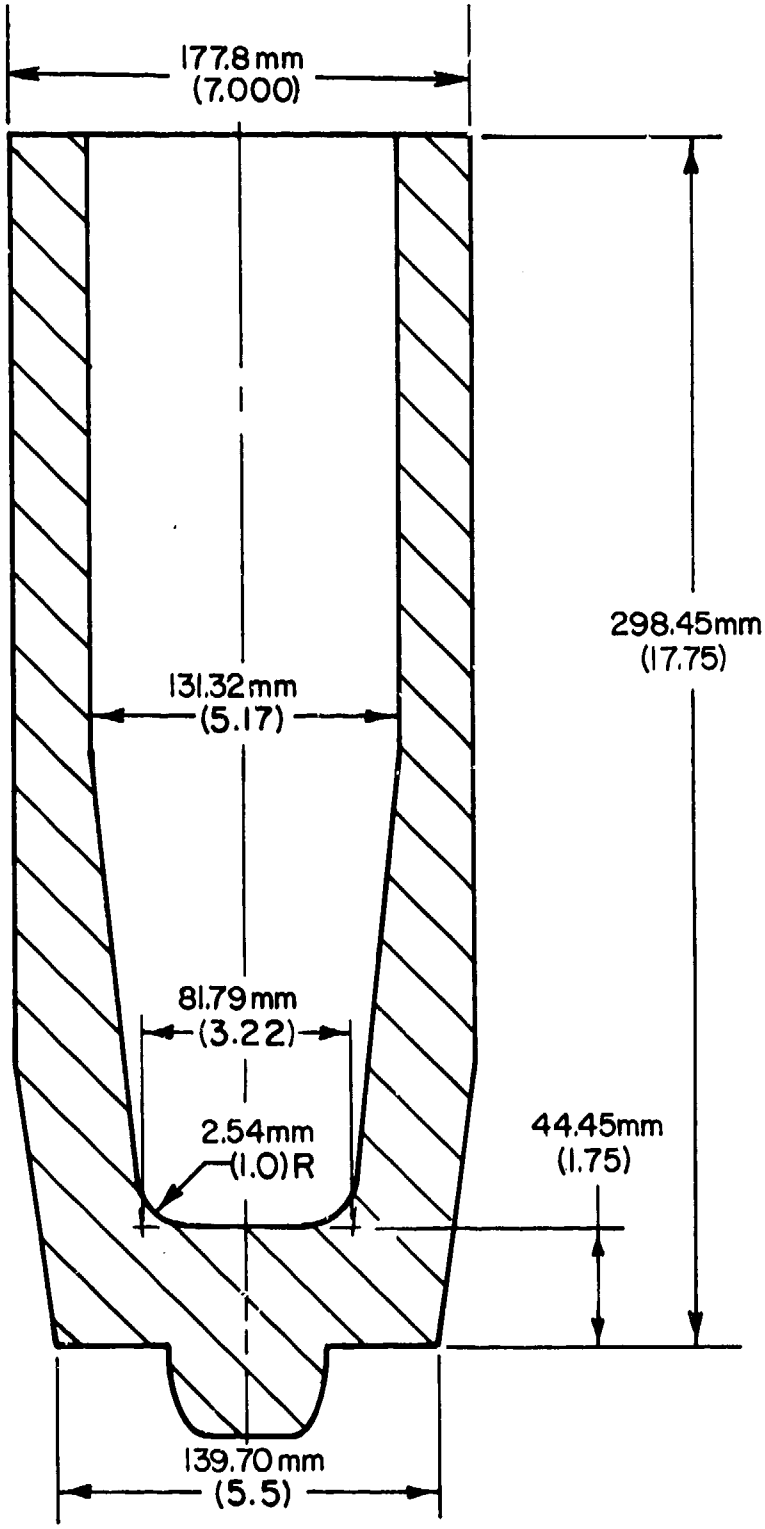

Figure 16(a). Body of 155 mm M107 shell prior to hot drawing.

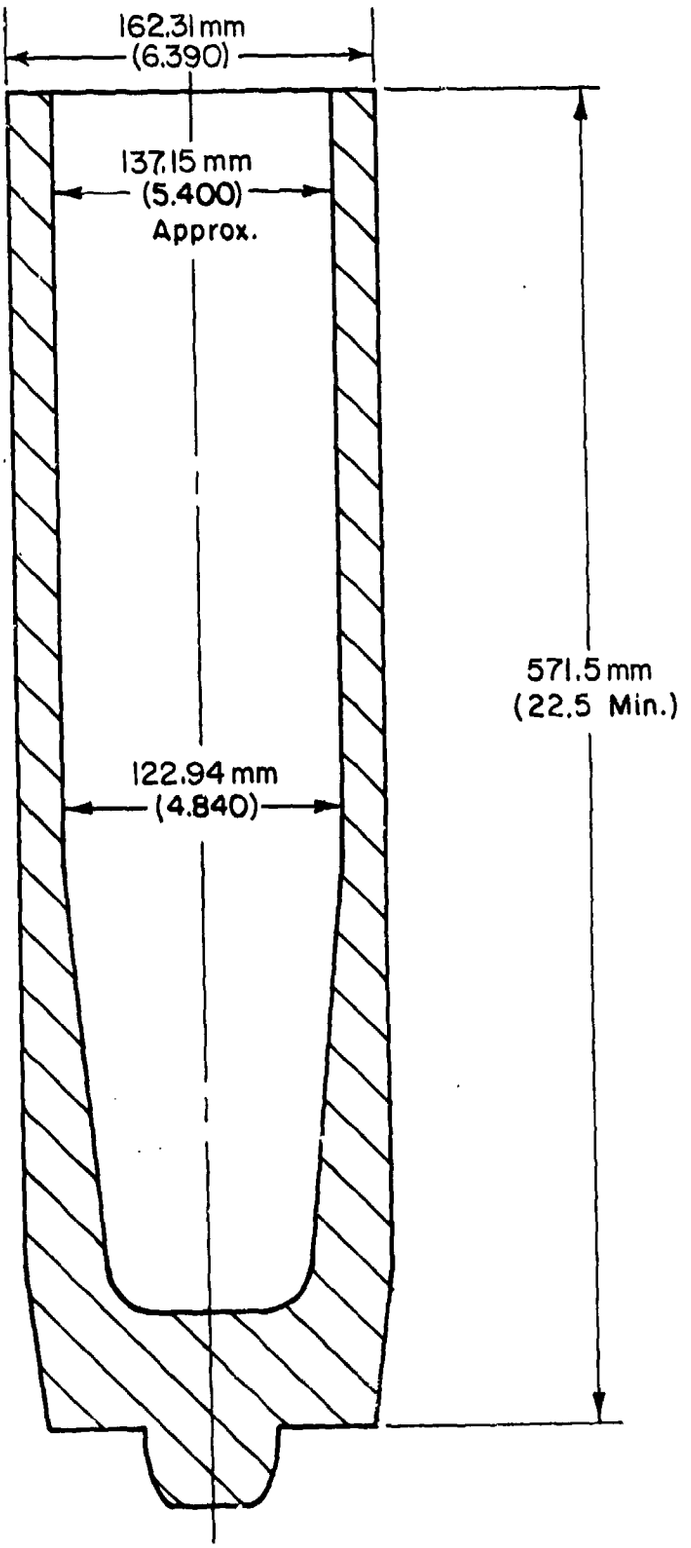

Figure 16(b). Body of 155 mm M107 shell after the hot drawing.

Figure 17. 155 mm M107 projectile bodies before and after hot drawing.

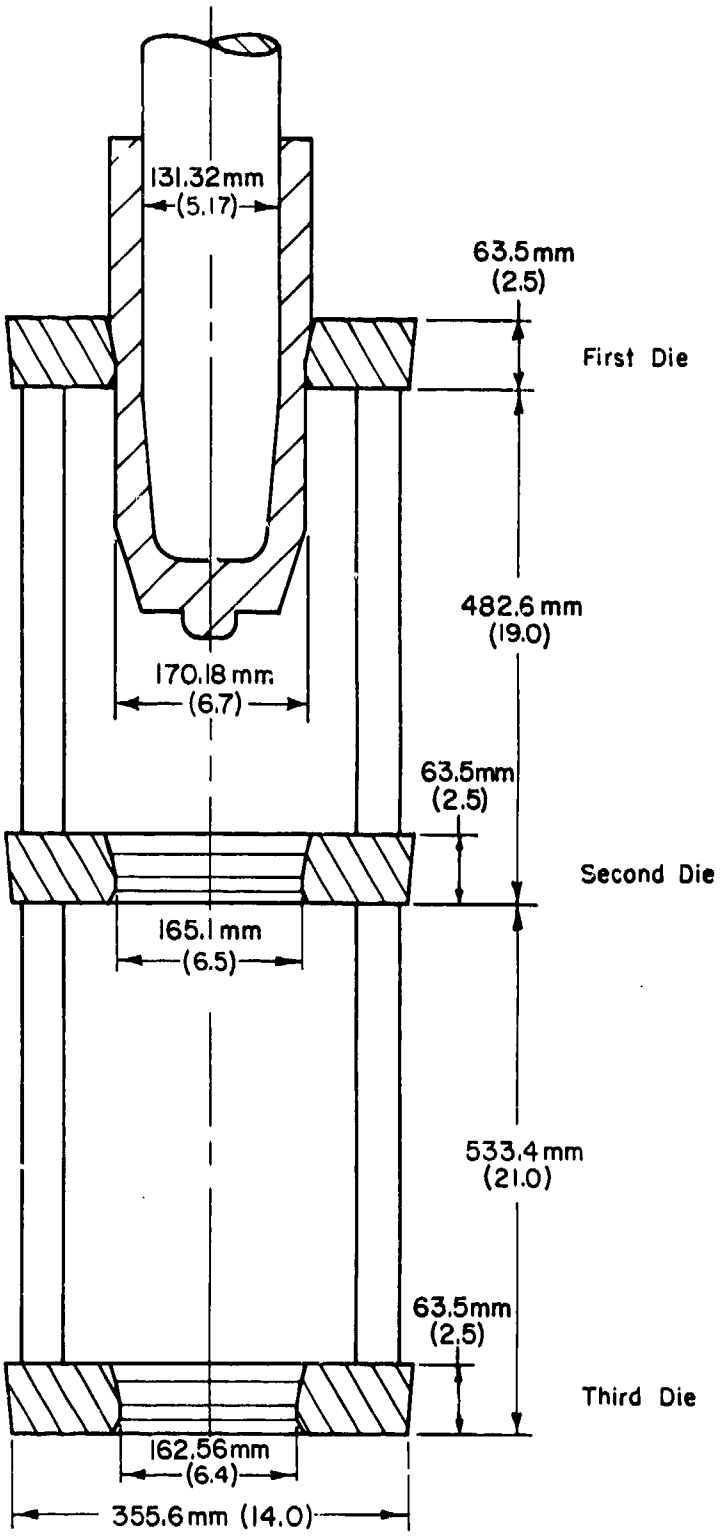

Figure 18. Schematic representation of hot drawing of 155 mm M107 shell under actual production.

under actual production is shown in figure 19. Incoming material first touches the dies on a 10-degree segment at the die entrance. The 12-degree segment on the die entrance is primarily for easy centering of the workpiece in the top die. These die blocks are machined from shell die steel (H-11) hardened to R_C 40-44, and bore diameter of the dies is machined 6.35 mm (0.25 inch) oversize to allow for hard facing by overlay welding. The die bore is first soft-welded with 6.35-mm (0.25-inch) electrodes of Lincoln LH-70 (mild steel), and then finish-welded using the electrodes from the hardfacing alloy. After the dies are cooled, the bore is finish-machined on a copier lathe using appropriate templates.

All the dies for hot drawing tests were fabricated and machined by Chamberlain Corporation's Scranton division. One set of conventional conical dies, identical to those used currently in production, and another set of streamlined dies, as shown in figure 20, were designed using the computer program CDVEL (ref. 1). Templates required for copy-turning of the die bore were numerically control (NC) machined at Battelle and supplied to Chamberlain. The details of design and machining of templates for streamlined dies used in this program are included in appendix C.

The punch configuration is somewhat complex and proprietary data of Chamberlain. However, the punch profile is similar to the inner configuration of the product, shown in figure 16(b). The punch is machined from hot-worked tool steel. It has an internal bore of approximately 63.5-mm (2.5-inch) diameter for continuous internal cooling by water. At the end of each stroke, the punch surface becomes quite hot and shows some red color; however, the color disappears rapidly as the punch cools. In addition, the punch is dipped in a thick oil prior to the next stroke (the press is equipped with two shuttle punches), which helps to cool the external surface, and the burnt residue acts as a parting agent between the punch and the billet material during stripping.

Drawing dies have considerable life (approximately 25,000 to 50,000 pieces). However, the punch must be replaced after approximately 1000 to 2000 shells are drawn.

First Die "A" = 170.18 mm (6.700 in.)
Second Die "A" = 165.10 mm (6.500 in.)
Third Die "A" = 162.56 mm (6.400 in.)

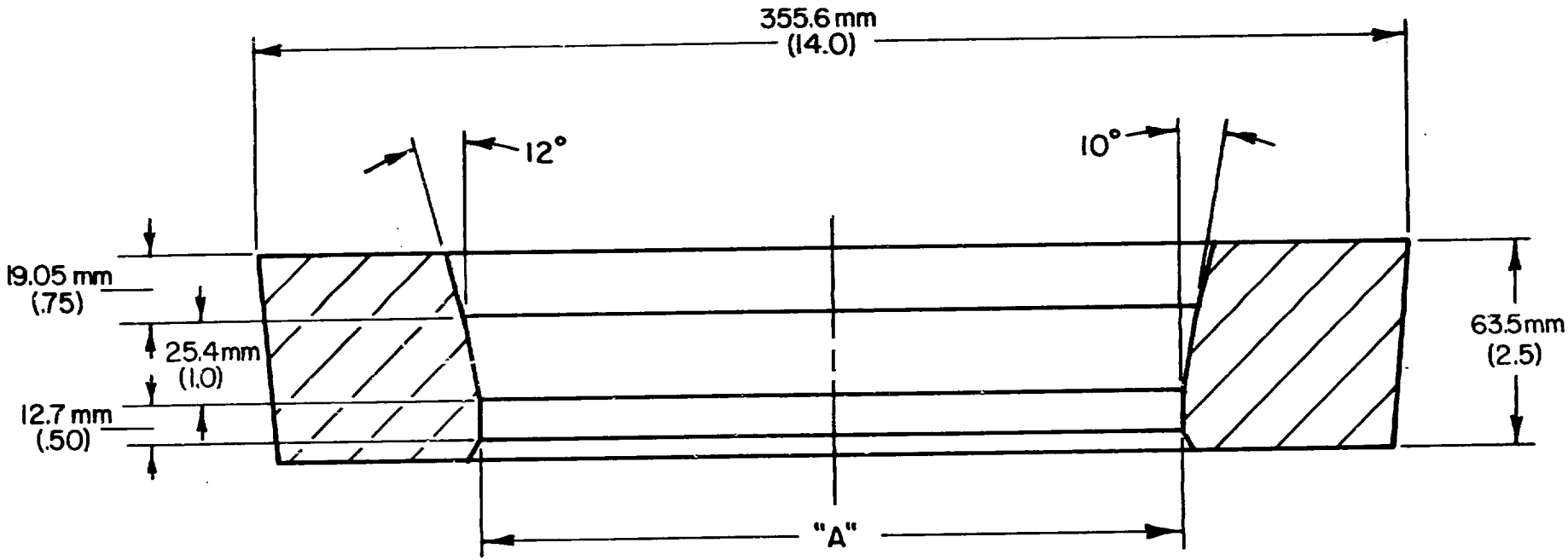

Figure 19. Conventional conical dies for hot drawing of 155 mm M107 shell.

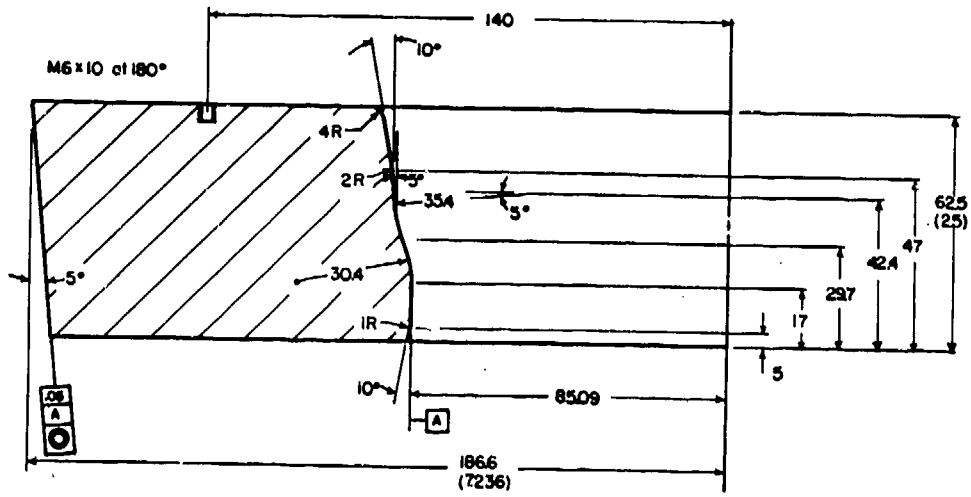

(a) First Die

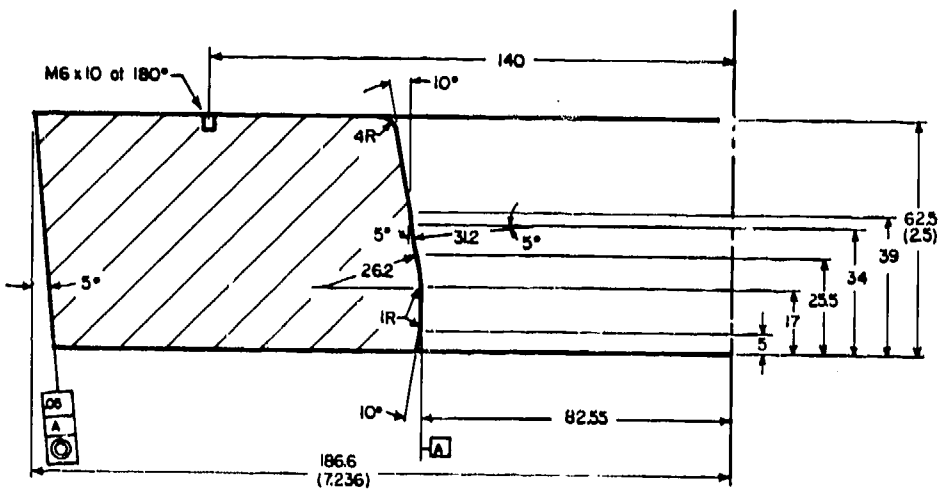

(b) Second Die

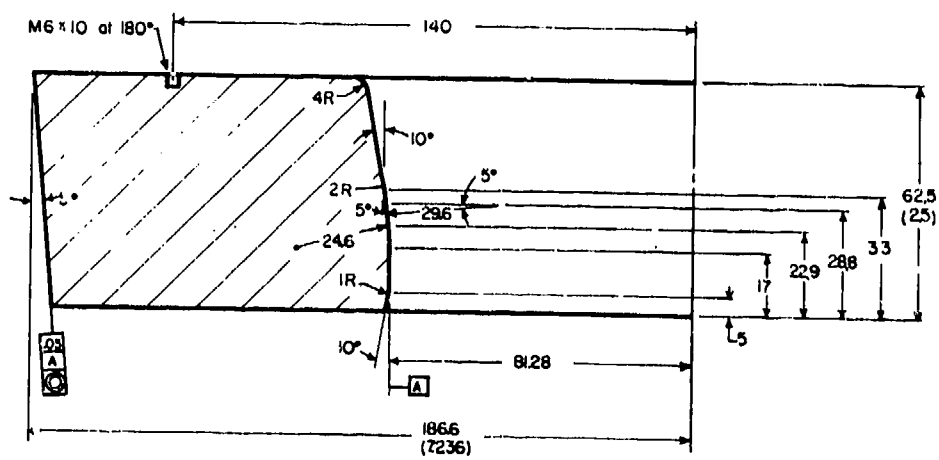

(c) Third Die

All dimensions in mm. (Dimensions in parentheses are in inches.)

Figure 20. Streamlined dies for hot drawing of 155 mm 1107 shell.

Tests with Conventional Conical Dies

The hot drawing tests with the conventional conical dies were performed during a production run on April 10, 1979 at Chamberlain's Scranton, Pennsylvania plant. Dies were replaced with a new set of conical dies during the night shift of April 9, 1979. But the drawing punch was not changed and no record of its change was kept. Prior to the beginning of the first shift on the day of the testing, the dies were flame heated as usual and the press was instrumented to record ram pressure and ram displacement on a two-channel strip recorder.

Drawing of shells was monitored from the beginning of the first shift at 7:00 a.m. Temperature of the incoming preform was measured with an optical pyrometer and the ram pressure and ram displacement was recorded on the strip chart. The first few shells were drawn with manual operation of the press and required higher load. Afterwards, the press was set on automatic mode to produce 180 shells per hour. After a few minutes, the process stabilized and the recorded loads were somewhat more consistent. Beginning at 7:45 a.m., the temperature of the incoming preform, the ram pressure and ram displacement were recorded at an interval of 15 minutes until lunch break at 11:15 a.m. During this production, two preforms were taken out of the production line to measure pertinent dimensions, as shown in figure 21. In addition, the first eleven shells were marked as they came out of the drawing press. After cooling, when these shells reached the inspection table, they were set aside and all important dimensions were measured, as shown in table 5. One preform and one shell were saved for preparing specimens for measuring mechanical properties.

Hot drawing tests were continued in the afternoon of April 10, 1979 and the preform temperature, ram pressure and ram displacement were recorded every 15 minutes, as during the morning session, until a total of twenty readings were taken. A typical ram pressure and ram displacement recording is shown in figure 22. Prior to beginning of the drawing operation, the press builds up pressure behind the ram as it moves downward (Zone I, figure 22). Then the preform goes through the first die. As it totally emerges from the first die, it enters the second die where the peak load is typically developed. Similarly, when the product emerges from the second die, it is picked up by the third die. As the product exits from the third die, ram pressure drops. But the ram still moves downward under nearly constant pressure (Zone II in figure 22) until the bottom dead center is reached, and when the pressure

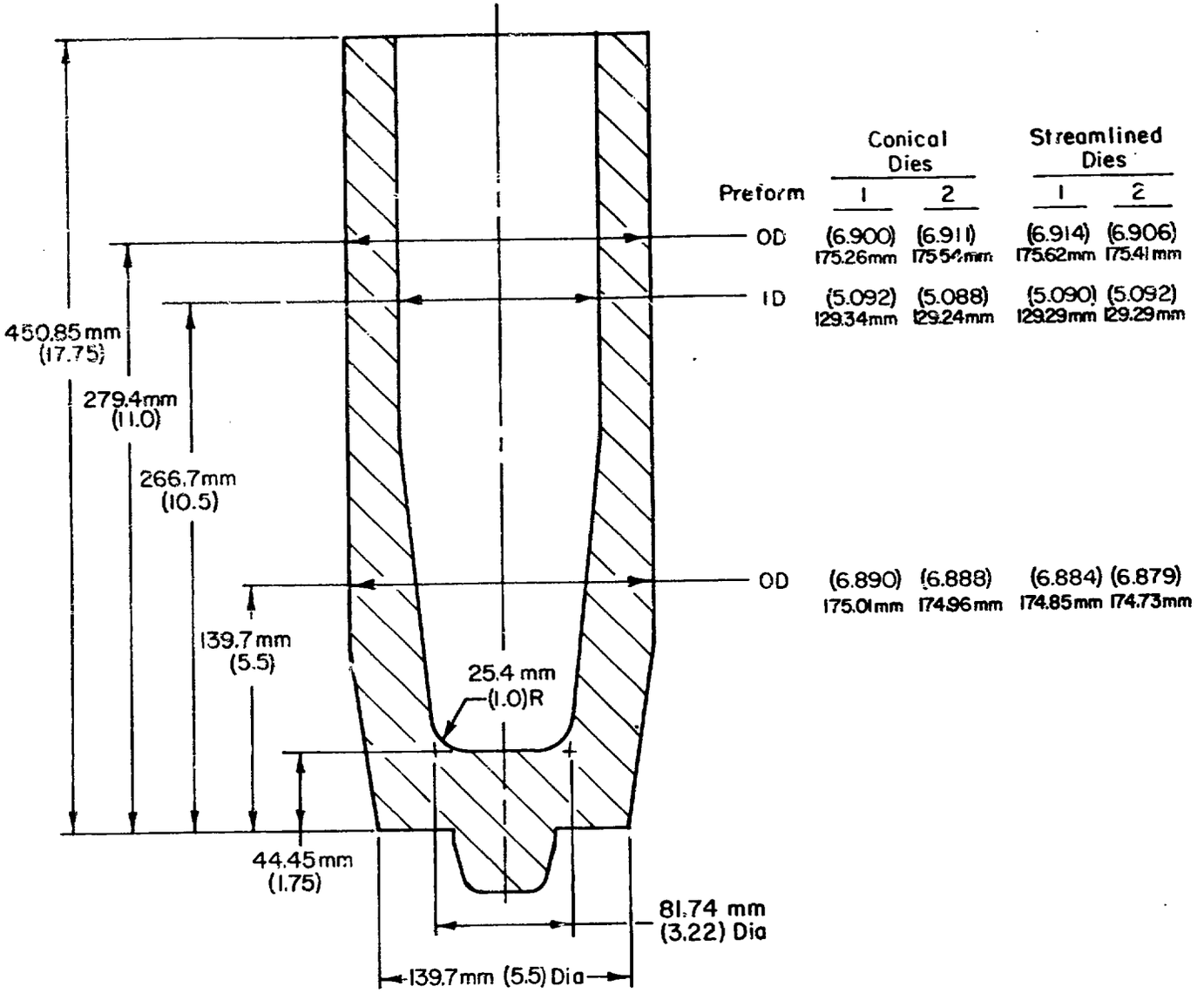

Figure 21. Dimensions of preforms for hot drawing of M107 shell.

Table 5. Pertinent dimension of shells hot drawn through conventional conical dies.

Shell No.	ID at 266.7 mm (10.500 in.) From Cavity Bottom, mm (inch)	ID at 514.4 mm (20.250 in.) From Cavity Bottom, mm (inch)	OD at 50.8 mm (2 in.) Boat Trail, mm (inch)	OD at Mid Length, mm (inch)	OD at Cut-off Length, mm (inch)	Base Thickness Over Nominal 44.5 mm (1.750 in.), mm (inch)		Cavity Length Over Nominal 571.5 mm (22.5 in.), mm (inch)	
N-1	122.94 (4.840)	137.11 (5.398)	159.77 (6.290)	160.02 (6.300)	160.53 (6.320)	Max	(Max)	+50.8	(+2)
N-2	122.94 (4.840)	137.11 (5.395)	159.77 (6.290)	160.02 (6.300)	160.40 (6.315)	Max	(Max)	+38.1	(+1.5)
N-3	122.80 (4.835)	137.11 (5.398)	159.77 (6.290)	160.02 (6.300)	160.27 (6.310)	Max	(Max)	+50.8	(+2)
N-4	123.06 (4.845)	137.41 (5.410)	160.02 (6.300)	160.53 (6.320)	160.78 (6.330)	Mean	(Mean)	+50.8	(+2)
N-5	122.94 (4.840)	137.16 (5.400)	160.27 (6.310)	160.02 (6.300)	160.78 (6.330)	Mean/Max	(Mean/Max)	+76.2	(+3)
N-6	122.94 (4.840)	137.29 (5.405)	160.02 (6.300)	160.02 (6.300)	160.78 (6.330)	Max	(Max)	+76.2	(+3)
N-7	123.06 (4.845)	137.24 (5.403)	160.02 (6.300)	160.27 (6.310)	160.66 (6.325)	Max	(Max)	+50.8	(+2)
N-8	122.94 (4.840)	137.16 (5.400)	160.02 (6.300)	160.02 (6.300)	160.40 (6.315)	Mean	(Mean)	+76.2	(+3)
N-9	122.94 (4.840)	137.16 (5.400)	160.02 (6.300)	160.27 (6.310)	160.53 (6.320)	Mean	(Mean)	+76.2	(+3)
N-10	122.94 (4.840)	137.29 (5.405)	160.02 (6.300)	160.02 (6.300)	160.53 (6.320)	+1.59	(+1/16)	+63.5	(+2.5)
N-11	122.68 (4.830)	137.10 (5.400)	160.53 (6.320)	160.53 (6.320)	160.78 (6.330)	+1.59	(+1/16)	+63.5	(+2.5)

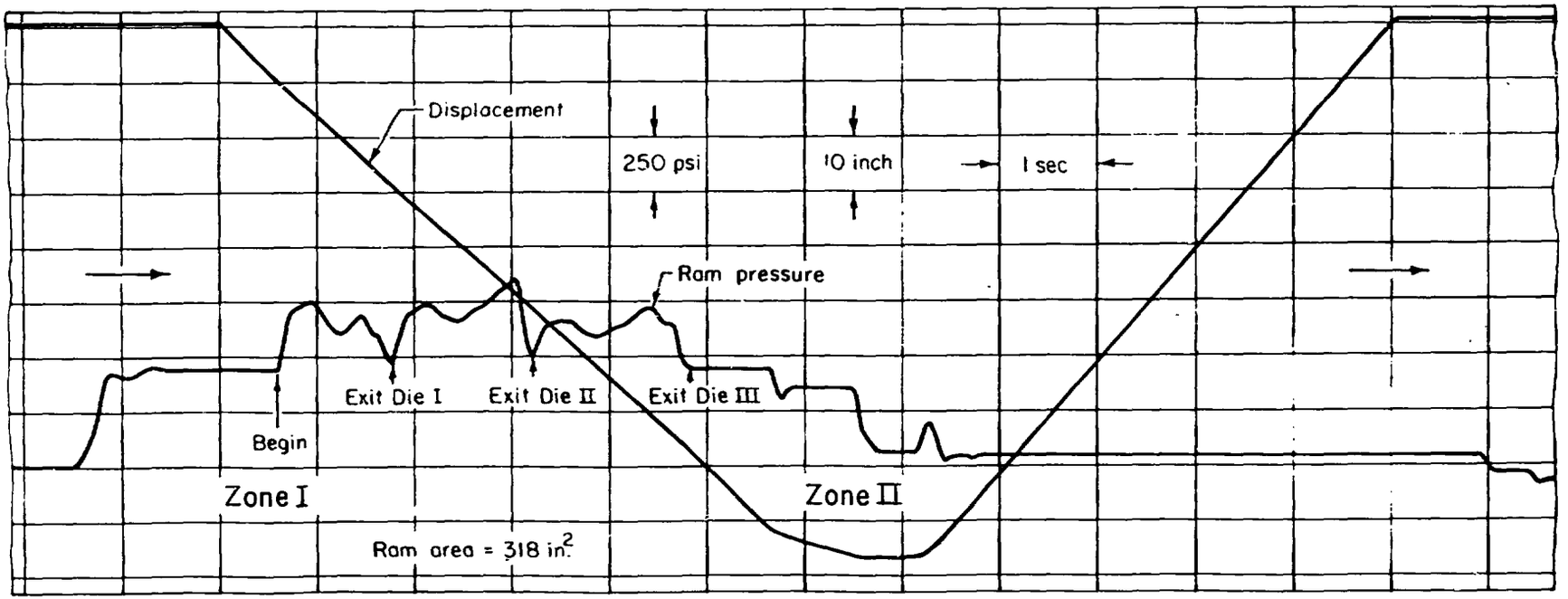

Figure 22. A typical ram pressure and ram displacement recording during hot drawing of M107 shell through conventional conical dies. (1 inch = 25.4 mm; 1 psi = 6.895 kN/m^2)

drops to nearly zero and the ram slows down. Table 6 shows preform temperatures and the peak ram loads through the first, second, and the third die for the twenty shells monitored during these trials. Preform temperature varied between 1027°C (1880°F) and 1068°C (1955°F). Peak ram load varied between 1.11 MN (125 tons) to 1.24 MN (139 tons).

Tests with Streamlined Dies

Following the tests with conventional conical dies, hot drawing tests with streamlined dies were conducted during a production run on April 11, 1979 at Chamberlain's Scranton, Pennsylvania plant. Again, the dies were changed during the night shift of April 10, 1979 and streamlined dies, designed by the computer program CDVEL, were installed. The punch, however, was not changed. On April 11, 1979, prior to the beginning of the morning shift, the press was instrumented to record ram pressure and ram displacement, and the dies were flame heated as usual.

Drawing of shell was monitored from the beginning of the first shift at 7:00 a.m. Again, the first few shells were drawn by operating the press manually, and when everything seemed normal, the press was set on automatic mode. Right from the beginning, the streamlined dies produced good parts, meeting all hot inspection requirements. As in the case of conventional conical dies, the temperature, ram pressure, and ram displacement were recorded every 15 minutes during the morning; and two preforms were taken out for measuring pertinent dimensions, as shown in figure 21. Also the first ten shells were marked after they were drawn, and all important measurements were made after they cooled, as shown in table 7. One preform and one drawn shell were retained for mechanical testing.

Production through the streamlined dies was monitored for about 6 hours, and a total of nineteen recordings were made. These dies consistently produced good products throughout this period. Typical ram pressure and ram displacement recordings for drawing through these dies, shown in figure 23, are very similar to those through the conical dies. Required peak loads for these dies, given in table 8, were slightly lower than those for conventional conical dies, given in table 6. However, the measured loads were more consistent with these dies compared to the conical dies, and the peak load typically varied within ±35.6 kN (±4 ton). In addition, the whole operation appeared somewhat smoother than drawing through conical dies. This observation was verified by plant personnel at Chamberlain.

Table 6. Data for hot drawn 155 mm M107 shells using conventional drawing.

Date	Sample No.	Time[1], hr	Preform Temp[2] °C (°F)	Mandrel[3] No.	Peak Draw Load, MN (tons) Die I	Die II	Die III	Remarks
4-10-79	N-1	7:45 am[1]	1060 (1940)	-	1.079 (121.28)	1.143 (128.43)	0.944 (106.17)	Line stopped 7:52 to 7:54, problems at mechanical press.
	N-2	8:00	1043 (1910)	-	1.075 (120.88)	1.189 (133.60)	0.973 (109.35)	
	N-3	8:15	1043 (1910)	2	1.100 (123.66)	1.196 (134.40)	0.990 (111.34)	Line stopped from 8:20 to 8:22; problem at mechanical press.
	N-4	8:30	949 (1740)	1	1.196 (134.40)	1.167 (131.22)	0.955 (107.36)	Considerable scale on preform, reading probably low. Line stopped 3 times between 8:30 and 9:00 for total of 9 minutes. (8:35-8:40; 8:40-8:41; 8:42-8:47)
	N-5	9:00	1038 (1900)	2	1.061 (119.29)	1.192 (134.00)	0.983 (110.54)	
	N-6	9:15	1032 (1890)	2	1.079 (121.28)	1.203 (135.19)	1.005 (112.93)	
	N-7	9:17	1027 (1880)	1	1.104 (124.06)	1.192 (134.00)	0.990 (111.34)	Line stopped at 9:20 to change #1 mandrel; Down 9:54 to 9:56.
	N-8	10:00	1066 (1950)	1	1.061 (119.29)	1.167 (131.22)	0.955 (107.36)	
	N-9	10:15	1060 (1940)	2	1.026 (115.31)	1.167 (131.22)	0.955 (107.36)	
	N-10	10:30	1068 (1955)	1	1.047 (117.70)	1.167 (131.22)	0.955 (107.36)	
	N-11	10:45	1060 (1940)	2	1.075 (120.88)	1.192 (134.40)	0.990 (111.34)	
	N-12	11:00	1054 (1930)	2	1.026 (115.31)	1.167 (131.22)	0.962 (108.15)	
	N-13	11:15	1060 (1940)	1	0.998 (112.13)	1.132 (127.24)	0.920 (103.38)	Line stopped at 11:20 to lubricate equip. at mech. press; 11:30 lunch.
	N-14	1:30 pm	1054 (1930)	1	1.040 (116.90)	1.132 (127.24)	0.983 (110.54)	
	N-15	1:45	1038 (1900)	2	1.061 (119.29)	1.167 (131.22)	0.983 (110.54)	1:52 break time.
	N-16	2:15	1066 (1950)	1	1.047 (117.70)	1.160 (130.42)	0.937 (105.37)	
	N-17	2:30	1066 (1950)	2	1.026 (115.31)	1.114 (125.25)	0.990 (111.34)	
	N-18	2:45	1066 (1950)	1	1.061 (119.29)	1.203 (135.19)	0.998 (112.13)	
	N-19	3:00	1060 (1940)	2	1.044 (117.30)	1.153 (129.63)	0.998 (112.93)	
	N-20	3:15	1043 (1910)	1	1.082 (121.67)	1.238 (139.17)	1.019 (114.52)	

(1) Production started at 7:10 a.m. with new conventional dies preheated to 149°C (300°F).
(2) Temperature readings obtained on the preform just prior to draw.
(3) Mandrel #1 is "yard side" or left/#2 is "shop side" or right side of press. These mandrels were both installed in the press at noon April 9, 1979, and have been used for 1-1/2 shifts of production prior to start-up today.

Table 7. Dimensions of shells hot drawn through streamlined dies.

Shell No.	ID at 266.7 mm (10.500 in.) From Cavity Bottom, mm (inch)	ID at 514.4 mm (20.250 in.) From Cavity Bottom, mm (inch)	OD at 50.8 mm (2 in.) Boat Trail, mm (inch)	OD at Mid Length, mm (inch)	OD at Cut-off Length, mm (inch)	Base Thickness Over Nominal 44.5 mm (1.750 in.), mm (inch)		Cavity Length Over Nominal 571.5 mm (22.5 in.), mm (inch)	
E-1	123.06 (4.845)	137.08 (5.397)	159.89 (6.295)	160.02 (6.300)	160.27 (6.310)	+3.18	(+1/8)	+38.1	(+1.5)
E-2	123.14 (4.848)	137.03 (5.395)	160.02 (6.300)	160.27 (6.310)	160.53 (6.320)	+1.59	(+1/16)	+38.1	(+1.5)
E-3	123.06 (4.845)	137.29 (5.405)	160.02 (6.300)	160.15 (6.305)	160.40 (6.315)	+3.18	(+1/8)	Min.	(Min.)
E-4	122.94 (4.840)	137.14 (5.400)	159.77 (6.290)	160.02 (6.300)	160.27 (6.310)	+3.18	(+1/8)	+63.5	(+2.5)
E-5	123.06 (4.845)	137.14 (5.400)	159.89 (6.295)	160.27 (6.310)	160.53 (6.320)	+1.59	(+1/16)	+63.5	(+2.5)
E-6	122.81 (4.835)	137.14 (5.400)	160.02 (6.300)	160.27 (6.310)	160.53 (6.320)	+1.59	(+1/16)	+76.2	(+3.0)
E-7	123.06 (4.845)	137.14 (5.400)	160.02 (6.300)	160.15 (6.305)	160.53 (6.320)	+1.59	(+1/16)	+63.5	(+2.5)
E-8	123.06 (4.845)	137.14 (5.400)	160.02 (6.300)	160.40 (6.315)	160.66 (6.325)	+1.59	(+1/16)	+88.9	(3.5)
E-9	123.01 (4.843)	137.14 (5.400)	160.02 (6.300)	160.15 (6.305)	160.53 (6.320)	+1.59	(+1/16)	+76.2	(+3.0)
E-10	123.14 (4.828)	137.11 (5.398)	160.02 (6.300)	160.27 (6.310)	160.66 (6.325)	+1.59	(+1/16)	+50.8	(+2.0)

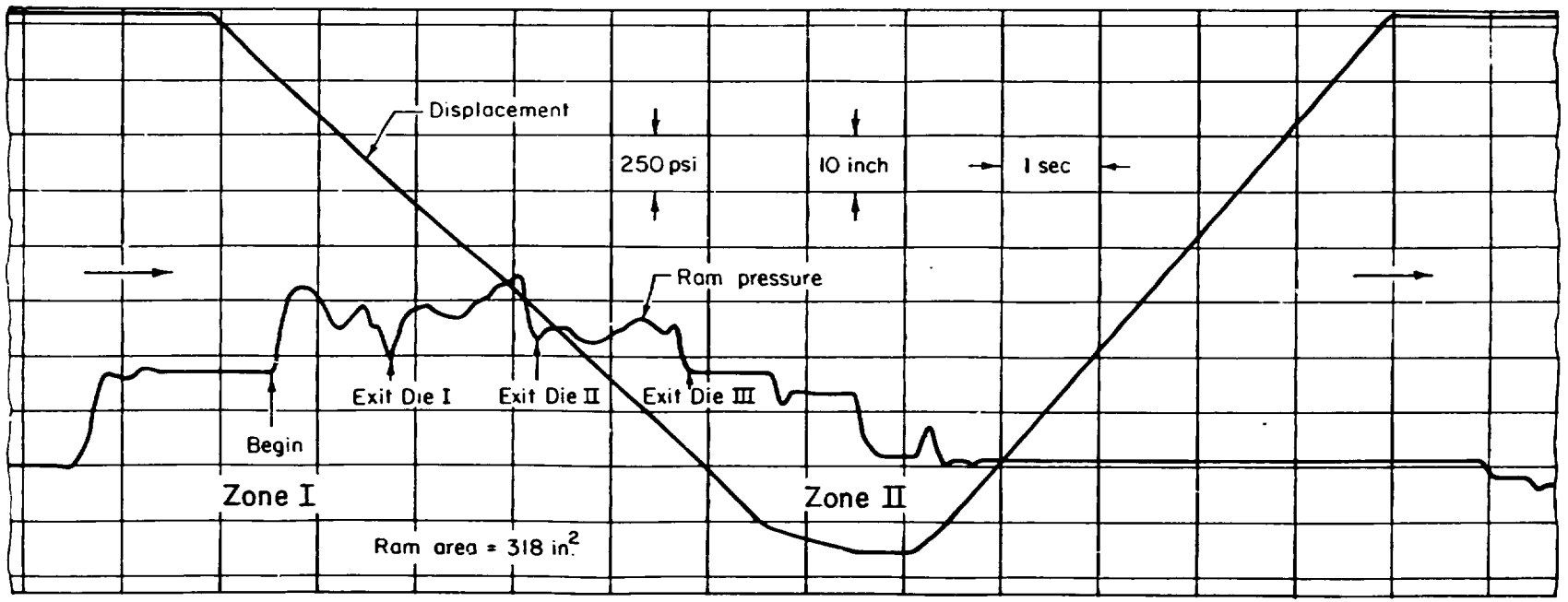

Figure 23. A typical ram pressure and ram displacement recording during hot drawing of M107 shell through streamlined dies. (1 inch = 25.4 mm, 1 psi = 6.895 kN/m^2)

Table 8. Data for hot drawn 155 mm M107 shells using streamlined dies.

Date	Sample No.	Time, hr.	Preform Temp. °C (°F)	Mandrel No.	Peak Draw Load, MN (tons) Die I	Die II	Die III	Remarks
6-11-79	E-1	7:15 am	1077 (1970)	1	1.054 (118.49)	1.167 (131.22)	0.952 (106.96)	
	E-2	7:30	1066 (1950)	2	1.121 (126.05)	1.220 (137.18)	0.959 (107.76)	Line down from 7:36-7:39 and 7:40-7:42 am.
	E-3	7:45	1054 (1930)	1	1.097 (123.26)	1.203 (135.19)	0.994 (111.73)	
	E-4	8:00	1054 (1930)	2	1.096 (123.26)	1.167 (131.22)	0.937 (105.37)	
	E-5	8:15	1032 (1890)	1	1.026 (115.31)	1.157 (130.02)	0.913 (102.59)	O.D. surface of preform appears to have less scale than those run before about 8:17 am.(1)
	E-6	8:30	1038 (1900)	2	1.125 (126.44)	1.167 (131.22)	0.920 (103.38)	
	E-7	8:45	1038 (1900)	1	1.114 (125.25)	1.167 (131.22)	0.955 (107.36)	
	E-8	9:00	1049 (1920)	2	1.150 (129.23)	1.167 (131.22)	0.930 (104.58)	
	E-9	9:15	1038 (1900)	1	1.111 (124.85)	1.167 (131.22)	0.923 (103.78)	Hydraulic press stopped to change #2 mandrel. Line down from 9:37 to 9:42 am.
	E-10	9:47	1038 (1900)	2	1.096 (123.26)	1.178 (132.41)	0.920 (103.38)	
	E-11	10:00	1054 (1930)	1	1.072 (120.48)	1.132 (127.24)	0.884 (99.41)	
	E-12	10:15	1043 (1910)	2	1.096 (123.26)	1.167 (131.22)	0.902 (101.39)	
	E-13	10:30	1043 (1910)	1	1.096 (123.26)	1.167 (131.22)	0.937 (105.37)	
	E-14	10:45	1027 (1880)	2	1.132 (127.24)	1.203 (135.19)	0.937 (105.37)	
	E-15	11:00	1027 (1880)	1	1.121 (126.05)	1.203 (135.19)	0.948 (106.56)	
	E-16	11:15	1038 (1900)	2	1.153 (129.63)	1.231 (138.37)	0.952 (106.96)	11:20 lunch
	E-17	1:15 pm	1043 (1910)	1	1.167 (131.22)	1.234 (138.77)	0.990 (111.34)	
	E-18	1:30	1043 (1910)	2	1.146 (128.83)	1.220 (137.18)	0.955 (107.36)	
	E-19	1:45	1041 (1905)	1	1.167 (131.22)	1.220 (137.18)	0.955 (107.36)	Line stopped at 1:54 pm. Major crack in water-cooled portion of piercing punch, required 1-1/2 hr. stop.

(1) Ron Kivac of Chamberlain remarked after these observations that the second shift leaves the furnace loaded with billets for the first shift. This means that for the first 1-1/4 hours of production, the billets had been in the furnace for up to 8 hours instead of the normal 1-1/4 to 1-1/2 hours.

Since the computer-designed streamlined dies produced consistently good parts, the plant personnel at Chamberlain's Scranton plant agreed to keep the dies in production until a replacement was needed. A total of 15,836 shells were drawn before removal of the dies. Engineers at Scranton state that the number is half of the normal production run on a set of dies. These dies were removed because of excessively deep draw marks, which is the normal criterion for die removal. Engineers at Scranton state that this short life may not be attributable to the streamlined dies alone, as it has happened before occasionally.

EVALUATION OF MATHEMATICAL MODELS

Under this section, the predictions from the computer program DRAWNG, described earlier, are evaluated with respect to both cold and hot confirmation testings of drawing operations conducted under production or near-production conditions. Evaluations of the mathematical models were conducted for drawing of artillery shells using conventional conical dies and computer-designed streamlined dies. Therefore, it became necessary to characterize the interface friction condition during drawing, and the flow stress of the deforming material. In addition, mechanical properties of the preform and the drawn shell materials were determined for evaluating the streamlined dies versus the conical dies.

Cold Drawing Operations

Flow Stress and Interface Friction

Incerface friction and flow stress are two basic inputs required in the program DRAWNG. Since deformation in shell drawing occurs primarily due to tensile stresses, the material flow stress should be determined under tensile loading. Therefore, a randomly-selected preform was cut and tension specimens of 6.35-mm (0.25-inch) gage diameter were machined. These specimens were tested in an Instron testing machine at a crosshead speed of 0.04 mm/s (0.100 inch/min.). Load versus displacement was recorded at a constant chart speed, and later it was reduced into true stress ($\bar{\sigma}$) versus true strain ($\bar{\varepsilon}$) curve, as shown in figure 24. In order to use this information in the computer program DRAWNG, a least square mean fit to the experimental points was developed as given below:

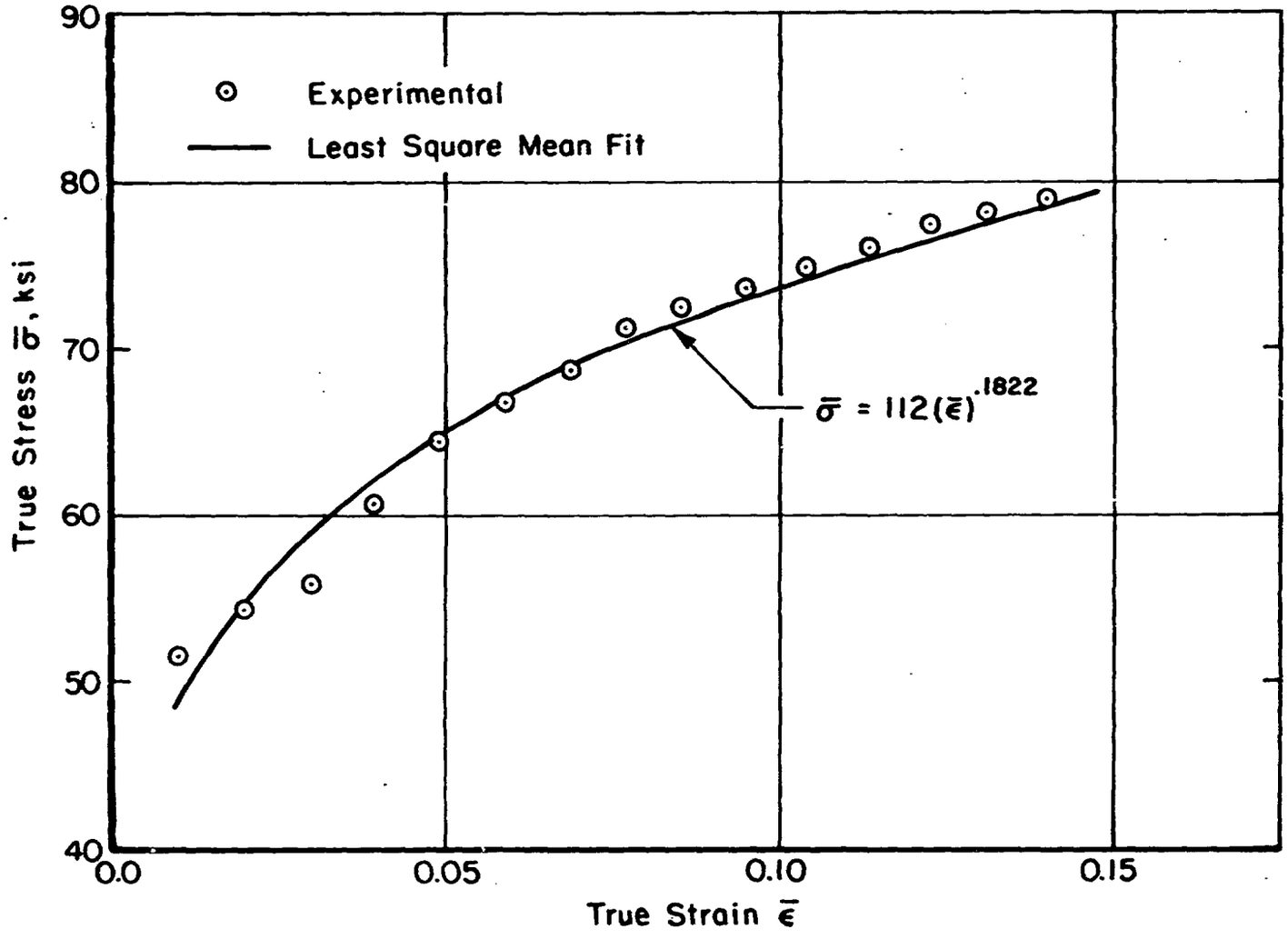

Figure 24. True stress versus true strain for annealed 1030 steel at room temperature. (1 ksi = 6.895 MN/m^2.)

$$\bar{\sigma} = 772\ (\bar{\varepsilon})^{0.1822}\ (MN/m^2). \qquad (1)$$

This equation seems to fit the experimental data well, as shown in figure 24. Therefore, it was also used for determining $\bar{\sigma}$ beyond $\bar{\varepsilon} = 0.15$ by extrapolation.

In the present mathematical modeling studies, the interface friction shear stress is defined by

$$\tau = \frac{m}{\sqrt{3}}\ \bar{\sigma} = f\ \bar{\sigma} \qquad (2)$$

where $f = \sqrt{3}\ m$ is the friction factor and its value could be between 0 and 0.577.

The interface friction shear factor in cold drawing was characterized using the well known ring test (ref. 3). Four rings of 38.1 mm (1.5 in.) OD x 19.05 mm (0.75 in.) ID x 12.7 mm (0.50 in.) height were machined from the preform material. These rings were cleaned, phosphated and lubricated with soap in exactly the same procedure as used for lubrication of preforms prior to cold drawing. The rings were then forged under flat parallel dies in a hydraulic press to 20 and 40 percent reduction in height. Change in bore diameter was plotted on theoretical calibration curves, as shown in figure 25. It is seen that friction shear factor $m \simeq 0.06$ ($f = 0.035$) characterize the interface friction between the dies and the workpiece. This value of interface friction factor was used for predicting the load-stroke curve using the computer program DRAWNG.

Load-Displacement Curves

As described earlier, cold drawing tests were conducted for the final double draw operation of M335 shell using the following arrangements of drawing dies:

(a) Two conventional conical dies in tandem

(b) Two double-curvature streamlined dies in tandem

(c) One double-curvature streamlined die.

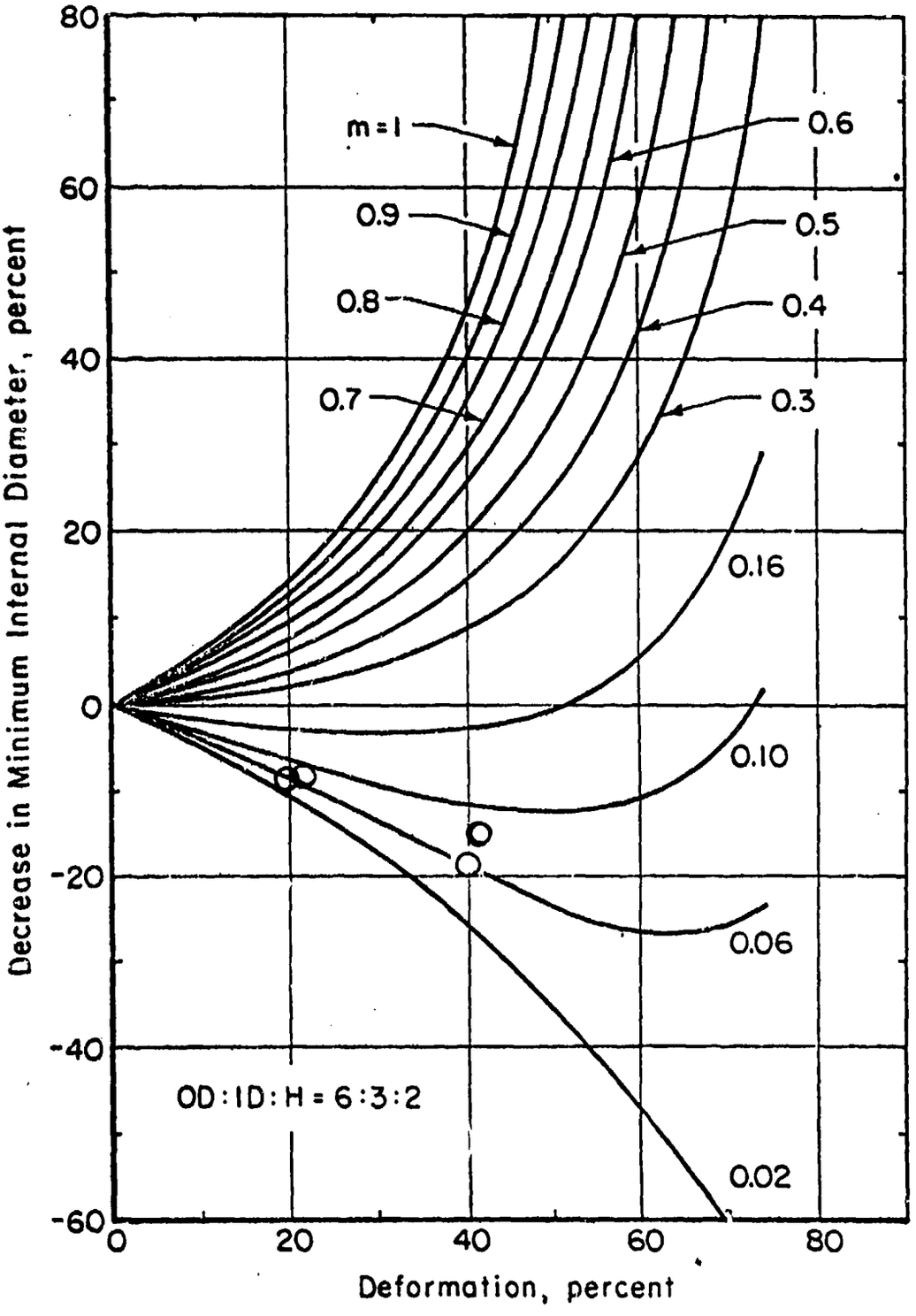

Figure 25. Theoretical calibration curves used for determining friction and experimental points for commercial soap from upsetting a ring with OD:ID:height ratio of 6:3:2.

All pertinent dimensions before and after the drawing operations were measured and the ram pressure and ram displacement were recorded individually with respect to time, as shown in figures 13 and 15. Using a digitizer attached to a PDP-11/40 computer, these curves were digitized and the data were processed on the same computer to generate the experimental load versus displacement curves.

These load-displacement curves, predicted by the computer program DRAWNG for each of the above three die arrangements, were then evaluated. For this purpose three cases were selected corresponding to the maximum, the minimum, and the average peak ram load recorded during each of the tests. For each of these selected cases, the theoretical load-displacement curve was generated using actual dimensions of the preform and the product. Theoretically predicted and experimentally measured load-displacement curves (corresponding to maximum recorded peak load), for drawing through two conical dies in tandem, are compared in figure 26. Overall agreement between predicted and measured curves is very good. Predicted peak loads are somewhat higher, however, the accuracy of prediction is well within the range of acceptable engineering accuracy. The slight mismatch on the displacement axis is primarily due to initial positioning of the preform in the second die, since its forward end is contoured (see figure 8) and does not match the die contour. Similarly, as shown in figures 27 and 28, the experimental load-displacements corresponding to the minimum and the average peak loads are in very good overall agreement with the theoretically predicted curves. Thus, the mathematical models and associated computer programs are capable of reliably simulating cold drawing of shells through conical dies in tandem.

Experimental load-displacement curves, corresponding to the maximum, the minimum and the average peak loads for cold drawing of M335 shell through two streamlined dies (designed by the computer program CDVEL (ref. 1)), are compared with the theoretically predicted load-displacement curves in figures 29 through 31. The mathematical model in these cases predicts higher peak loads compared to measured peak loads. However, overall agreement between predictions and measurements is good for all engineering purposes. In addition, these dies proved to produce good parts, required approximately 13 percent less force and energy, and the breakthrough peak was typically absent compared to the conical dies in a similar tooling arrangement. The fact that streamlined dies are more efficient was further confirmed by measuring the temperature of the

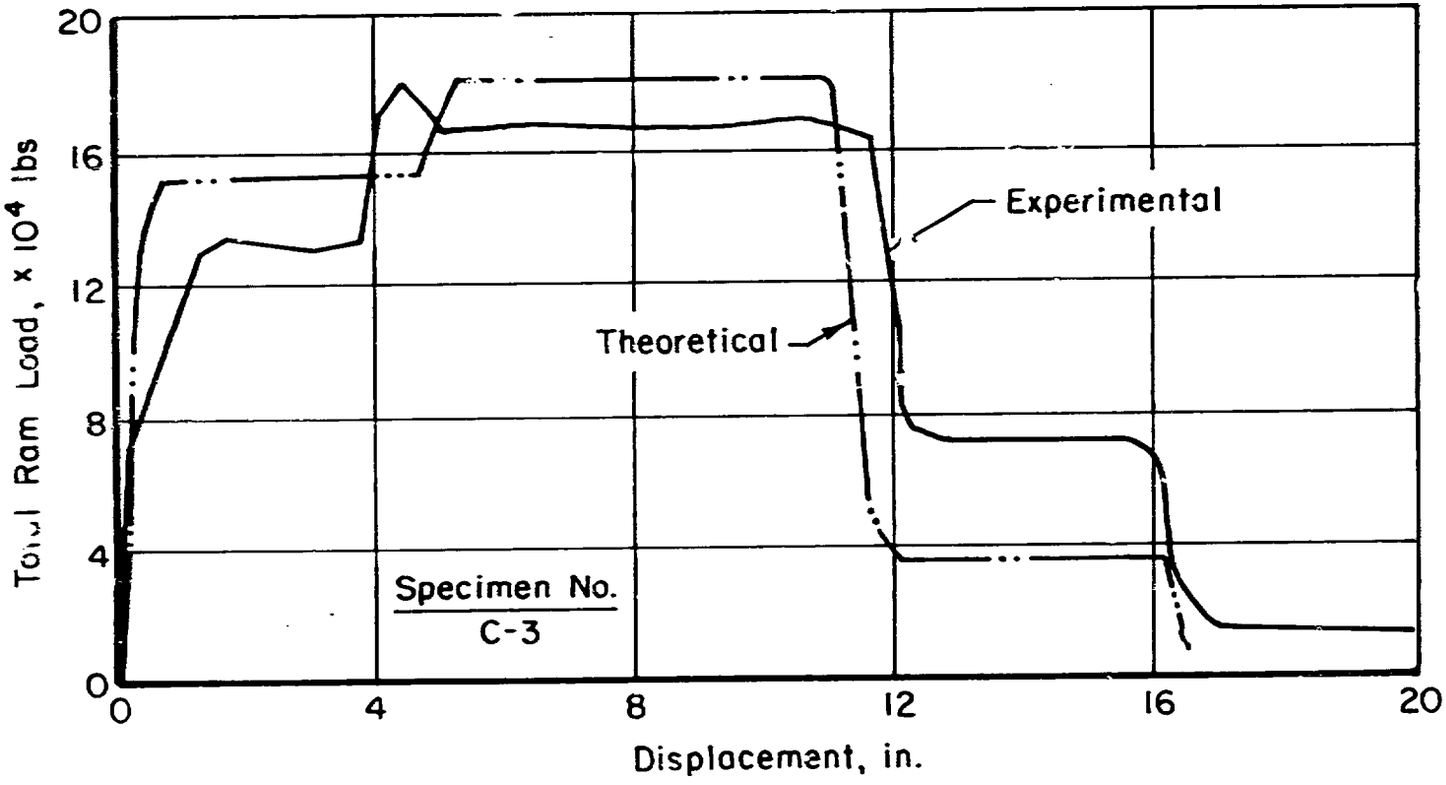

Figure 26. Theoretical and experimental (corresponding to maximum peak load) load-displacement curves for cold drawing of M335 shell through two conical dies in tandem. (1 inch = 25.4 mm, 1 lb = 4.448 N)

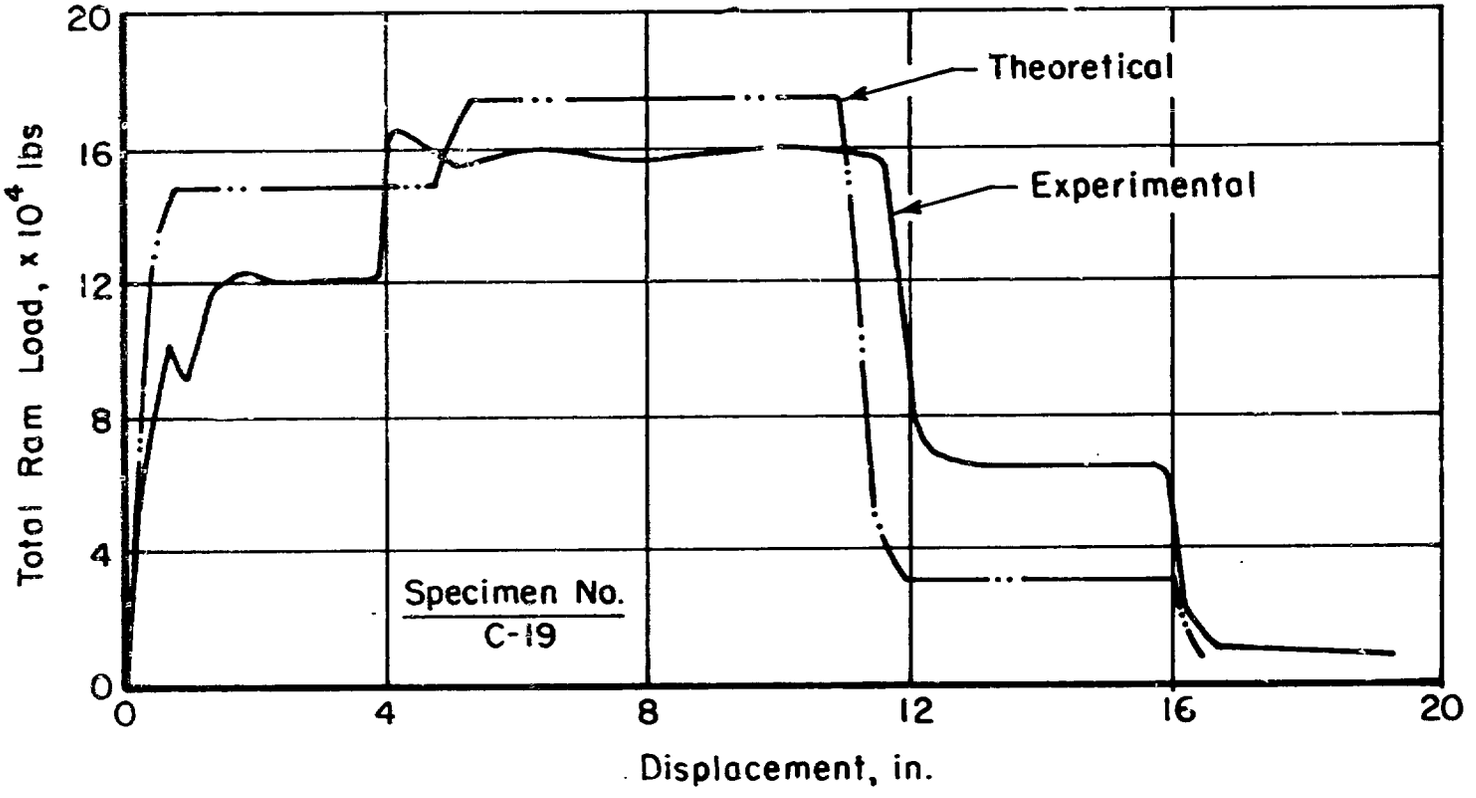

Figure 27. Theoretical and experimental (corresponding to minimum peak load) load-displacement curves for cold drawing of M335 shell through two conical dies in tandem. (1 inch = 25.4 mm, 1 lb = 4.448 N)

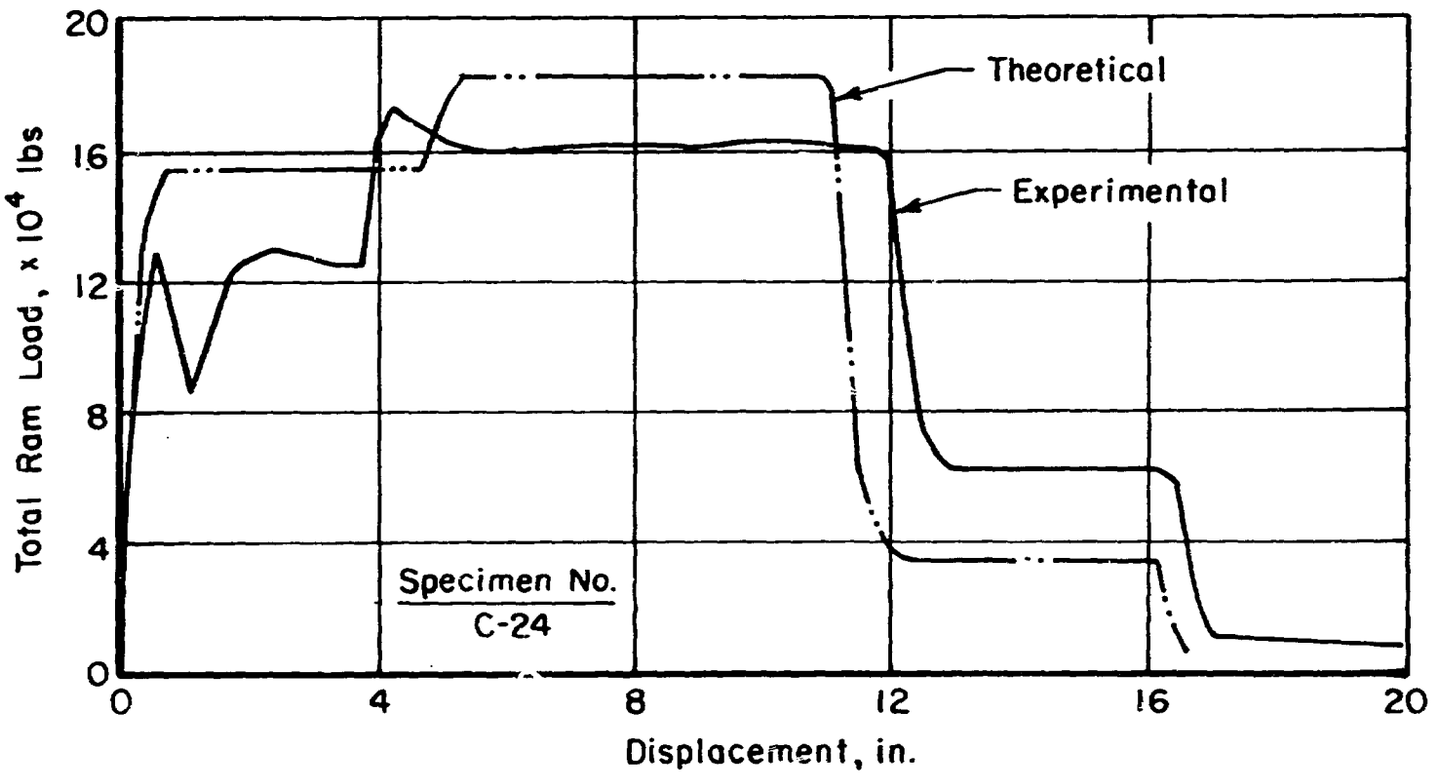

Figure 28. Theoretical and experimental (corresponding to average peak load) load-displacement curves for cold drawing of M335 shell through two conical dies in tandem. (1 inch = 25.4 mm, 1 lb = 4.448 N)

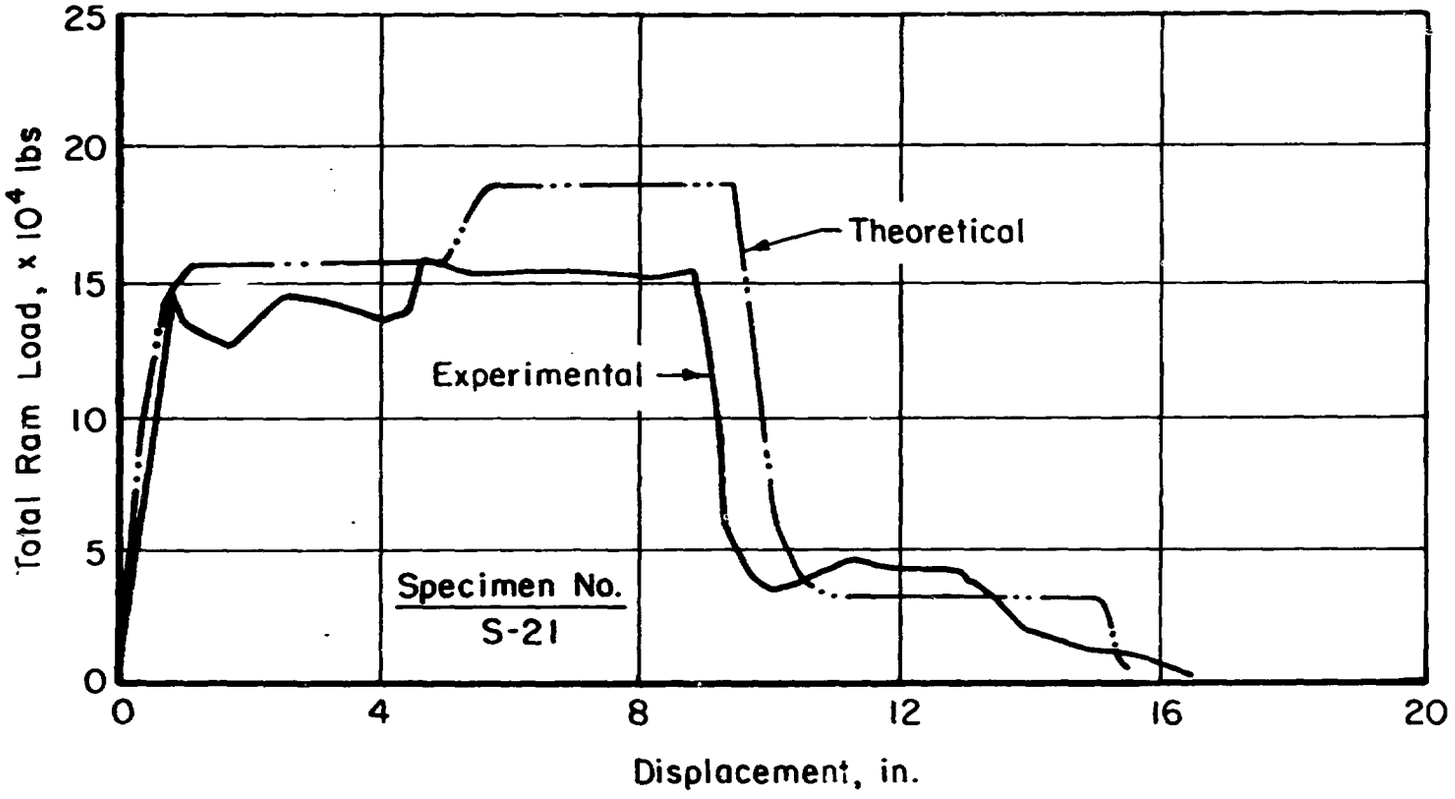

Figure 29. Theoretical and experimental (corresponding to maximum peak load) load-displacement curves for cold drawing of M335 shell through two streamlined dies in tandem. (1 inch = 25.4 mm, 1 lb = 4.448 N)

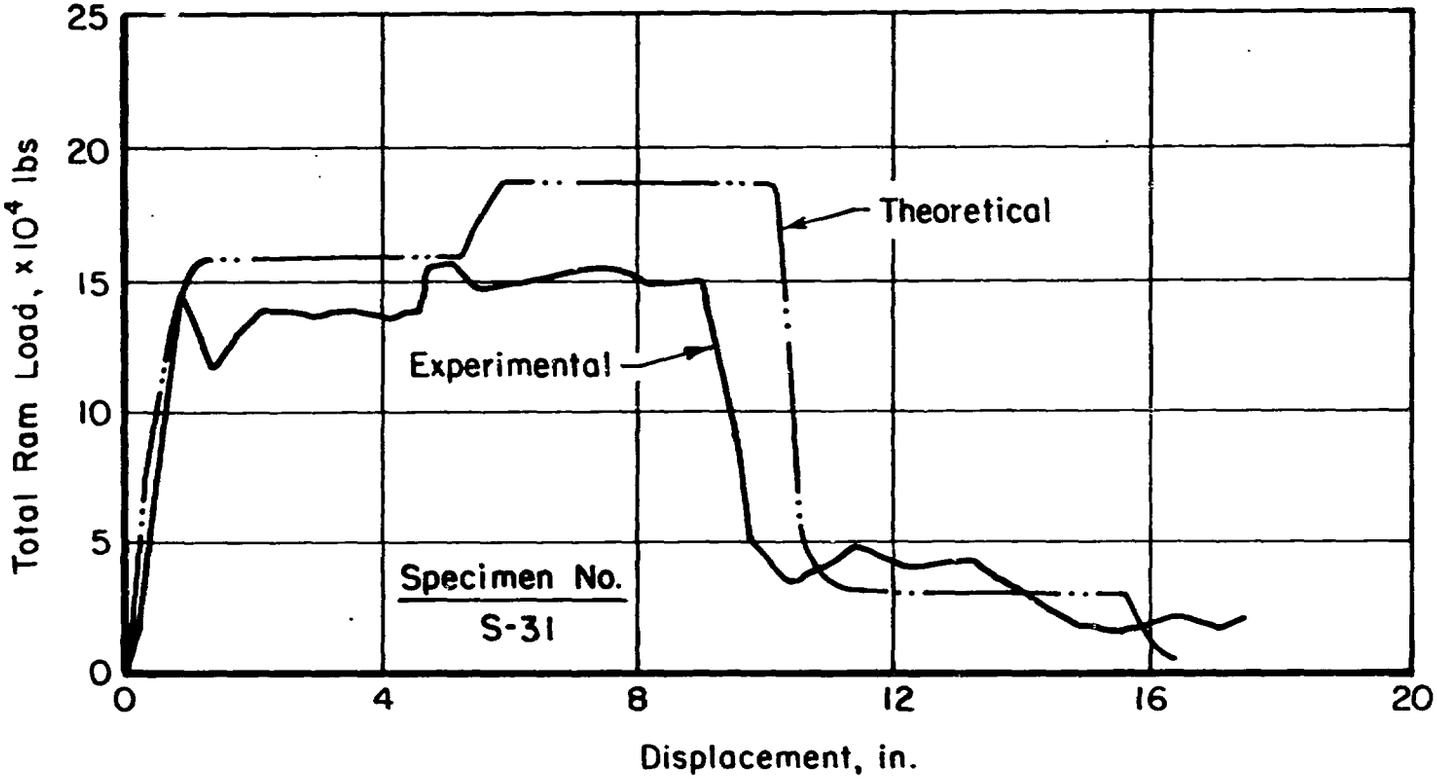

Figure 30. Theoretical and experimental (corresponding to minimum peak load) load-displacement curves for cold drawing of M335 shell through two streamlined dies in tandem. (1 inch = 25.4 mm, 1 lb = 4.448 N)

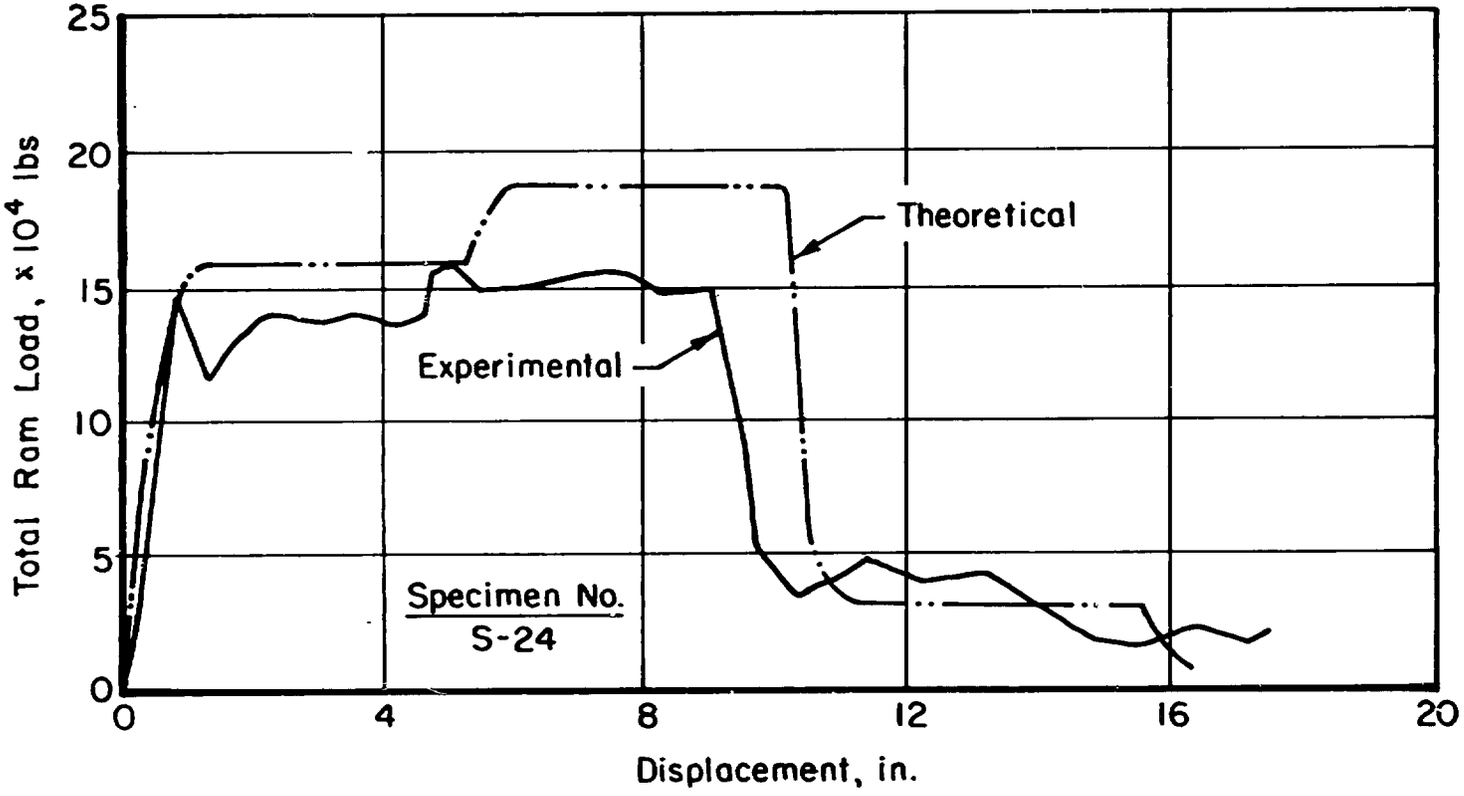

Figure 31. Theoretical and experimental (corresponding to average peak load) load-displacement curves for cold drawing of M335 shell through two streamlined dies in tandem. (1 inch = 25.4 mm, 1 lb = 4.448 N)

product after drawing through conical and streamlined dies. Under steady conditions of the operations, the product temperature was found to be 11° to 14°C (20° to 25°F) lower when drawn through streamlined dies. Thus, the metal flow through streamlined dies seems to be smoother and requires less redundant work compared to conical dies. These observations were in accordance with theoretical predictions regarding the efficiency of streamlined dies.

Since streamlined dies could produce the part with lower forces, it was felt that the deformation in the present double drawing operation could be accomplished with single streamlined die without causing punch through. Therefore, as described earlier, tests were run to produce the required reduction with a single streamlined die. A single streamlined die produced good parts and required less force and energy even compared with two streamlined dies in tandem. Figures 32 through 34 show the comparison between theoretically predicted and experimentally measured (corresponding to the maximum, the minimum and the average peak loads, respectively) load-displacement curves through these dies. Again, the agreement is very good in all three cases.

Thus, computer programs DRAWNG are capable of predicting load-displacement curves for drawing through a single die or through multiple dies in tandem. The accuracy of predictions is very good for practical applications and reliability appears to be excellent.

Prediction of Punch Through

The computer program DRAWNG is capable of predicting the tensile stress in the drawn shell wall with respect to punch displacement. Punch through or wall tear occurs when this stress is larger than the flow stress of the product material. Figures 35 through 37 show wall stress versus displacement, corresponding to maximum ram loads, for two conical dies in tandem, two streamlined dies in tandem, and a single streamlined die, respectively. In all three cases, punch through or wall tear was not predicted since the wall stress was well below the yield strength of the product material (approximately 689.5 MPa (100 ksi)). During the confirmation testings, no punch through or wall tear was observed. Thus, the predictions from the computer program DRAWNG are in accordance with the experimental observations.

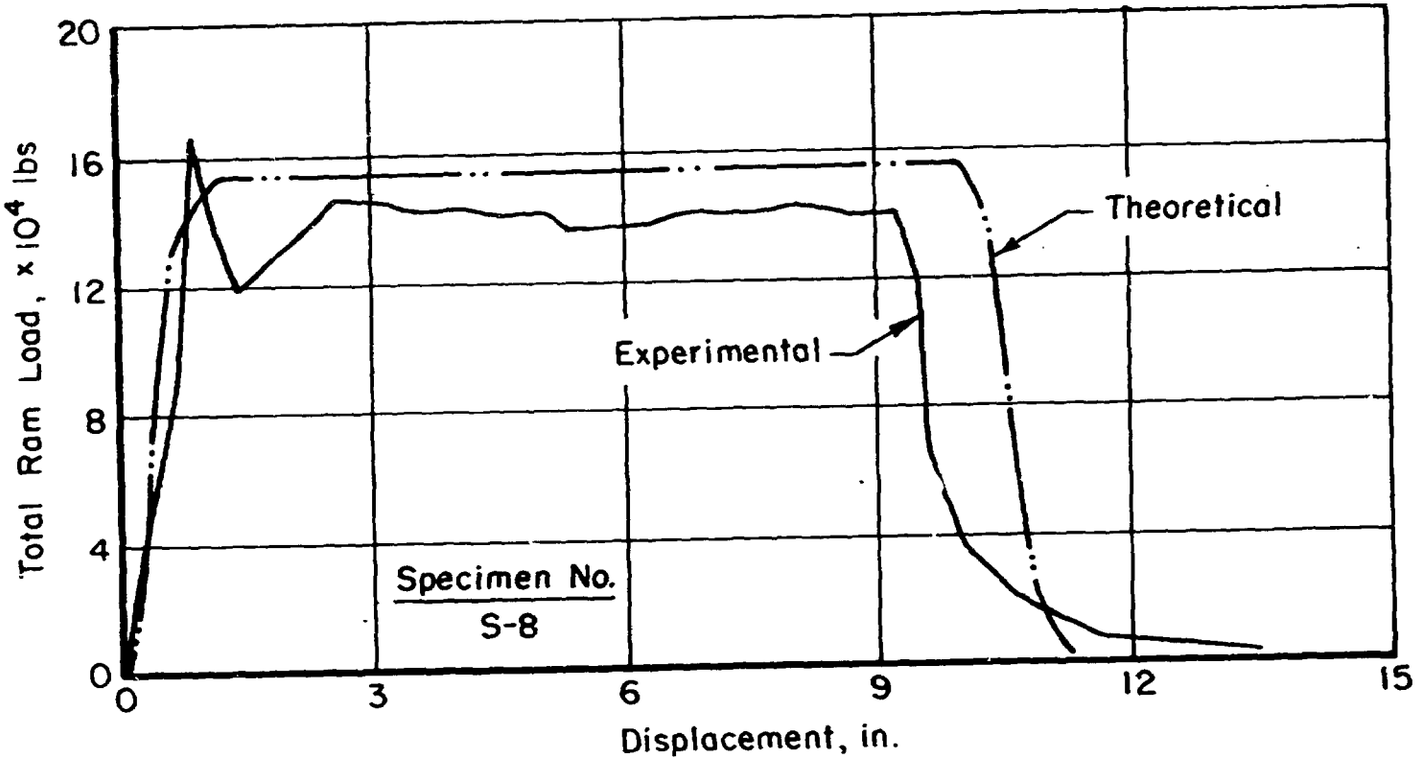

Figure 32. Theoretical and experimental (corresponding to maximum peak load) load-displacement curves for cold drawing of M335 shell through a single streamlined die. (1 inch = 25.4 mm, 1 lb = 4.448 N)

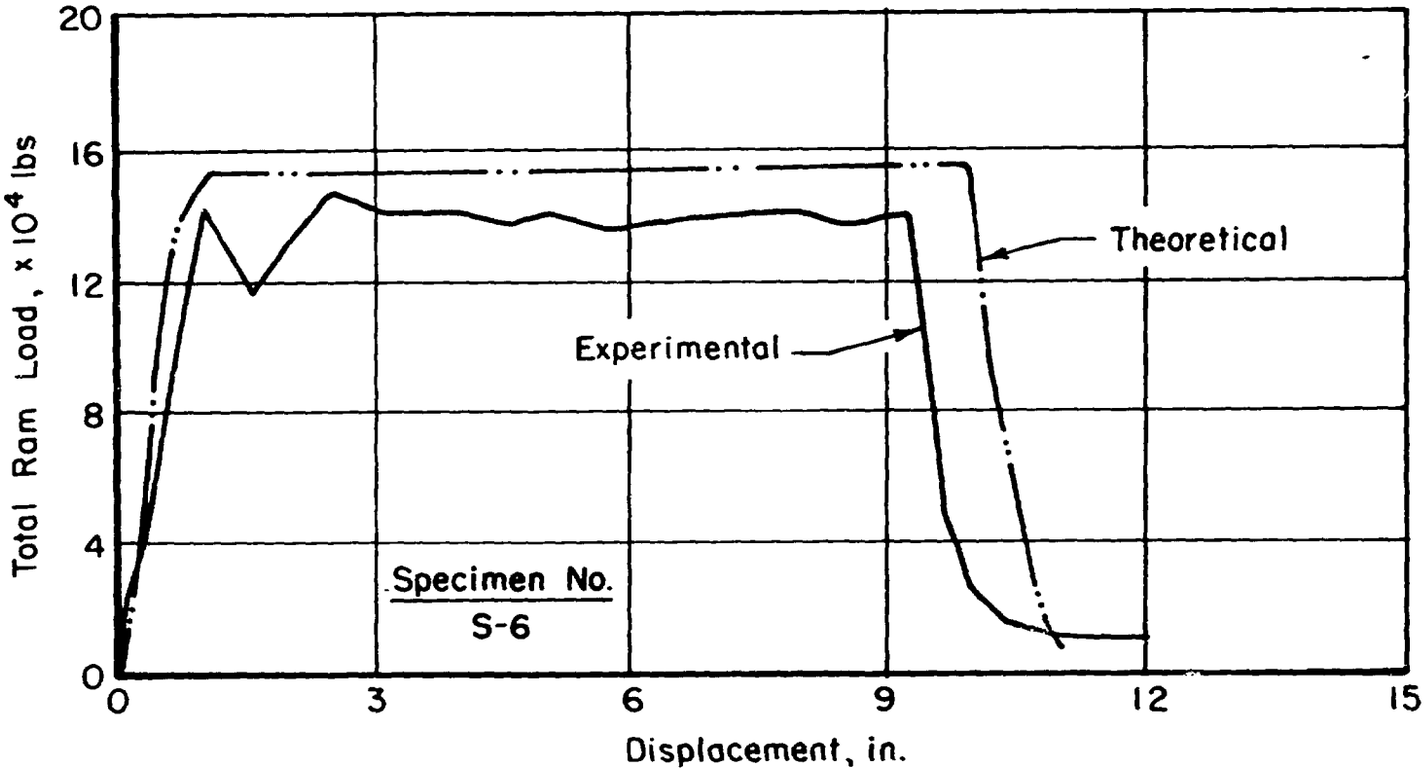

Figure 33. Theoretical and experimental (corresponding to minimum peak load) load-displacement curves for cold drawing of M335 shell through a single streamlined die. (1 inch = 25.4 mm, 1 lb = 4.448 N)

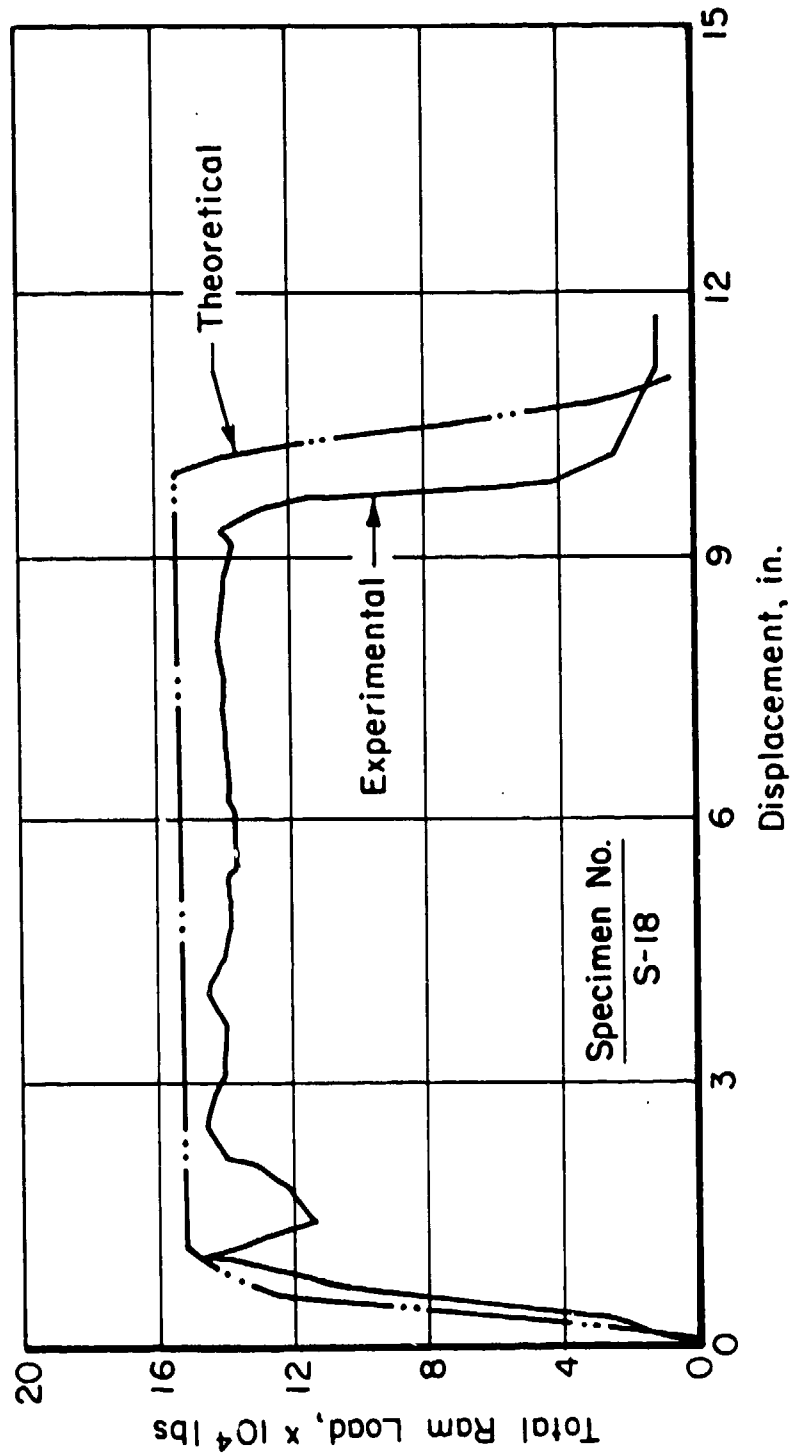

Figure 34. Theoretical and experimental (corresponding to average peak load) load-displacement curve for cold drawing of M335 shell through a single streamlined die. (1 inch = 25.4 mm, 1 lb = 4.448 N)

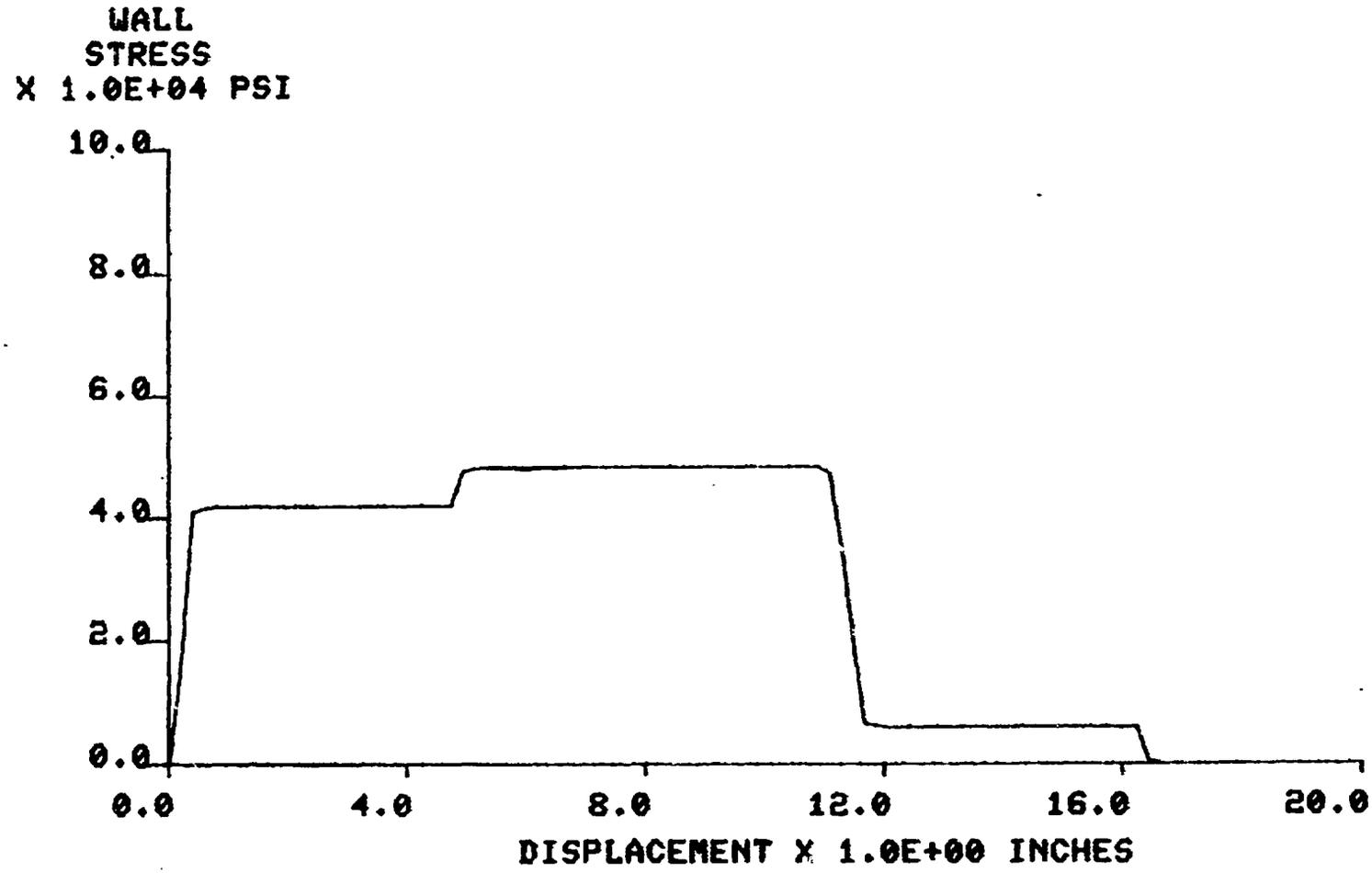

Figure 35. Theoretically predicted wall stress versus displacement during cold drawing of M335 shell through two conical dies. (1 inch = 25.4 mm, 1 lb = 4.448 N)

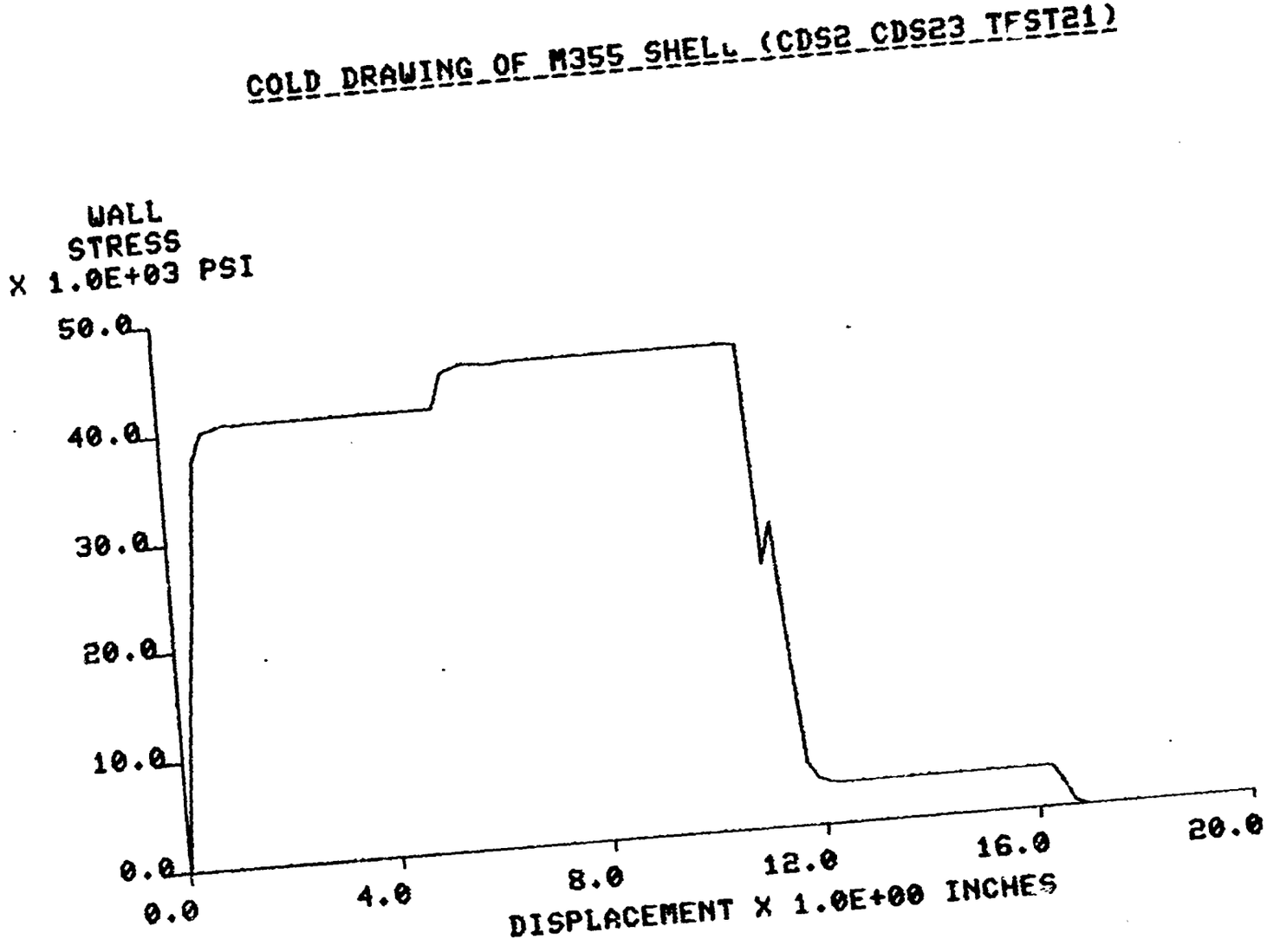

Figure 36. Theoretically predicted wall stress versus displacement during cold drawing of M335 shell through two streamlined dies. (1 inch = 25.4 mm, 1 lb = 4.448 N)

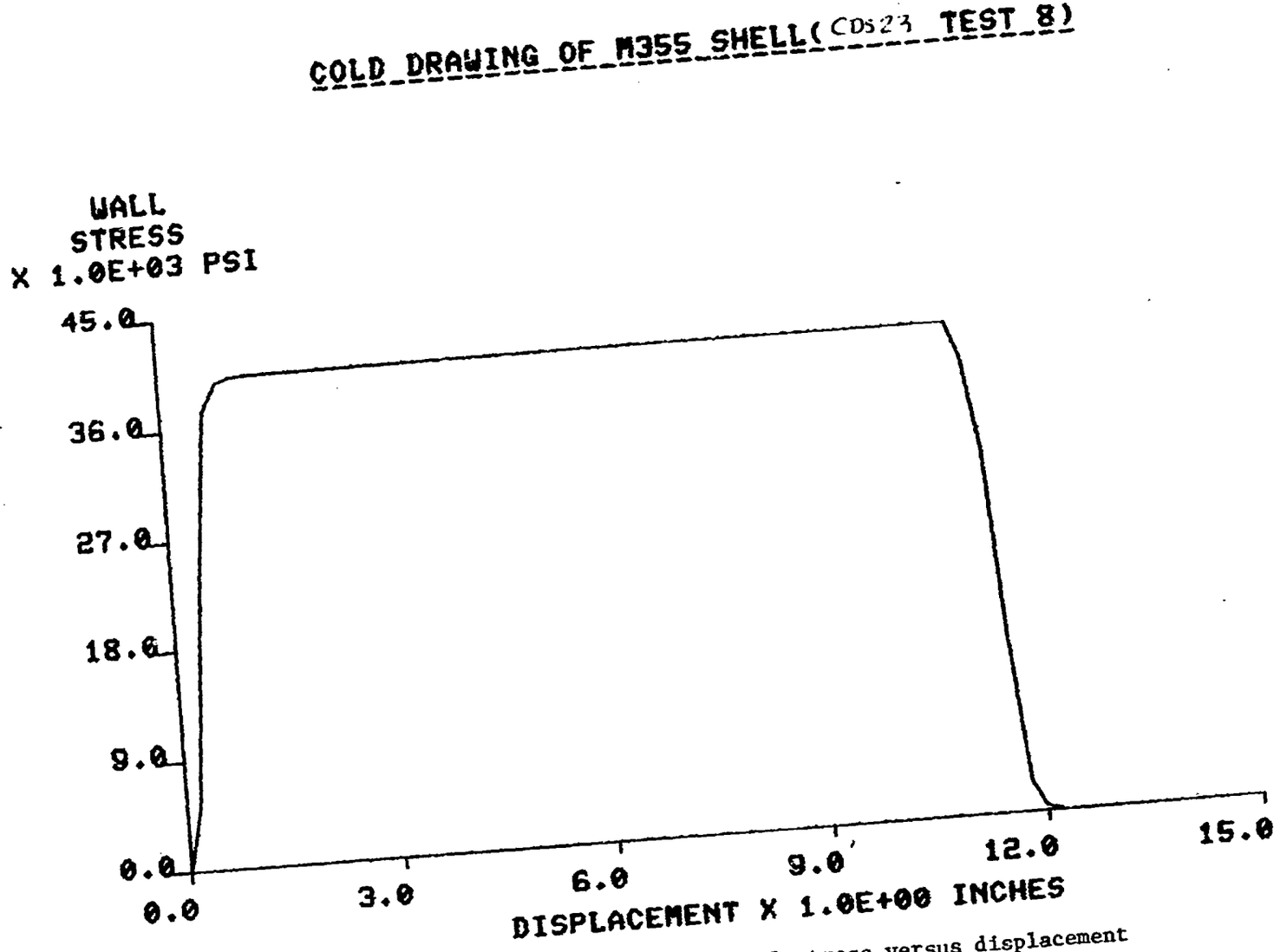

Figure 37. Theoretically predicted wall stress versus displacement during cold drawing of M335 sheil through a single streamlined die. (1 inch = 25.4 mm, 1 lb = 4.448 N)

Properties

In order to evaluate the cold drawing operations, tensile properties of the incoming material and various products were determined by conducting tension tests on an Instron machine. Table 9 shows typical tensile data for incoming material and for the product drawn through two conical dies in tandem, two streamlined dies in tandem, and a single streamlined die. It is worth noting that considerable work hardening takes place due to cold drawing. However, tensile properties of the product are not affected significantly by type of dies used and can be predicted using Equation (1). Thus, streamlined dies can be used to produce shells by cold drawing without affecting the tensile properties.

In addition to the tensile properties, Vickers hardness readings were taken across the wall of shells drawn through two conical dies in tandem and two streamlined dies in tandem. These readings, along with their location, are given in table 10. The average hardness of the product drawn through conical dies was higher than that for shell drawn through streamlined dies. Distribution across the thickness of the shell wall was not significant in either case and did not follow any specific pattern. One interesting phenomenon, however, occurred while the drawn shells were being sectioned for hardness measurement. As seen in figure 38, the section of the shell drawn through conical dies bowed twice as much as the section of the shell from streamlined dies, indicating that residual stresses in the latter case were lower than those in the former case. Although this does not mean that stress relieving is not necessary for shells drawn through streamlined dies, it does indicate that streamlined dies work the shell material somewhat more uniformly compared to the conical dies and thus produce less residual stresses in the product.

Hot Drawing Operations

As described earlier, hot drawing tests were conducted with 155 mm M107 shell using both conventional conical and double-curvature streamlined dies. These shells are manufactured from AISI 1046 steel between 1038°C (1900°F) to 1093°C (2000°F). However, in the following evaluation, the flow stress data for AISI 1045 steel from reference 4 are used. It is believed that this approximation in material flow stress will not introduce errors of any significance. Further, in a separate study using the hot ring compression test, the friction factor, f, for hot forging of steels was found to vary

Table 9. Tensile test data for M335 shell

Typical Data Prior to Drawing

Specimen No.	1		2		3	
Diameter, mm (in.)	6.2230	(.2450)	6.3500	(.2500)	6.3627	(.2505)
Area, mm^2 ($in.^2$)	30.4151	(.0471)	31.6692	(.0491)	31.7960	(.0493)
YL (0.2%), MN (lb)	0.0129	(2890)	0.0135	(3040)	0.0132	(2960)
UL, MN (lb)	0.0144	(3230)	0.0153	(3430)	0.0153	(3440)
YS, MPa (ksi)	422.63	(61.3)	426.79	(61.9)	414.37	(60.1)
US, MPa (ksi)	472.29	(68.5)	481.94	(69.9)	481.25	(69.8)
Elongation, (%)		(40.0)		(40.0)		(40.0)
Reduced Diameter, mm (in.)	3.0404	(.1197)	3.2766	(.1290)	2.9845	(.1175)
Reduced Area, mm^2 ($in.^2$)	7.2602	(.0113)	8.4321	(.0131)	6.9957	(.0108)
Reduction of Area, (%)		(76.1)		(73.4)		(78.0)

Typical Data After Production Double Draw (Conical Dies)

Specimen No.	1		2		3	
Diameter, mm (in.)	4.0259	(.1585)	4.0386	(.1590)	3.9497	(.1555)
Area, mm^2 ($in.^2$)	12.7296	(.0197)	12.8101	(.0199)	12.2523	(.0190)
YL (0.2%), MN (lb)	0.00863	(1940)	0.00859	(1930)	0.00850	(1910)
UL, MN (lb)	0.00899	(2020)	0.00903	(2030)	0.00859	(1930)
YS, MPa (ksi)	677.75	(98.3)	670.17	(97.2)	693.61	(100.6)
US, MPa (ksi)	706.02	(102.4)	704.64	(102.2)	700.51	(101.6)
Elongation, (%)		(16.5)		(17.9)		(15.6)
Reduced Diameter, mm (in.)	2.7305	(.1075)	2.5908	(.1020)	2.6314	(.1036)
Reduced Area, mm^2 ($in.^2$)	5.8556	(.0091)	5.2718	(.0082)	5.438	(.0084)
Reduction of Area, (%)		(54.0)		(58.8)		(55.6)

Typical Data After Experimental Draw (Streamlined Dies)

	Double Draw				Single Draw			
Specimen No.	1		2		1		2	
Diameter, mm (in.)	4.0259	(.1585)	3.9497	(.1550)	4.0132	(.1580)	4.0640	(.1600)
Area, mm^2 ($in.^2$)	12.7296	(.0197)	12.2523	(.0189)	12.6494	(.0196)	12.9717	(.0201)
YL (0.2%), MN (lb)	.00827	(1860)	.00825	(1855)	.00843	(1895)	.00852	(1915)
UL, MN (lb)	.00865	(1945)	.00843	(1895)	.00861	(1935)	.00883	(1985)
YS, MPa (ksi)	650.16	(94.3)	677.75	(98.3)	666.72	(96.7)	656.38	(95.2)
US, MPa (ksi)	679.82	(98.6)	692.23	(100.4)	680.51	(98.7)	680.51	(98.7)
Elongation, (%)		(16.1)		(14.6)		(14.8)		(14.5)
Reduced Diameter, mm (in.)	2.7178	(.1070)	2.6543	(.1045)	2.7661	(.1089)	2.7178	(.1070)
Reduced Area, mm^2 ($in.^2$)	5.8013	(.0090)	5.5333	(.0086)	6.0092	(.0086)	5.8013	(.0090)
Reduction of Area, (%)		(54.4)		(54.5)		(52.5)		(55.3)

Table 10. Vickers hardness across wall of drawn M335 shell

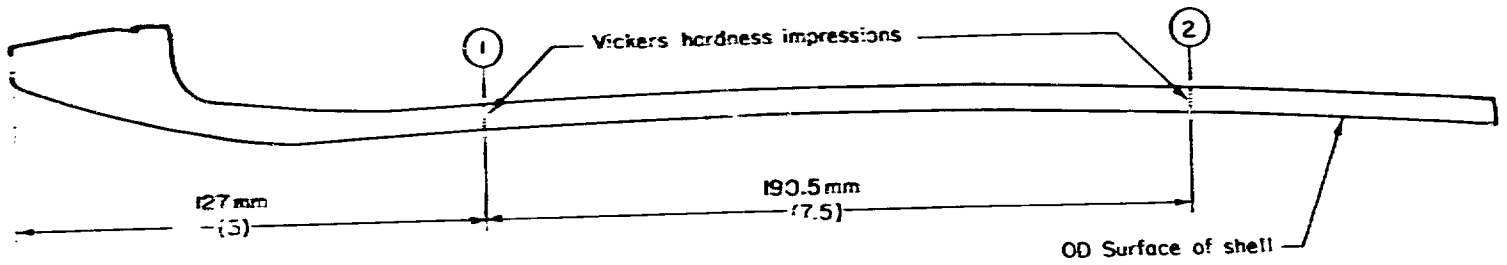

Shell Drawn Through Conical Dies			Shell Drawn Through Streamlined Dies		
	Location 1	Location 2		Location 1	Location 2
	232	249 ← ID of Shell		232	232 ← ID of Shell
	228	242		233	233
	230	240		238	227
	232	236		228	225
	235	233		230	219
	245	236 ← OD of Shell		222	225 ← OD of Shell
Average	234	239	Average	230	227

Note: The surface was not polished for these hardness readings. It was a flat ground surface.

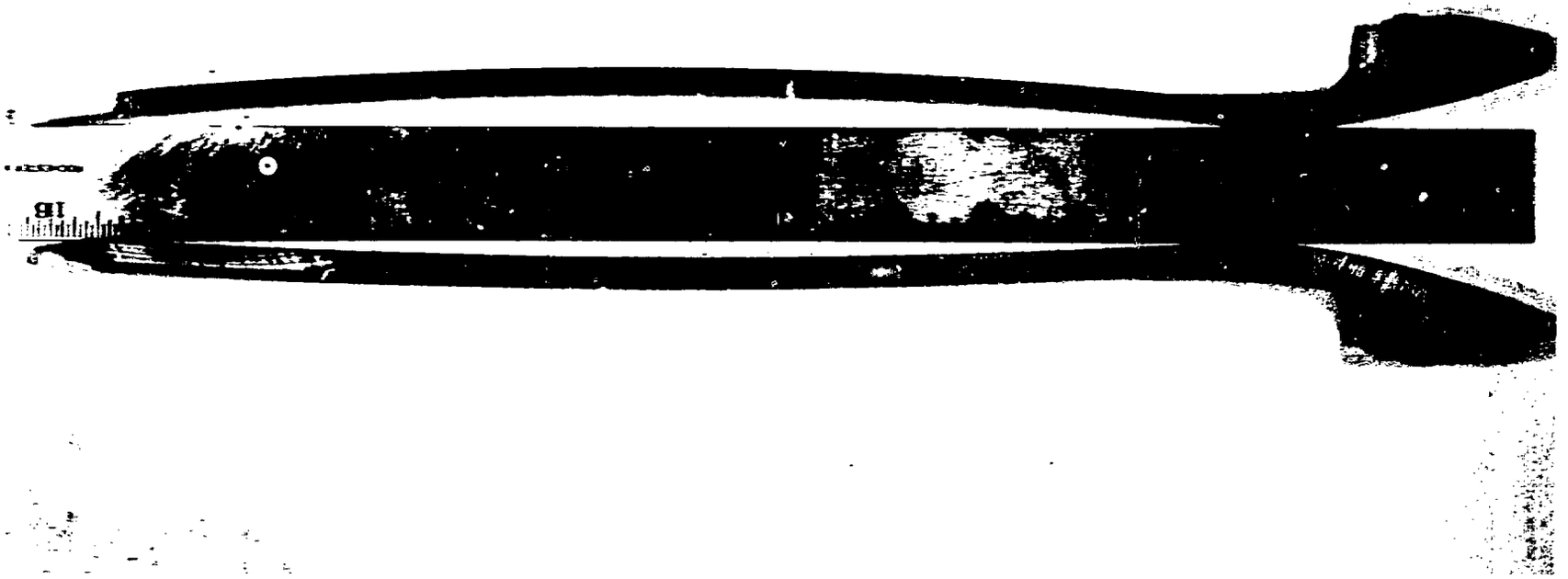

Top: Conventional Conical Dies,
Bottom: Streamlined Dies.

Figure 38. Deflection due to residual stresses in cold-drawn M335 shell bodies.

between 0.3 to 0.4, depending upon the amount of scale on the specimen. Therefore, in the present evaluation of the computer program DRAWNG, an average value of the friction factor f = 0.35 was selected.

To evaluate the load-displacement curves predicted by the computer program DRAWNG for hot drawing of M107 shell through conical and streamlined dies, three different cases for each type of dies were selected. Hot dimension of the preform was calculated from cold dimensions of the preform measured during trials. However, the effective length of the preform varied considerably, from 342.9 mm (13.5 inch) to 368.3 mm (14.5 inch). Punch dimensions were taken from the shape of the base of the finished product, as shown in figure 16(b). Tool assembly, as shown in figure 18, was also considered.

Length of the preform has considerable effect on overall shape of the load-displacement diagram. If the preform length is on the shorter side, the load drops nearly to zero as the product exits the first die and the peak near the exit from the second die is small. This behavior is shown in the theoretical curve in figure 39, where the preform length was taken as 342.9 mm (13.5 inch). On the other hand, if the length of the preform is on the higher side, the product is picked up by the second die as soon as it exits from the first die, and the peak near the exit from the second die is relatively high, since the shell is in the second and the third die at the same time. This behavior is shown in the theoretical curve in figure 40, where the effective preform length is taken as 368.3 mm (14.5 inch). Therefore, for evaluation purposes, an average preform length (effective) of 355.6 mm (14.00 inch) was taken. With this length of the preform, the trend observed in experiments were also reproduced by computer predictions, as shown in figure 41. Similar evaluations of the load-displacement curves for hot drawing through conical dies are included in figures 42 and 43 for Specimen No. N-10 and N-20, respectively. Overall agreement is good; peaks and valleys in the theoretical curves are somewhat sharper than measured. This is basically due to the simplified heat generation and heat transfer analysis used in the present model. However, the peak loads correlate well with the experimental measurements, except under the third die. This is, again, believed to be due to simple heat transfer analysis to a certain extent and due to the complex preform shape used in production compared to one assumed in the present analysis. (The actual preform shape is a proprietary information of Chamberlain.) In general, agreement between the theory and experiment appears good.

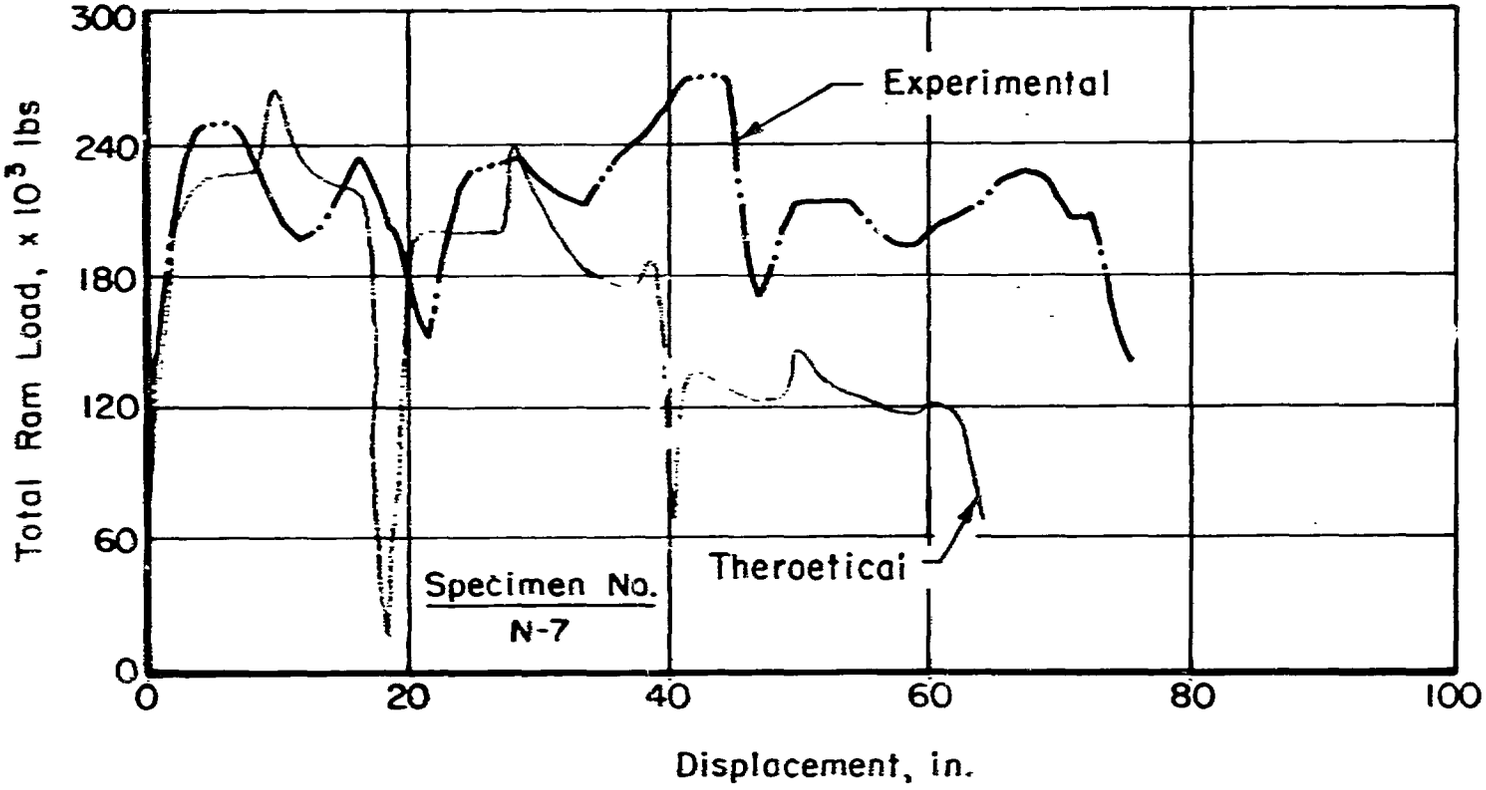

Figure 39. Theoretical and experimental load-displacement curves for hot drawing of M107 shell through conical dies for preform length = 342.9 mm (13.5 inch). (1 inch = 25.4 mm, 1 lb = 4.448 N)

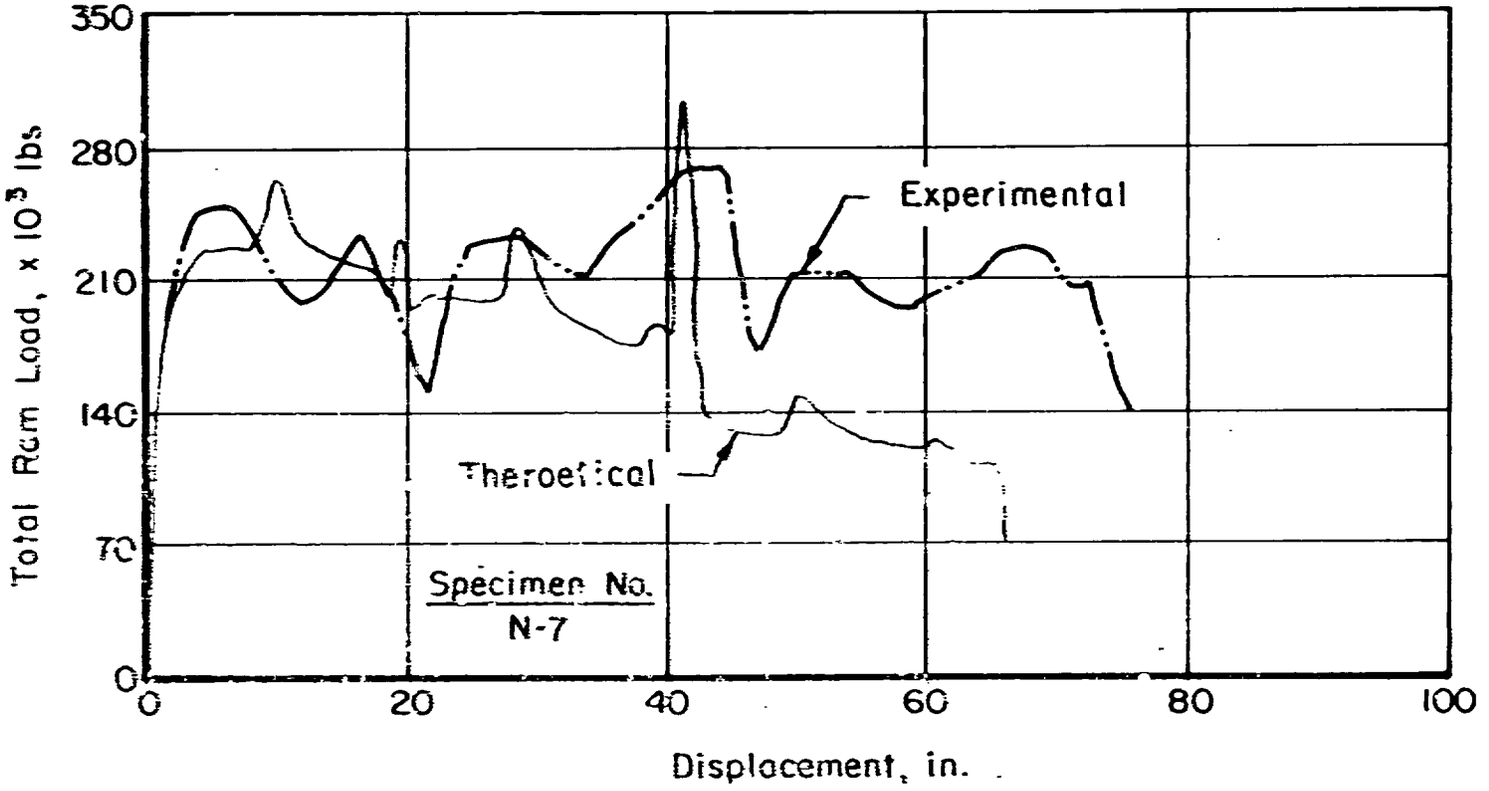

Figure 40. Theoretical and experimental load-displacement curves for hot drawing of M107 shell through conical dies for preform length = 368.3 mm (14.5 inch). (1 inch = 25.4 mm, 1 lb = 4.448 N)

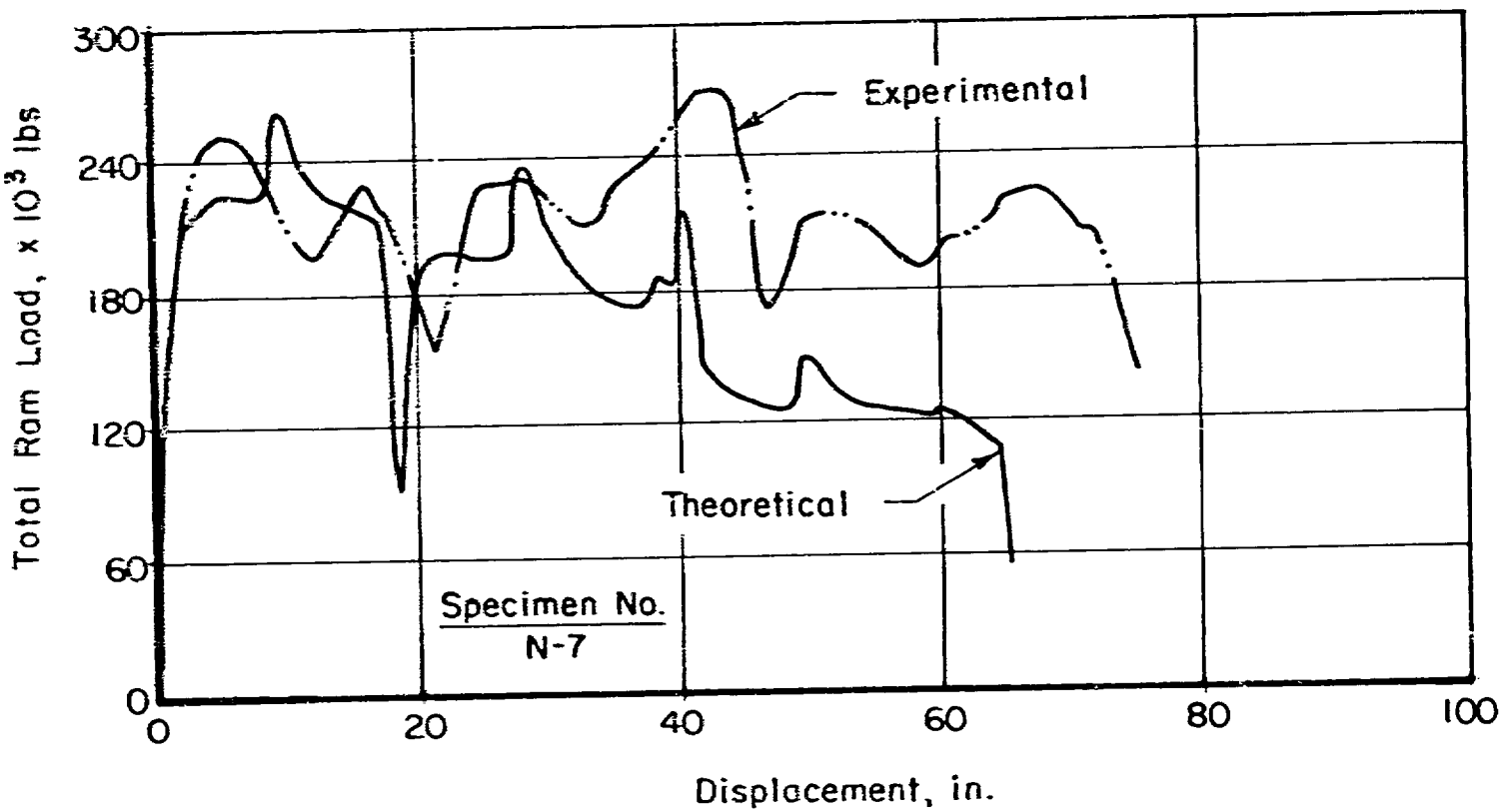

Figure 41. Theoretical and experimental load-displacement curves for hot drawing of M107 shell through conical dies for preform length = 355.6 mm (14.0 inch). (1 inch = 25.4 inch, 1 lb = 4.448 N)

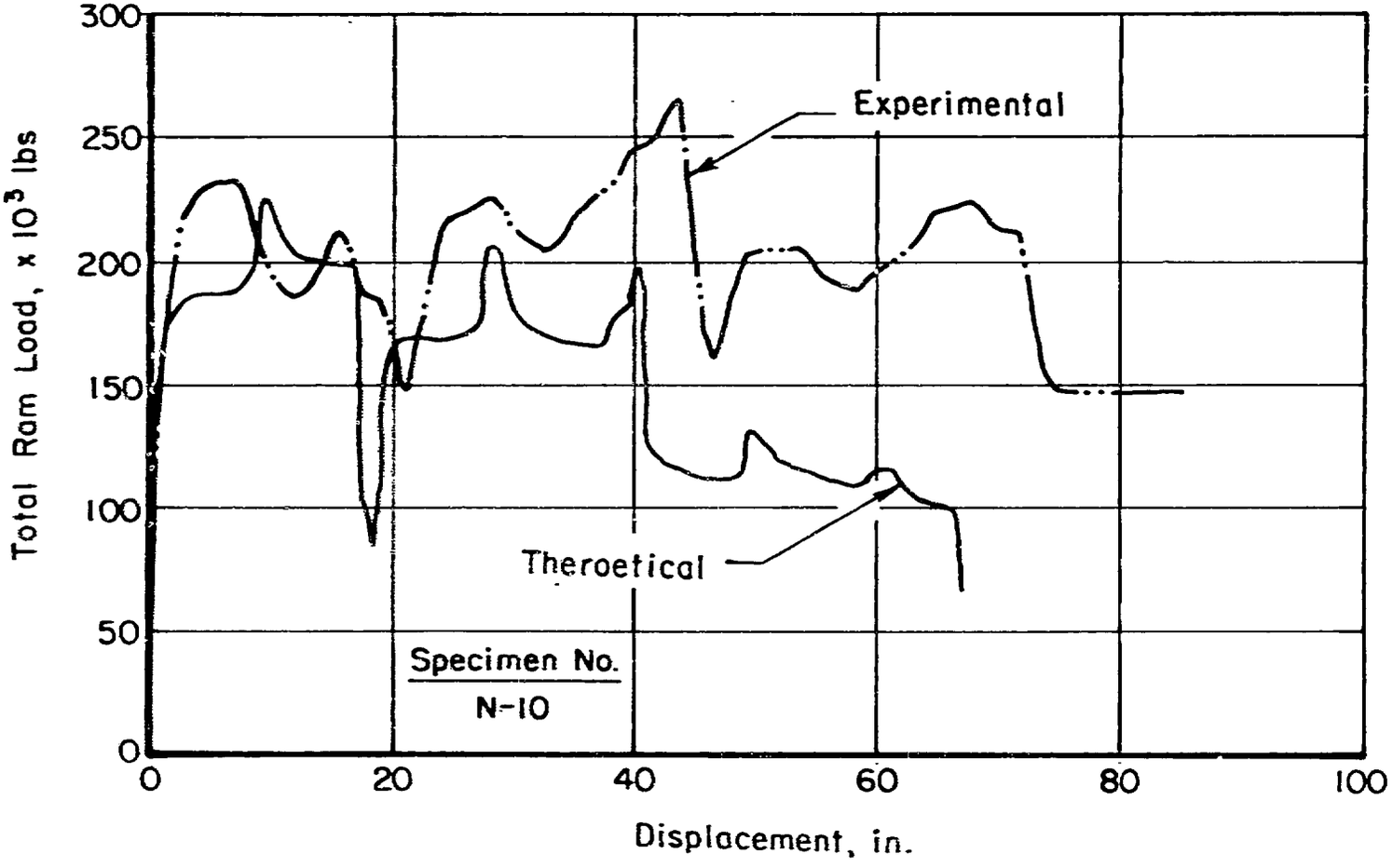

Figure 42. Theoretical and experimental load-displacement curves for hot drawing of M107 shell through conical dies for preform length = 355.6 mm (14.0 inch). (1 inch = 25.4 mm, 1 lb = 4.448 N)

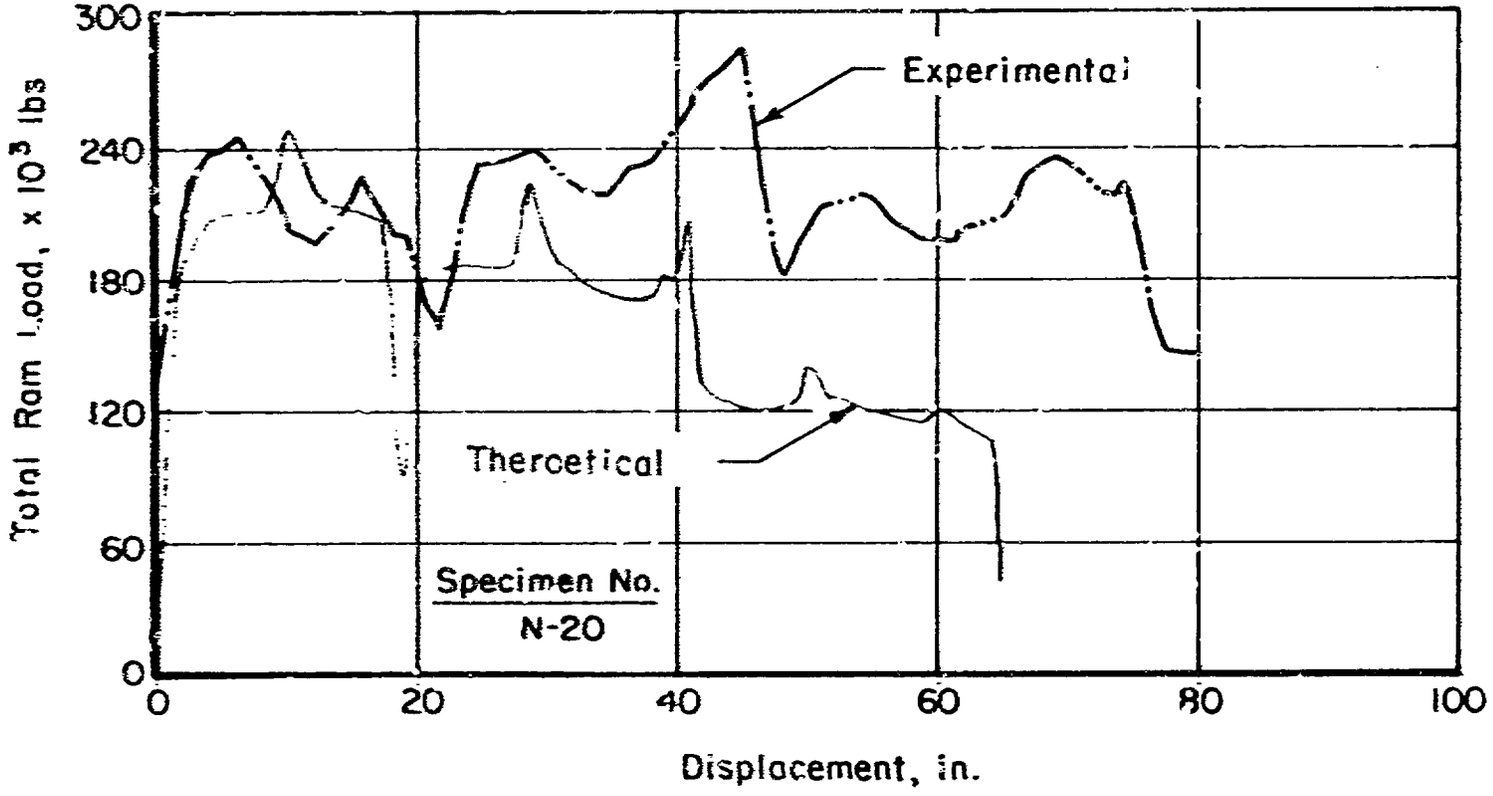

Figure 43. Theoretical and experimental load-displacement curves for hot drawing of M107 shell through conical dies for preform length = 355.6 mm (14.0 inch). (1 inch = 25.4 mm, 1 lb = 4.448 N)

Similar comparisons of load displacement curves for hot drawing through streamlined dies are made in figures 44 to 46. Considering the fact that preform dimensions and friction at the interfaces (due to different amount of scale) in hot drawing vary from piece to piece, correlation between the theoretically predicted and experimentally measured load displacement curves is very good. Again, predicted loads through the third die are lower than measured values. This discrepancy is partially due to the difference between theoretical and actual preform shape, as discussed earlier. However, this error is not considered of any significance since process design and equipment selection in reality is primarily based on the peak loads in the process.

Further, the computer program DRAWN predicted product wall stresses below the yield strength of the product, and thus no warning of punch through or wall tear were printed. This is in accordance with the observations where not a single shell during the day of the trial showed any signs of material failure.

Properties

In order to evaluate the hot drawing operations, tensile properties of the incoming material and various products were determined by conducting tension tests at room temperature. Table 11 shows typical tensile data for incoming material and for the product drawn through three conventional conical dies and streamlined dies in tandem. Tensile properties of the material are not changed significantly due to hot drawing. Further, these properties are also not affected significantly by type of dies used. Thus, streamlined dies can be used to produce shells by hot drawing without affecting the tensile properties of the drawn shell.

CONCLUSIONS AND RECOMMENDATIONS

Mathematical models for optimization of the shell drawing process were expanded to consider drawing through multiple dies in tandem and tapered punch and coded in computer program DRAWNG. DRAWNG is capable of simulating the shell drawing process, both hot and cold, and generate the ram load and the product wall stress versus ram displacement diagrams during simulation on a Cathode Ray Tube (CRT). Predictions from these models were evaluated with respect to hot and cold drawing confirmation testings conducted under actual

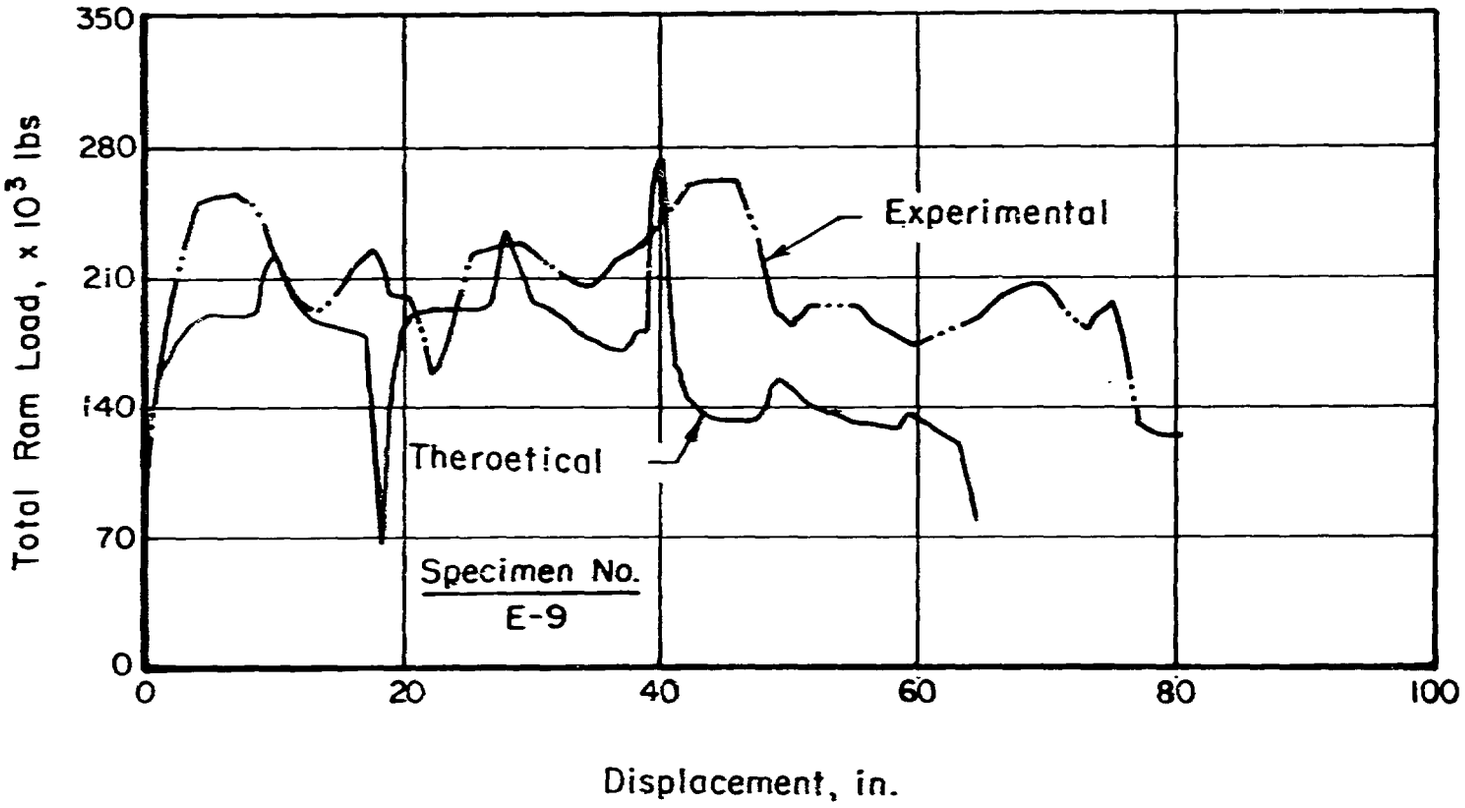

Figure 44. Theoretical and experimental load-displacement curves for hot drawing of M107 shell through streamlined dies for preform length = 355.6 mm (14.0 inch). 1 inch = 25.4 mm, 1 lb = 4.448 N)

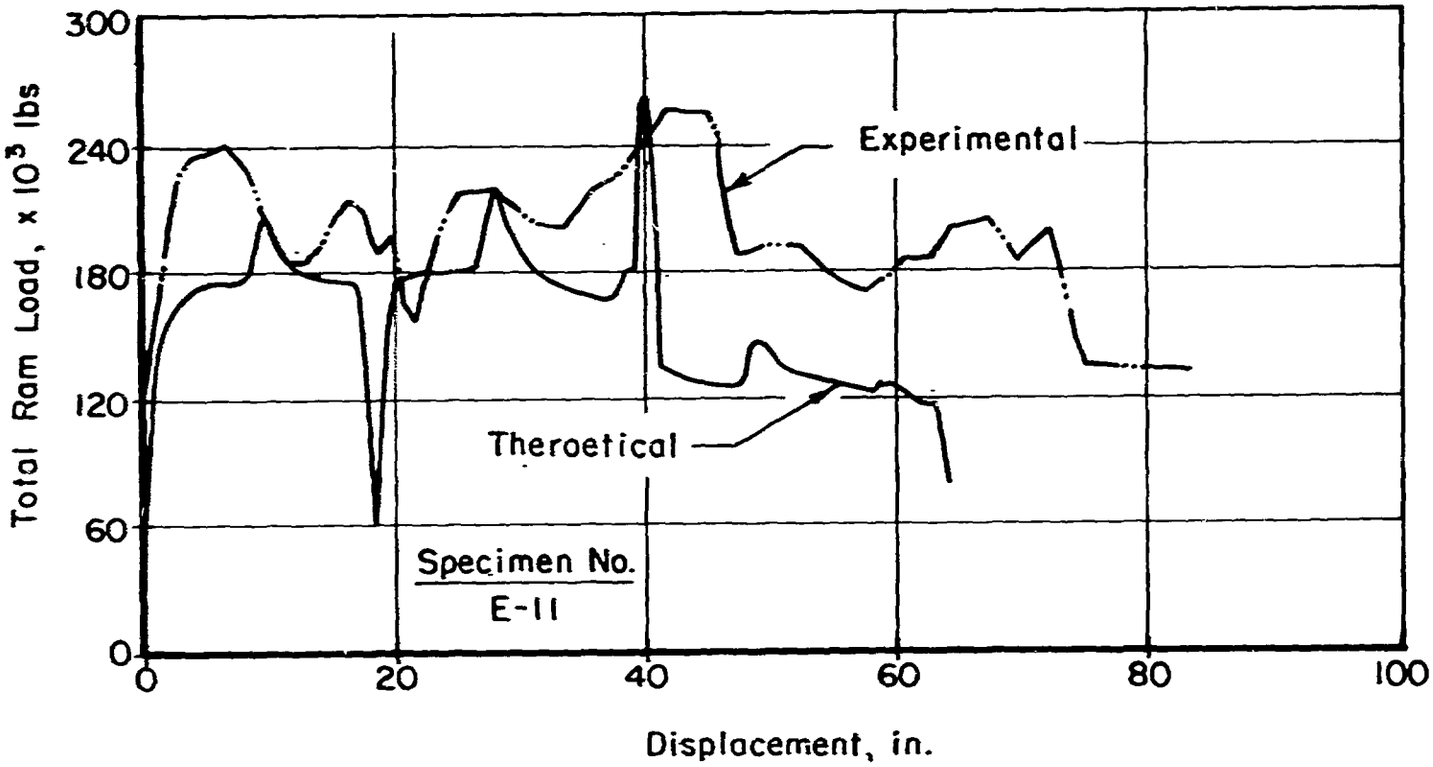

Figure 45. Theoretical and experimental load-displacement curves for hot drawing of M107 shell through streamlined dies for preform length = 355.6 mm (14.0 inch). (1 inch = 25.4 mm, 1 lb = 4.448 N)

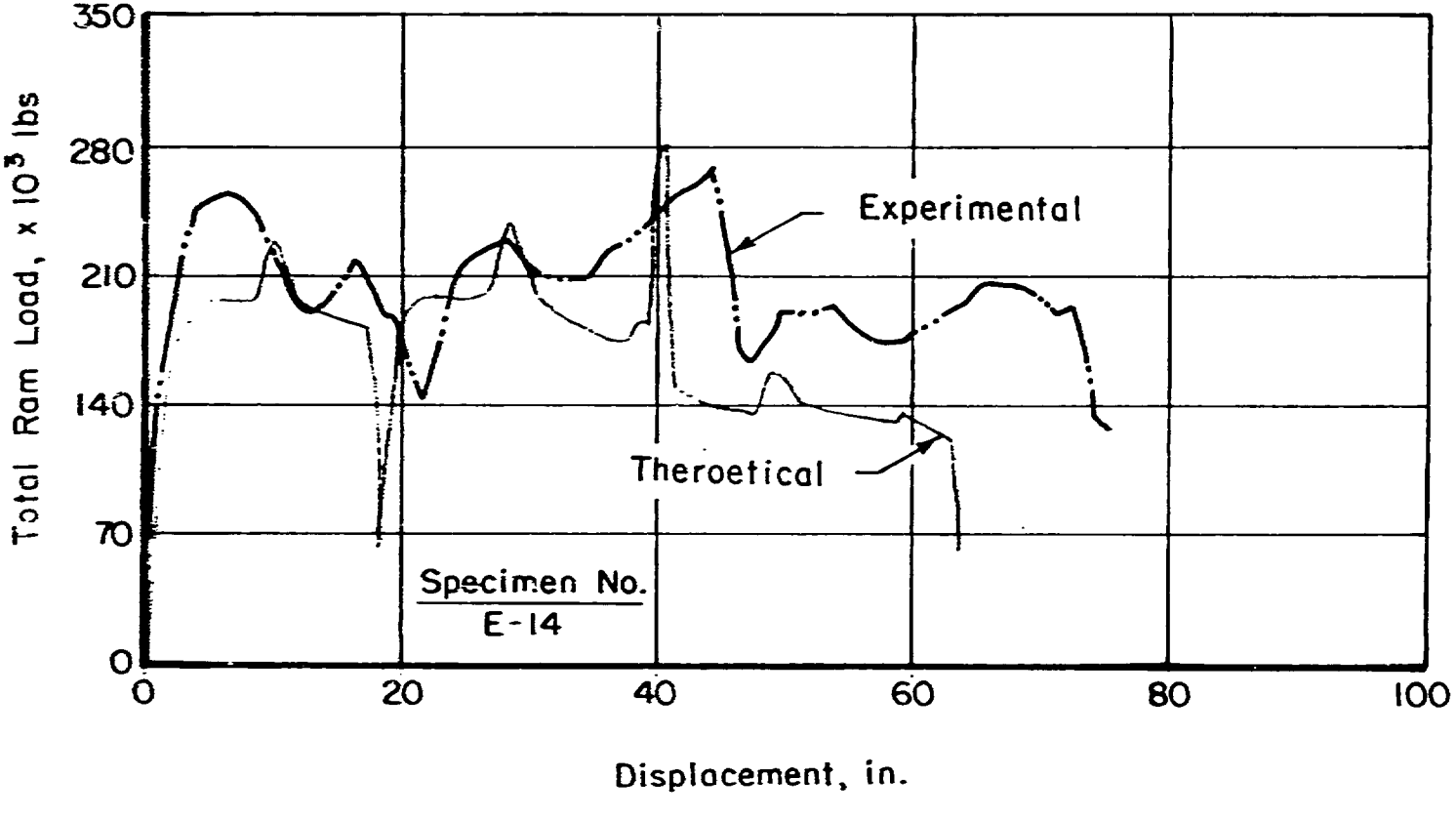

Figure 46. Theoretical and experimental load-displacement curves for hot drawing of M107 shell through streamlined dies for preform length = 355.6 mm (14.0 inch). (1 inch = 25.4 mm, 1 lb = 4.448 N)

Table 11. Tensile test data for M107 shell.

Typical Data Before Draw

	1		2	
Diameter, mm (in.)	6.3373	(.2495)	6.2992	(.2480)
Area, mm^2 ($in.^2$)	31.5427	(.0489)	31.1645	(.0483)
YL (0.2%), MN (lb)	.0133	(2,980)	.0131	(2,940)
UL, MN (lb)	.0232	(5,210)	.0229	(5,140)
YS, MPa (ksi)	420.60	(61.0)	419.91	(60.9)
US, MPa (ksi)	735.01	(106.6)	733.63	(106.4)
Elongation, (%)		(22.1)		(23.1)
Reduced Diameter, mm (in.)	4.6609	(.1835)	4.6101	(.1815)
Reduced Area, mm^2 ($in.^2$)	17.0620	(.0264)	16.6921	(.0259)
Reduction of Area, (%)		(45.9)		(46.4)

Typical Data After Drawing Through Production Dies (Conical Dies)

	1		2	
Diameter, mm (in.)	6.2992	(.2485)	6.2357	(.2455)
Area, mm^2 ($in.^2$)	31.1645	(.0485)	30.5394	(.0473)
YL (0.2%), MN (lb)	.0138	(3,100)	.0134	(3,020)
UL, MN (lb)	.0218	(4,910)	.0218	(4,900)
YS, MPa (ksi)	440.59	(63.9)	439.90	(63.8)
US, MPa (ksi)	697.77	(101.2)	713.63	(103.5)
Elongation,(%)		(24.0)		(21.1)
Reduced Diameter, mm (in.)	4.3688	(.1720)	4.3561	(.1715)
Reduced Area, mm^2 ($in.^2$)	14.9904	(.0232)	14.9034	(.0231)
Reduction of Area, (%)		(52.1)		(51.2)

Typical Data After Drawing Through Experimental Dies (Streamlined Dies)

	1		2	
Diameter, mm (in.)	6.2611	(.2465)	6.2992	(.2485)
Area, mm^2 ($in.^2$)	30.7887	(.0477)	31.1645	(.0485)
YL (0.2%), MN (lb)	.0126	(2,840)	.0134	(3,010)
UL, MN (lb)	.0230	(5,180)	.0233	(5,240)
YS, MPa (ksi	410.25	(59.5)	428.18	(62.1)
US, MPa (ksi)	748.11	(108.5)	744.66	(108.0)
Elongation, (%)		(19.2)		(23.2)
Reduced Diameter, mm (in.)	4.5593	(.1795)	4.5720	(.1800)
Reduced Area, mm^2 ($in.^2$)	16.3259	(.0253)	16.4173	(.0254)
Reduction of Area, (%)		(47.0)		(47.5)

or near production conditions. In addition, these tests included an evaluation of the streamlined dies, designed by the computer program CDVEL developed earlier (ref. 1).

Conclusions of the present study are:

(1) The system of computer programs DRAWNG is capable of simulating both the cold and hot shell drawing process using single or multiple dies (both conical and streamlined) in tandem with a tapered punch.

(2) Comparisons between theoretically predicted and experimentally measured ram load versus ram displacement curves indicate that computer programs DRAWNG are capable of predicting load-displacement curves, both under hot and cold drawing conditions, with acceptable engineering accuracy. All important trends and salient points in the experimental curves are reproduced accurately by the mathematical model, and the peak load values were within 5 to 10 percent of measured values.

(3) Material failure due to punch through or wall tear during the drawing operation were predicted accurately in all cases.

(4) Streamlined dies designed by using the computer program CDVEL produced good parts, both dimensionally and property-wise, under actual production environment. As predicted by mathematical models, in cold drawing of M335 shell, double curvature streamlined dies were found to be approximately 13 percent more efficient than conical dies, and they produced parts with lesser degree of residual stresses. Streamlined dies used in hot drawing of M107 shell were slightly more efficient compared to conical dies. However, drawing operation with streamlined dies appeared smoother compared to conical dies.

(5) Computer program CDVEL (ref. 1) can be used for designing the dies and DRAWNG can be used for simulating the shell drawing operations under both cold and hot working conditions.

Based on results of this study, recommendations are:

(1) Computer program DRAWNG should be stored in a central location from which it can be accessed through interactive terminals by various shell manufacturers. Since this program can simulate

cold and hot drawing operations accurately, it is recommended it be used for designing in future applications.

(2) Streamlined dies have produced good parts. Thus, computer program CDVEL can be used for designing streamlined dies for actual production applications.

(3) Since streamlined dies are proven to be more efficient compared to conical dies, these dies can possibly be used to (a) reduce the number of draws to make a part, (b) handle larger jobs which could not be handled before, due to marginal press tonnage, and (c) allocate smaller presses for existing jobs which are currently using larger presses.

(4) Finally, these computer programs should be integrated into a single comprehensive system for designing and optimizing the entire shell manufacturing activity. Such a system will be very useful in reducing the lead time during the period of emergency and will lessen the need for highly experienced people for designing shell manufacturing processes, tooling, and the production line.

REFERENCES

1. G.D. Lahoti, T. L. Subramanian, and T. Altan, "Development of a Mathematical Model and Computer Programs Capable of Optimizing the Drawing Process for Actual Artillery Shells and Cartridge Cases", Final Report, Contract No. DAAA25-74-C0557, Frankford Arsenal, May, 1975.

2. E. G. Thomsen, et al., Mechanics of Plastic Deformation in Metal Processing, McMillan, N.Y., 1965.

3. C. H. Lee, and T. Altan, "Influence of Flow Stress and Friction Upon Metal Flow in Upset Forging of Rings and Cylinders", Trans. ASME, J. Engrg. Industry, Vol. 94, August, 1972, p 775.

4. T. Altan, and F. W. Boulger, "Flow Stress of Metals and Its Application in Metal Forming Analysis", Trans. ASME, J. Engrg. Industry, Vol. 95, November, 1973, p 1009.

APPENDIX A.

ANALYSIS OF STRESSES, STRAINS, STRAIN RATES, AND TEMPERATURES DURING TANDEM DRAWING OF SHELLS

The mathematical model developed earlier at Battelle (ref. 1) is valid for drawing through a single die with a straight punch. Very often during hot drawing more than one drawing dies are used in tandem, as shown in figure A-1. Further, in actual shell drawing operations, the front portion of the punch is invariably tapered, as shown in figure A-1. Therefore, the existing math model was modified to include dies in tandem and a tapered punch in drawing. The present model simulates the actual drawing process by dividing the punch movement in a finite number of discrete steps. The slab method of analysis (ref. 2) was used to calculate stresses and the drawing loads at each step.

This analysis is also valid for streamlined dies, since the die profile can be approximated with a series of straight lines.

Analysis of Stresses

Figure A-2 shows a segment of a drawing die and the punch, where the dies are stationary and the punch is moving to the right. This operation consists of drawing a tube of outside radius R_o, inside radius R_i through a die to an outside radius r_o, inside radius r_i. Referring to page 439 of reference 2, neglecting friction, drawing stress can be expressed as:

$$\sigma_z = \bar{\sigma} \frac{2}{\sqrt{3}} \ln \left(\frac{R_o^2 - R_i^2}{r_o^2 - r_i^2} \right) \qquad \text{(A-1)}$$

where σ_z and $\bar{\sigma}$ are axial stress and flow stress of the deforming material, respectively.

Equation (A-1) is valid for plane strain conditions encountered in thin wall tubing. For thick walled tubing, this can be modified to:

$$\sigma_z = \bar{\sigma} \ln \left(\frac{R_o^2 - R_i^2}{r_o^2 - r_i^2} \right) \qquad \text{(A-2)}$$

The estimate can be improved when friction at the die-material and mandrel-material interfaces are considered. Referring to figure A-2, the friction force at the die-material interface can be expressed as:

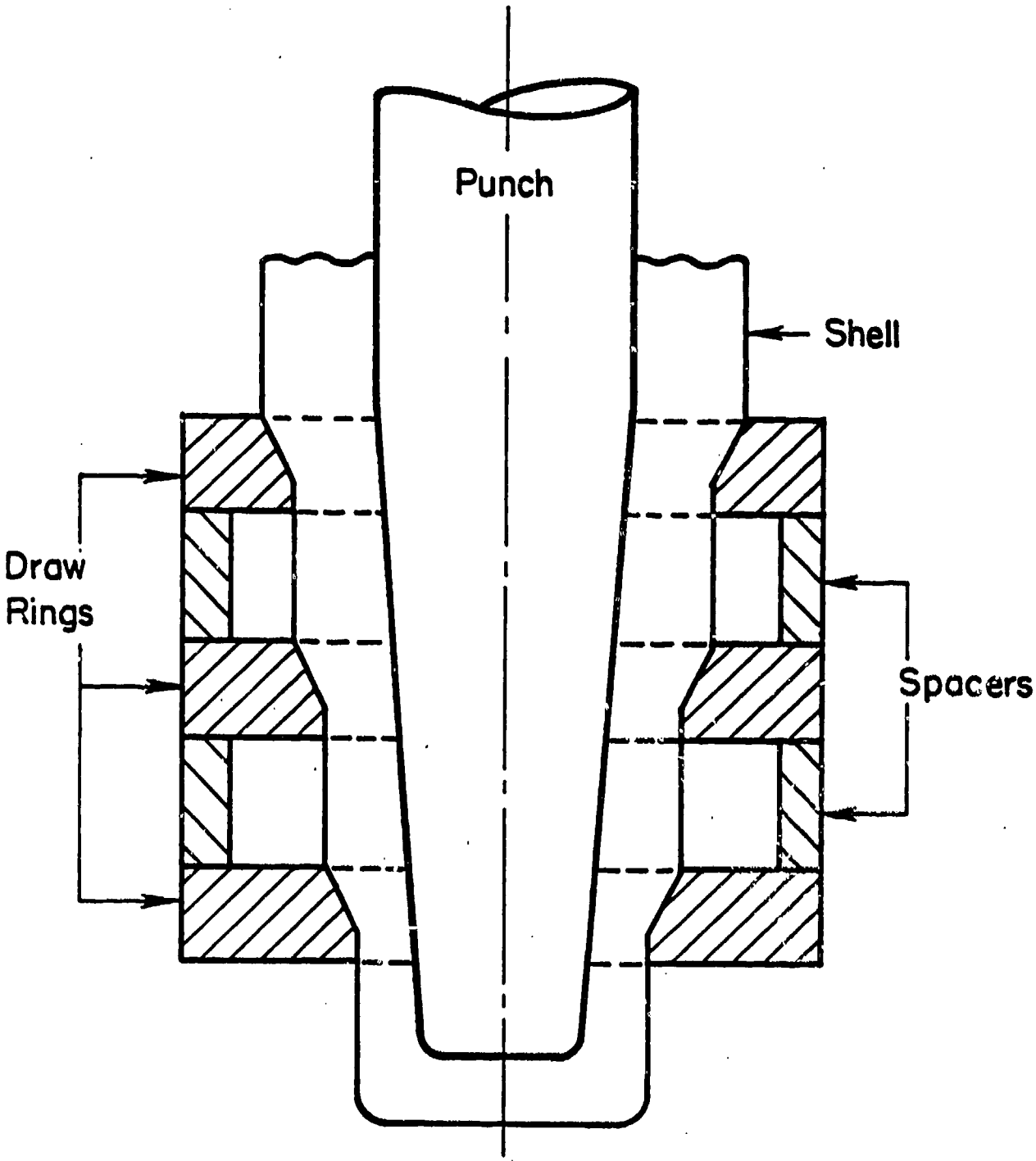

Figure A-1. Shell drawing with dies in tandem and with a conical punch.

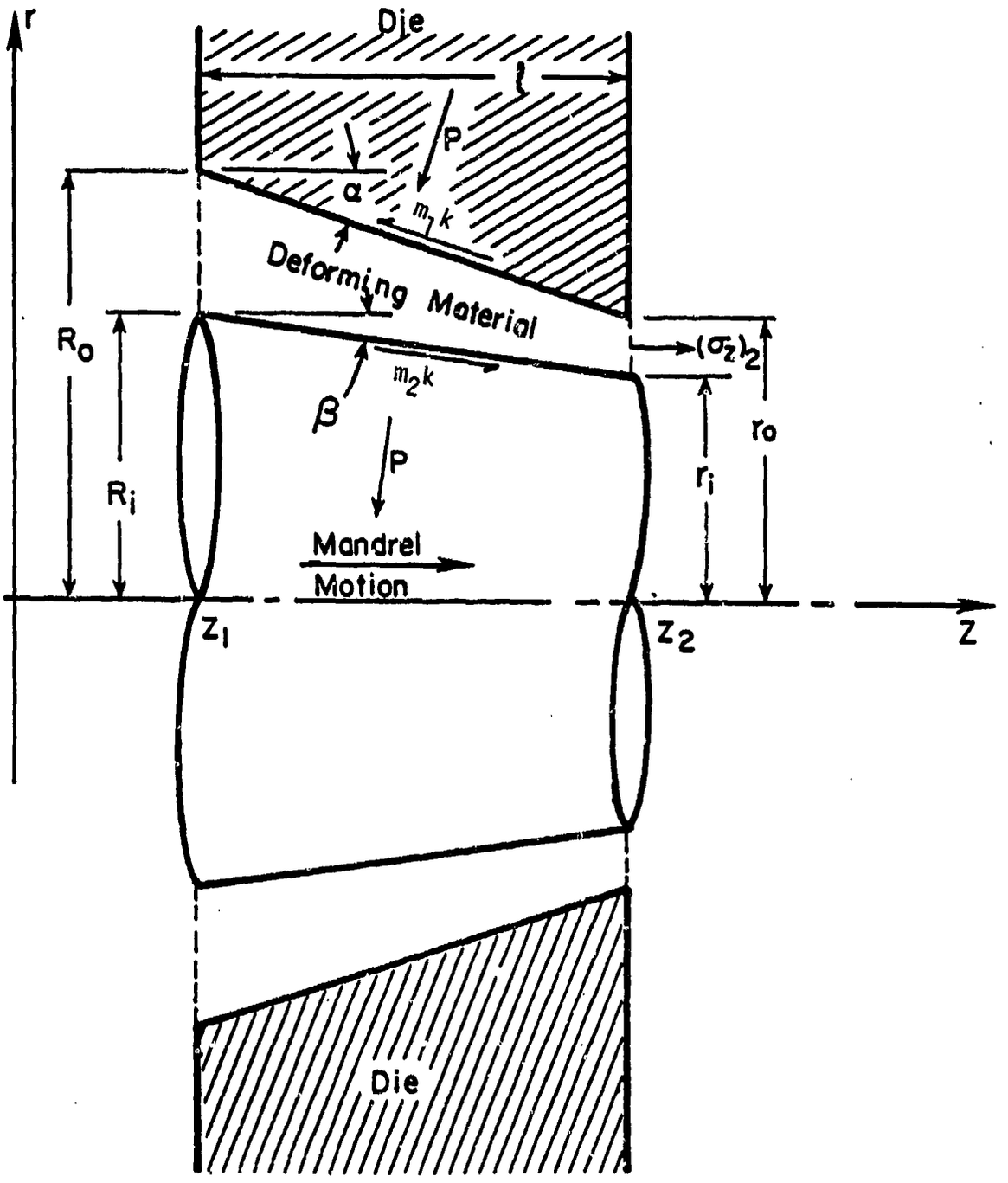

Figure A-2. Drawing with a conical moving mandrel.

$$F_o = m_1 \frac{\bar{\sigma}}{\sqrt{3}} \cdot \cos \alpha \, (R_o^2 - r_o^2) \, \pi / \sin \alpha \qquad \text{(A-3)}$$

where m_1 is the friction shear factor at die-workpiece interface. Similarly, the friction force at the punch-material interface can be expressed as:

$$F_i = m_2 \frac{\bar{\sigma}}{\sqrt{3}} \cdot \cos \beta \, (R_i^2 - r_i^2) \, \pi / \sin \beta \qquad \text{(A-4)}$$

where m_2 is the friction shear factor at the punch-workpiece interface. By dividing F_o and F_i with the cross sectional area and adding them to σ_z of Equation (A-2), an overall expression for stress is obtained. Due to the motion of the mandrel, F_i and F_o act in opposite directions. Thus,

$$\sigma_z = \bar{\sigma} \ln \left[\frac{R_o^2 - R_i^2}{r_o^2 - r_i^2} \right] + \frac{(F_o - F_i)}{(r_o^2 - r_i^2)\pi} \qquad \text{(A-5)}$$

The manner in which Equations (A-3) and (A-4) are expressed above is not suitable for computer programming. They contain a pseudo-singularity; that is, whenever one of the angles α or β is zero, a division by zero results. This can be alleviated by considering another expression for the area of a frustrum of a cone:

$$A = \pi \, (R + r) \sqrt{(z_1 - z_2)^2 + (R - r)^2} \qquad \text{(A-6)}$$

$$\text{and } F_i = m_2 \frac{\bar{\sigma}}{\sqrt{3}} \cdot \cos \beta \cdot A_i \qquad \text{(A-7)}$$

$$F_o = m_1 \frac{\bar{\sigma}}{\sqrt{3}} \cdot \cos \alpha \cdot A_o \qquad \text{(A-8)}$$

cos β and cos α can also be replaced as:

$$\cos \beta = \frac{(z_2 - z_1)}{\sqrt{(z_2 - z_1)^2 + (R_i - r_i)^2}} \tag{A-9}$$

$$\cos \alpha = \frac{(z_2 - z_1)}{\sqrt{(z_2 - z_1)^2 + (R_o - r_o)^2}} \tag{A-10}$$

Substitutions of Equations (A-6) through (A-10) into Equation (A-5) yields the final expression without pseudo-singularities.

$$\sigma_z = \bar{\sigma} \ln \left(\frac{R_o^2 - R_i^2}{r_o^2 - r_i^2}\right) + \frac{\bar{\sigma}(z_2 - z_1)}{(r_o^2 - r_i^2)} \left[\frac{m_1}{\sqrt{3}} (r_o + R_o) - \frac{m_2}{\sqrt{3}} (r_i + R_i)\right] \tag{A-11}$$

When the shell is drawn through more than one die, friction force acts between the portions of the punch in between the dies and the material. However, the magnitude of this friction force is significantly less than F_1, the friction force at the punch-material interface under the dies. Therefore, another friction factor, m_3, is used to describe this force.

Analysis of Strains

Under axial symmetry conditions, it can be shown that the radial strain (ε_r) and circumferential strain (ε_θ) are equal. Thus,

$$\varepsilon_r = \varepsilon_\theta \tag{A-12}$$

From the incompressibility condition, axial strain (ε_z) can be derived to be

$$\varepsilon_z = -2\varepsilon_r = -2\varepsilon_\theta \tag{A-13}$$

The effective strain $\bar{\varepsilon}$ is then given by

$$\bar{\varepsilon} = \frac{2}{3}\left\{\frac{1}{2}[(\varepsilon_z - \varepsilon_\theta)^2 + (\varepsilon_\theta - \varepsilon_r)^2 + (\varepsilon_r - \varepsilon_z)^2]\right\}^{\frac{1}{2}}$$

$$= \varepsilon_z$$

$$= \ln\left\{\frac{R_o^2 - R_i^2}{r_o^2 - r_i^2}\right\} \qquad \text{(A-14)}$$

Analysis of Strain Rates

Let us consider metal flowing through an arbitrarily shaped die, as shown in figure A-3. For the purpose of calculating strain rates only, it is assumed that, for a small axial segment of width Δz, the die profile can be approximated with a conical surface of angle α, and that the punch is straight with a constant radius r_o. Then, referring to appendix B of reference 1, a kinematically admissible velocity field can be derived as given below:

$$U_r = \frac{V_e}{r} \cdot \frac{(R_e^2 - r_o^2)(r^2 - r_o^2)\, R(z)\, R'(z)}{(R^2(z) - r_o^2)^2}$$

$$U_\theta = 0 \qquad \text{(A-15)}$$

$$U_z = V_e \cdot \frac{R_e^2 - r_o^2}{R^2(z) - r_o^2} \quad ,$$

where U_r, U_θ and U_z are the velocity components in the radial (r-), circumferential (θ-), and axial (z-) directions, respectively, and where R(z) describes the die profile. The prime denotes derivative with respect to z.

Components of the strain-rate tensor $\dot{\varepsilon}_{ij}$ can be obtained from Equation (A-15) as follows:

$$\dot{\varepsilon}_r = V_e \cdot \frac{(R_e^2 - r_o^2)\,(r^2 + r_o^2)\, R(z)\, R'(z)}{r^2 (R^2(z) - r_o^2)^2}$$

$$\dot{\varepsilon}_\theta = V_e \cdot \frac{(R_e^2 - r_o^2)\,(r^2 - r_o^2)\, R(z)\, R'(z)}{r^2 (R^2(z) - r_o^2)^2} \qquad \text{(A-16)}$$

$$\dot{\varepsilon}_z = -V_e \cdot \frac{2(R_e^2 - r_o^2)\, R(z)\, R'(z)}{(R^2(z) - r_o^2)^2}$$

$$\dot{\gamma}_{rz} = V_e \cdot \frac{(R_e^2 \cdot r_o^2)\,(r^2 - r_o^2)\, G(z)}{r\,(R^2(z) - r_o^2)^3} \qquad \text{(A-16) (continued)}$$

$$\dot{\gamma}_{r\theta} = \dot{\gamma}_{\theta z} = 0 \quad ,$$

where

$$G(z) = R(z)\, R''(z)\,(R^2(z) - r_o^2) - R'^2(z)\,(3R^2(z) + r_o^2) \quad .$$

In axisymmetric case, effective strain rate is then obtained by the relation:

$$\dot{\bar{\varepsilon}} = \frac{2}{\sqrt{3}} \sqrt{\frac{1}{2}\, \dot{\varepsilon}_{ij}\, \dot{\varepsilon}_{ij}} = \sqrt{\frac{2}{3}\,(\dot{\varepsilon}_r^2 + \dot{\varepsilon}_\theta^2 + \dot{\varepsilon}_z^2 + \frac{1}{2}\,\dot{\gamma}_{rz}^2)} \quad . \qquad \text{(A-17)}$$

Analysis of Temperatures

During shell drawing, heat is generated in the billet material under the dies due to plastic deformation and friction at the die workpiece and punch-workpiece interfaces. Simultaneously, heat is transported with the moving material, and heat transfer takes place. Some of the generated heat remains in the product, some is conducted to the tooling, and some may even increase the temperature of the material coming into the deformation zone. Thus, the general problem to be examined is that of time-dependent heat flow in an incompressible moving medium with heat generation in the medium.

In the present approximate analysis, it is assumed that heat is generated uniformly in the workpiece material in the deformation zone, and a steady state of temperatures is reached after an initial period of transients. Since the temperature gradients in the axial direction are not large, heat transfer in the radial direction alone is considered. Furthermore, the heat loss to drawing dies is considered. Figure A-4 shows a simplified model for calculating temperatures in drawing of shells. Since the outside radius of the tube depends upon the axial location of the cross section shown in figure A-4, radius r_3 is a function of axial location under the dies.

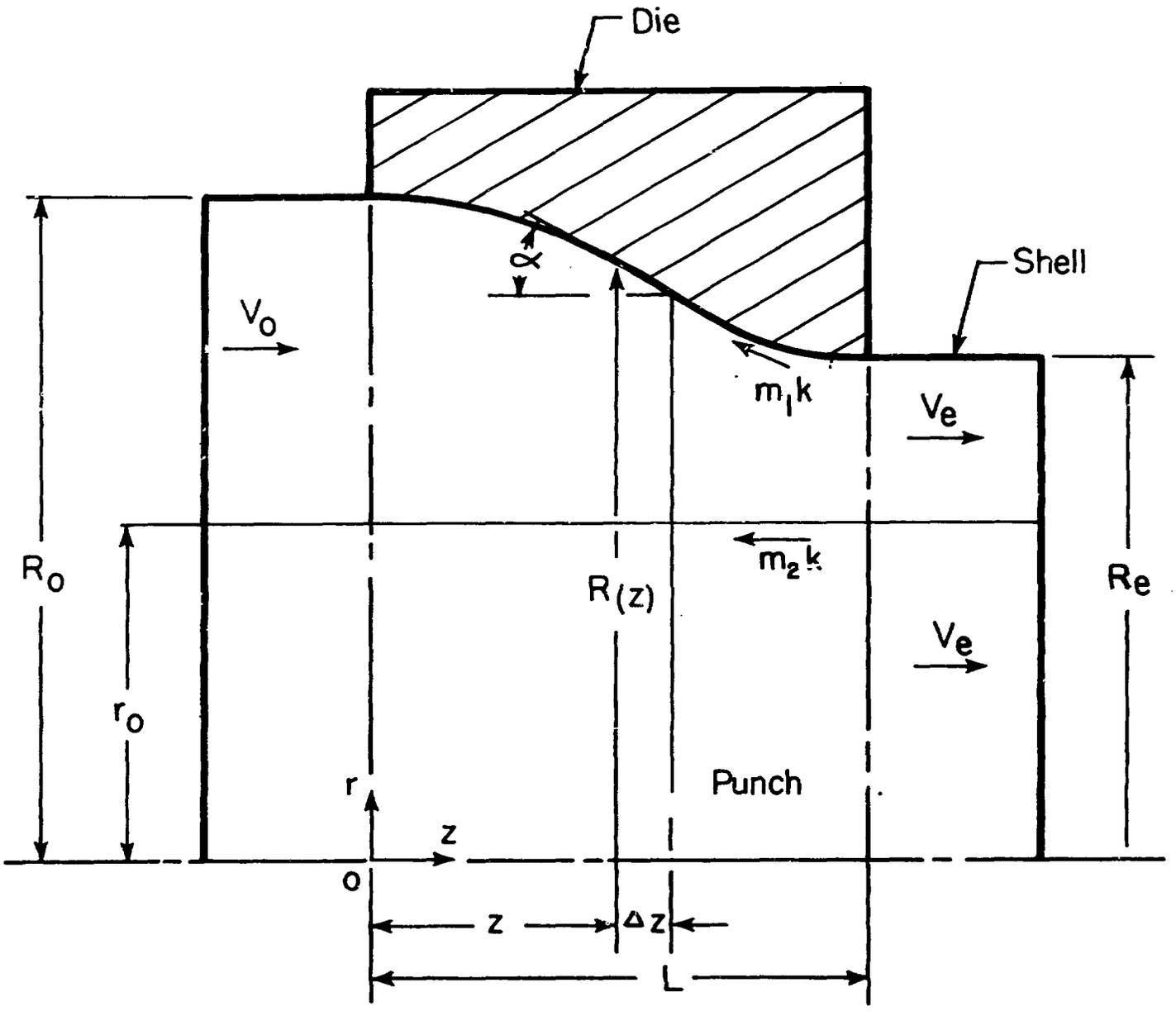

Figure A-3. Schematic diagram of shell drawing through a curved die.

Nomenclature

C = Specific heat of billet material, BTU/lb F (J/Kg C)

h_a = Coefficient of heat transfer for air, BTU/in.^{2} sec F (W/m^2 C)

h_w = Coefficient of heat transfer for water, BTU/in.^{2} sec F (W/m^2 C)

J = Factor for work to heat ratio, lb in./ BTU (1)

k_d = Thermal conductivity of die material, BTU/in. sec F (W/m C)

k_m = Thermal conductivity of punch material, BTU/in. sec F (W/m C)

L = Length of the deformation zone, inch (m)

l = Punch travel, inch (m)

$P(z)$ = Ram load as a function of punch position, lb (Kg)

r_1 = Punch inside radius, inch (m)

r_2 = Punch outside radius, inch (m)

r_3 = Product outside radius, inch (m)

r_4 = Die outside radius, inch (m)

t_1 = Punch coolant temperature, F (C)

t_3 = Billet initial temperature, F (C)

t_f = Billet final temperature, F (C)

t_o = Ambient temperature, F (C)

V = Volume of the deforming material, in.^{3} (m^3)

V_e = Punch velocity, in./sec (m/s)

$\Delta\tau$ = Time interval, sec

ρ = Density of billet material, lb/in.^{3} (Kg/m^3)

Heat Generation:

Heat is generated in the deformation zone due to dissipation of plastic energy and friction energy. Total energy supplied to the deforming material can be calculated from knowledge of load-displacement curve for the forging tools. Thus, if $P(z)$ is the average ram load at a displacement z, the energy spent in deforming the material from z_1 to z_2 is given by

$$\Delta Q_g = \int_{z_1}^{z_2} P(z)\, dz \qquad \text{(A-18)}$$

That is, energy spent is the area under the load-displacement curve. Billet temperature before heat loss is then:

$$t'_3 = t_3 + \frac{\Delta Q_g}{\rho C V} \qquad \text{(A-19)}$$

Heat Loss to Punch:

Heat is lost to water-cooled punch continuously. Part of the billet heat is conducted through the punch to water film at the inside diameter of the punch, where it is carried away by water via forced convection. Combined heat loss, Q_m, is given by:

$$\Delta Q_m = \frac{2\pi \ell \cdot (t'_3 - t_1)}{\ln\left(\frac{r_2}{r_1}\right)/k_m + 1/h_w r_1} \cdot \Delta\tau \qquad \text{(A-20)}$$

where $\Delta\tau = \Delta\ell/V_e$ the time increment due to a discrete movement $\Delta\ell$ of the punch. In case of a solid punch, above analysis is not valid. Approximate results can be obtained by selecting a small hole of radius r_1 with air in it.

Heat Loss to the Die

Heat is lost to the die whenever billet is in contact with the die. Heat loss to die during a small movement of the punch is given by

$$\Delta Q_d = \frac{2\pi \ell\ (t'_3 - t_o)}{\ln(r_4/r_3)/k_d + 1/h_a r_4} \cdot \Delta\tau \qquad \text{(A-21)}$$

Steady-State Temperature

The net heat, ΔQ_n, retained by the deforming material is then:

$$\Delta Q_n = \Delta Q_g - \Delta Q_m - \Delta Q_d \cdot \qquad \text{(A-22)}$$

Resultant increase in temperature of the deforming material, when added to initial billet temperature, gives the final billet temperature. Thus,

$$t_f = t_3 + \frac{\Delta Q_n}{\rho C V} \quad . \qquad \text{(A-23)}$$

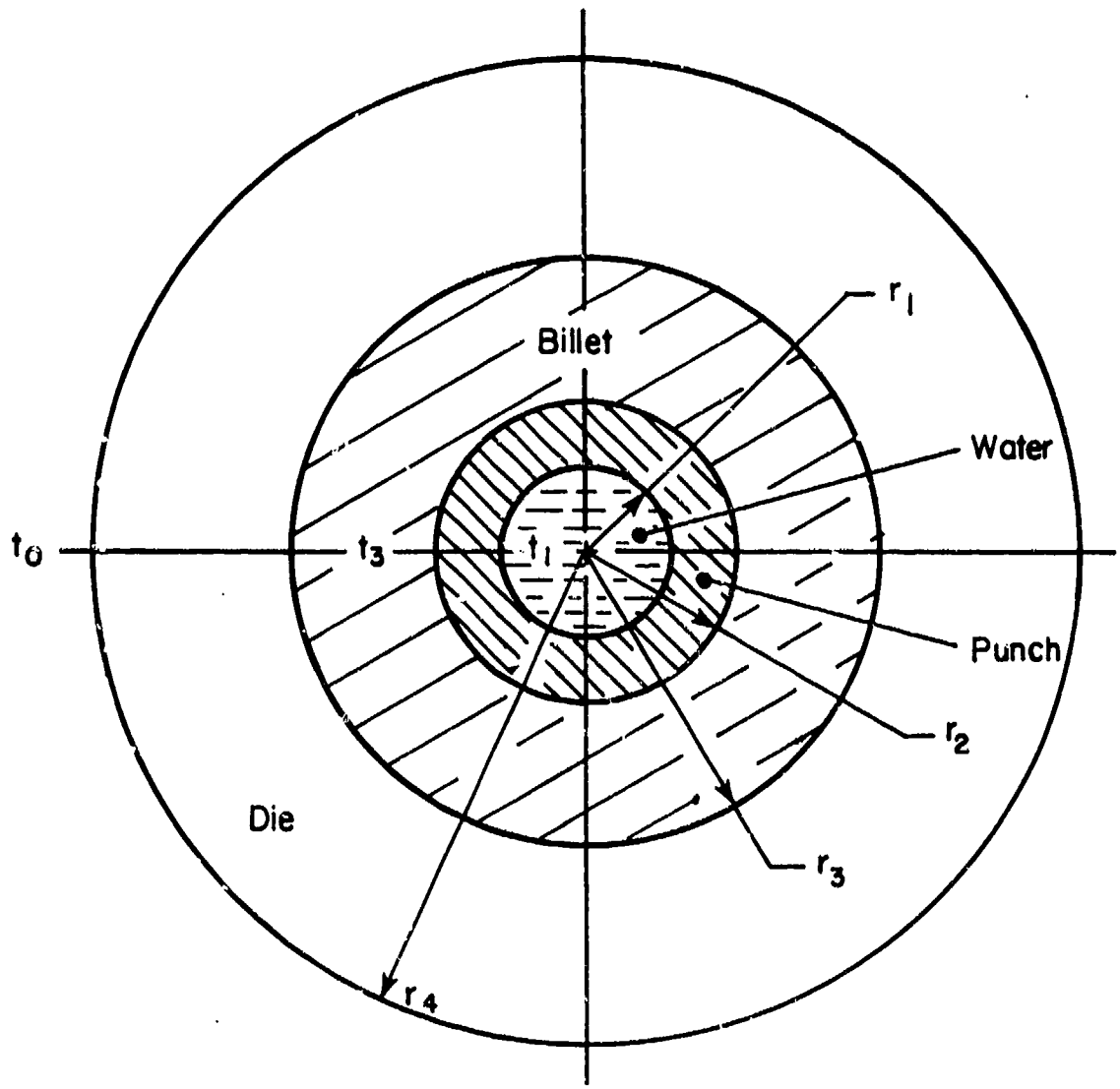

Figure A-4. Model for approximate heat transfer analysis in drawing of shells.

APPENDIX B.

DESCRIPTION OF THE SYSTEM OF COMPUTER PROGRAMS "DRAWNG"

A system of computer programs named DRAWNG, was developed at Battelle Columbus Laboratories to simulate the cold and hot tandem drawing process for producing artillery shells. Using the slab method of analysis, DRAWNG estimates the total ram load and the stress in the wall of the drawn shell at various stages of the process. To simulate the process on a real time basis, step-by-step results are displayed on computer's graphic display terminal as shown in figure B-1. Die configurations, punch position and billet geometry at various stages of the process are shown in the upper one third of the screen. Ram load versus ram displacement and stress in the shell wall versus punch displacement graphs are shown below the die and billet geometries. (Knowledge of the stress in the shell wall is important because the shell wall would fail if wall stress is larger than tensile strength of the shell wall during drawing). The lower portion of the screen is allocated for messages. In the present form, the computer program DRAWNG can be used on a CDC system in the interactive mode only.

Starting Procedure

To run the computer program DRAWNG, its load module file must be prestored in the computer as a cataloged file. After the local log-in procedure, the load module file is attached and executed. Since simulation requires a certain amount of computer time, it is necessary to increase the execution time limit, if the installation default time limit is less than 30 seconds. Also when using the Tektronix 4014 terminal, a "SCREEN, 140" command will be helpful to avoid overwriting. Thus, in a CDC system, the total starting procedure should involve inputting the following commands:

PLEASE LOGIN login
ENTER USER'S NAME user
ENTER PASSWORD password
COMMAND - et1,30
COMMAND - screen.140
COMMAND - attach,d,file name, ID=file id
COMMAND - d

In the above example, all computer commands are shown in upper case letters while the user's responses are underlined. If the starting procedure has been correctly followed, the computer will, after erasing the screen, respond with the message:

PROGRAM TESTING: DRAWING SIMULATION

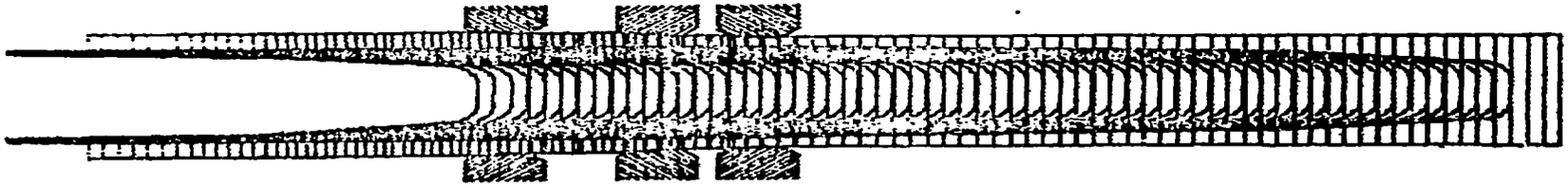

MATERIAL: STEEL 1045 NO. OF SIMULATION STEPS: 67
RAM SPEED: 80. INCH/MIN DRAWING TEMPERATURE: 2000.00 F

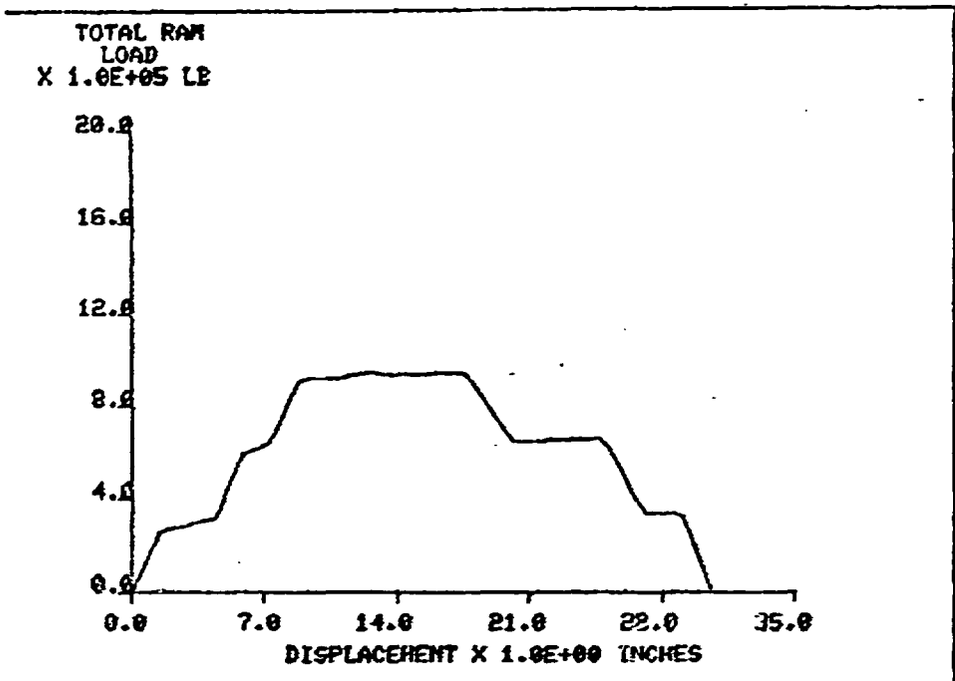

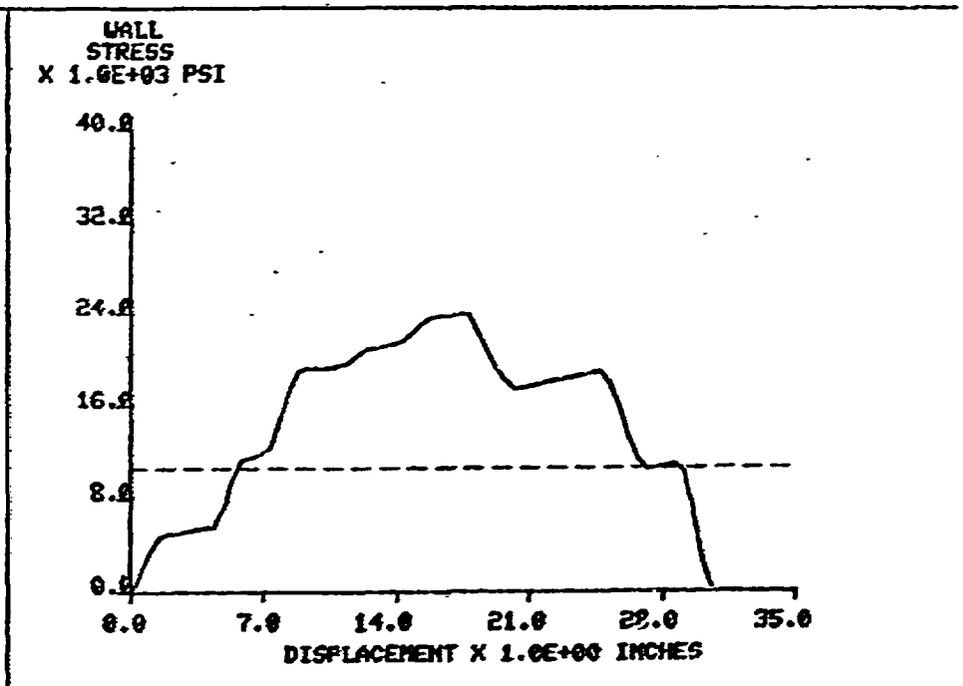

** WARNING ** ESTIMATED DRAWING PRESSURE IS MORE THAN THE FLOW STRESS

ENTER 1 TO DISPLAY DIE - PUNCH GEOMETRIES ON FULL SCREEN
2 RAM LOAD - DISPLACENT GRAPH
3 WALL STRESS - DISPLACEMENT GRAPH
0 NOT TO DISPLAY ANY PLOT ON FULL SCREEN

TO VIEW MORE THAN ONE PLOT ON FULL SCREEN, ENTER ANY
COMBINATION OF 1, 2, AND 3 123

THE PRESENT SIMULATION HAS 67 STEPS

ENTER THE SIMULATION STEP NUMBER, TO DISPLAY
THE PUNCH AND THE BILLET AT THE END THAT STEP
ENTER 999, TO DISPLAY ALL STEPS. OR,
ENTER 0, NOT TO DISPLAY ANY STEP

Figure B-1. Simulation of tandem drawing on a CRT screen.

WELCOME TO -DRAWNG- A SYSTEM OF PROGRAMS TO SIMULATE
TANDEM DRAWING OF SHELLS.

Inputting Die and Punch Geometries

Die and punch geometries for the tandem drawing simulation can either be read from a prestored data file or entered through the keyboard of the interactive terminal. Hence, after the welcome message, the computer displays the question

WANT TO READ THE DIE AND PUNCH GEOMETRIES THROUGH THE KEYBOARD?
ENTER YES OR NO.

Input From the Data File

To read data from the data file, the data file should be prepared in a special format as described below and prestored in the computer as a cataloged file. Prior to execution of the load module of DRAWNG, the data file should be attached under a local file name TAPE4.

Format of the data file is in 80 column card images or records. The first record is the title for the plots, and may contain any alpha numeric or special characters up to a maximum of 80 characters. The second record contains the number of dies and the number of points in each die in an I10 format. That is, the number of dies is entered in column 10. There can be a maximum of five dies. In columns 20, 30, ..., the number of points in the first, second, ... dies are entered. Each die can have a maximum number of ten points. In defining the die, only points on surfaces which will be in direct contact with the shell are specified. The remaining portion of the die is automatically appended by DRAWNG. For example, the die shown in figure B-2, is defined by points 3, 4 and 5 only. Points 1, 2, 6, and 7 are added by DRAWNG.

The third record contains the X and Y coordinates of points, describing the die surface, in an 8F10.4 format. That is, the X coordinate of the first point is entered between columns 1 and 10 and the Y coordinate between columns 11 and 20. If a decimal point is not present in any one of the first ten columns, the digits appearing in columns 7 to 10 will be considered as being to the right of the decimal point. For example, a 51321 in columns 6 to 10 will be read as 5.1321, whereas the same 51321 in columns 1 to 5 will be read as 51321.0. On the other hand, a 51.321 anywhere in

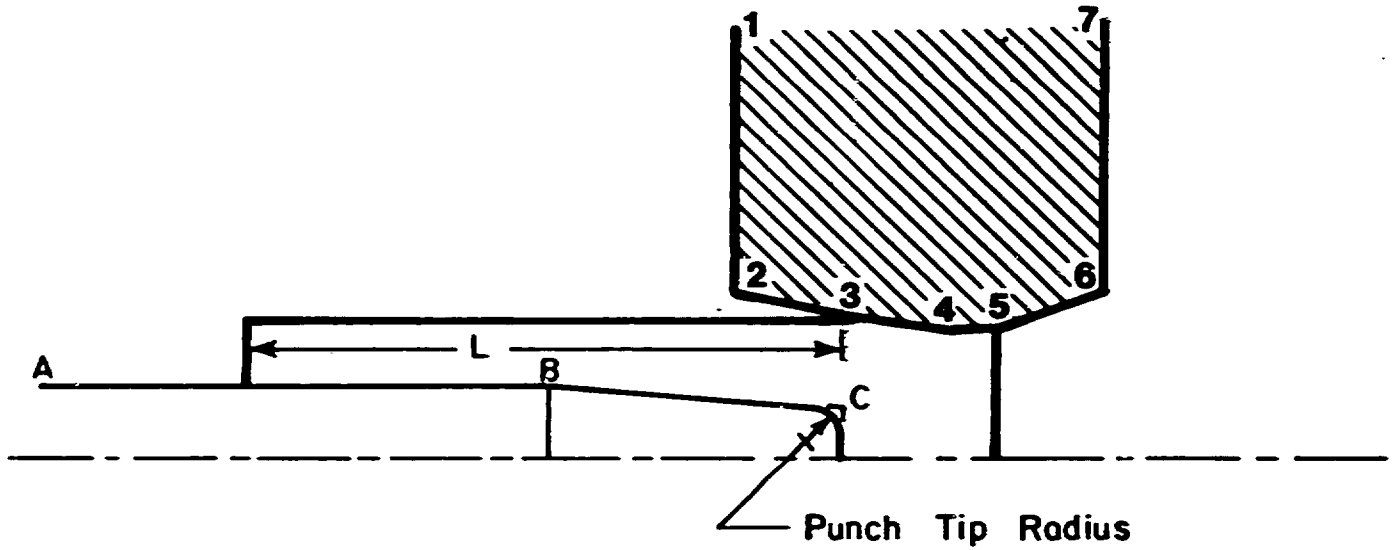

Figure B-2. Definition of die, billet, and punch geometries for simulation.

the first ten columns will be read as 51.321. The X and Y coordinates of the second point are entered between columns 21 and 30, and 31 and 40 respectively; and so on. If the first die has more than 4 points, the X and Y coordinates of the fifth point are entered between columns 1 and 10 and columns 11 and 20 of the next card, i.e. the next record. All points should be sequenced from left to right.

Similarly, the coordinates of the other dies are recorded with the same 8F10.4 format in subsequent records. In order to be specific about the relative positions of the dies, it is imperative that the same coordinate system be used to define points on all dies.

The next and fourth record in the data file contains the number of points on the punch in an I10 format. Due to symmetry about the axis, only points above the axis are supplied. DRAWNG adds additional points to define the lower half of the punch. Thus, to define the punch shown in figure B-2, it is sufficient to specify the points A, B, and C. Hence a 3 should be entered in column 10 of the next record. Total number of points to define the punch should not exceed 10. The next record contains the X and Y coordinates of points A, B, C ... in an 8F10.4 format. And, the last record contains the punch tip radius, figure B-2, and punch inner diameter in 2F10.4 format. The coordinate system used to define the points on the punch need not be the same as that used to define the dies. However, the units used should be the same in both cases.

At the beginning of the simulation, DRAWNG positions the front end of the punch to be in flush with the first effective point on the first die as shown in figure B-2. The billet configuration is defined only by its length, L, shown in figure B-2. The front end of the billet is assumed to have a boat tail which conforms the geometry of the first die as seen in figure B-2.

Input Through the Keyboard

The same data set on die and punch geometries can be read in through the key board also. If the answer to the question "WANT TO READ THE DIE AND PUNCH GEOMETRIES?" is yes, DRAWNG displays a number of appropriate messages to direct the user for proper input and reads the data. If the data set is small, it will be advantageous to read it through the keyboard.

Process Variables

After reading die and punch geometries, DRAWNG reads process variables via the namelist PRODAT. Supplying data by namelist has one major advantage. In namelist inputs, only those variables that need changing are assigned new values. For this reason, almost all variables included in a namelist are assigned default values by the system. Hence, even though a namelist may contain several variables, new values would have to be assigned to only a few of these.

When entering data by namelists, the first column is always left blank. Following a $ sign in the second column, the namelist name PRODAT, is entered without any embedded blanks. Following at least one blank space after the name PRODAT, various parameters are entered and are equated to their values with commas between each parameter. The order in which parameters appear within a namelist input is immaterial. Namelist data listing is terminated by another $ sign.

To help the user to type the name of the namelist correctly, a message containing the name of the namelist, such as "ENTER PRODAT VARIABLE LIST" is displayed prior to the namelist input. If a wrong name is entered, or the name is misspelled, there will be no response from the computer.

To inform the user as to the names of all variables included in the namelist, a list of names, as shown below is also displayed:
$PRODAT MATERL, NSMSTP, DELTAZ, RAMSPD, DRWTMP, COOLNT, AMBTMP, FSTRES, FFID, FFOD, FFBTWN, BILLET, INPRNT, .ISTATS.$
In the above list, ISTATS is a logical variable and is identified by period marks (.) before and after the variable name.

The following is the list of descriptions of the variables in alphabetical order. Following each description, units, wherever applicable, are given in brackets. Default values, if any, are given in parentheses.

AMBTMP Ambient temperature [F] (70.0)

BILLET Billet length, L, as shown in figure B-2 [inch]

COOLNT Coolant temperature [F] (70.0)

DELTAZ Incremental step for simulation [inch] (0.100)

DRWTMP Drawing temperature [F] (70)

FFBTWN Friction factor between the billet and the punch outside of the deformation zone under the die (0.01)

FFID Friction factor between the billet and the punch inside the

deformation zone, under the die (C.40)

FFOD — Friction factor between the billet and the die (0.20)

FSTRES — Flow stress in the deforming material. Used only when flow stress characteristics of the billet material are not known. Then, an approximate average value is assigned to FSTRES. FSTRES is valid only when MATERL = 0. Refer to the description of MATERL below. [psi] (1000)

IPRNT — If the final results are not as expected, intermediate results may be obtained by setting values greater than zero to the variable IPRNT. When IPRNT is set to 1, the following results are written on a separate file, named TAPE3, which may be disposed to a line printer at the end of program execution. Results written on TAPE3 are:

1. Punch and die geometries as read in
2. Process variables as read in
3. At each step of simulation,
   - (a) simulation step number
   - (b) pointers identifying the deformation elements
   - (c) coordinates of the corners of the deformation elements and the stress in each element, and
   - (d) total ram load.

ISTATS — A logical variable. When set to true, current values of the variables in the namelist PRODAT will be listed. Also, the user will be given a chance to modify any of these values as necessary.

MATERL — Material code. Flow stress as a function of strain, strain rate and temperature for different materials can be stored in DRAWNG. By assigning a suitable number to the material code, MATERL, appropriate flow stress in the material under study can be obtained. Currently DRAWNG has flow stress data for steel AISI 1045, for which the material code is 1. Flow stress data for steels AISI 9260, 52100 or any other material can be stored without any change in the program structure.

NSMSTP — Number of simulation steps. Number of simulation steps preformed in one operation may be limited by assigning a value to NSMSTP. If NSMSTP is not assigned a value, DRAWNG automatically assigns a value to NSMSTP, equal to the number of steps required to draw the entire billet through all dies.

RAMSPD — Ram speed. [inch/min] (100.).

DRAWING SIMULATION

After the namelist PRODAT is read, simulation of the drawing operation begins. As the process continues, the die geometry, instantaneous punch position, the deforming billet geometry, ram load versus ram displacement and wall stress versus ram displacement plots are all displayed as shown in figure B-1.

At the end of the simulation, the following message is displayed at the bottom of the screen:

ENTER 1 TO DISPLAY DIE-PUNCH GEOMETRIES ON FULL SCREEN
2 RAM LOAD-DISPLACEMENT GRAPH
3 WALL STRESS-DISPLACEMENT
0 NOT TO DISPLAY ANY PLOT ON FULL SCREEN
To REVIEW MORE THAN ONE PLOT ON FULL SCREEN, ENTER ANY COMBINATION OF 1, 2 AND 3.

When 1 is selected, the following message also appears at the bottom of the screen:

THE PRESENT SIMULATION HAS XXX STEPS. ENTER THE SIMULATION STEP NUMBER, TO DISPLAY THE PUNCH AND THE BILLET AT THE END OF THAT STEP.
ENTER 999, TO DISPLAY ALL STEPS, OR ENTER 0, NOT TO DISPLAY ANY STEP.

Upon entering a number greater than zero and less than XXX, the actual number of simulation step, die, punch and billet geometries at the beginning and at the end of the specified simulation step will be displayed as seen in figure B-3. If 2 and 3 were also selected, the load-displacement and stress-displacement plots will be displayed on the full screen as seen in figures B-4 and B-5 respectively.

Although the computer program DRAWNG is developed for the simulation of tandem drawing, the same program can also be used to simulate the single die drawing operation as seen in figure B-6.

PROGRAM TESTING: DRAWING SIMULATION

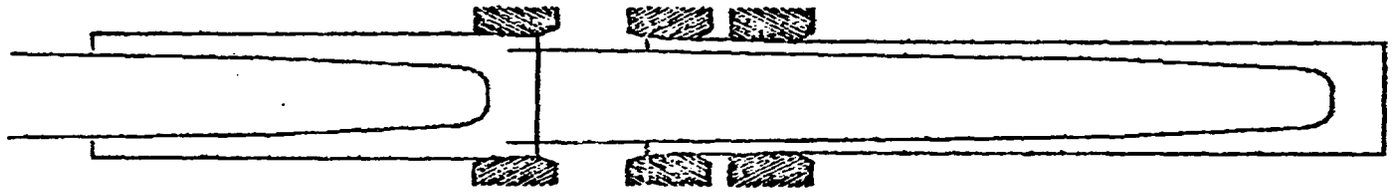

AT THE END OF SIMULATION STEP 50

MATERIAL: STEEL 1045 NO. OF SIMULATION STEPS: 67
RAM SPEED: 80. INCH/MIN DRAWING TEMPERATURE: 2000.00 F

TO CONTINUE, TYPE ANY CHARACTER AND STRIKE THE RETURN KEY

Figure B-3. Die and punch geometries on a full screen.

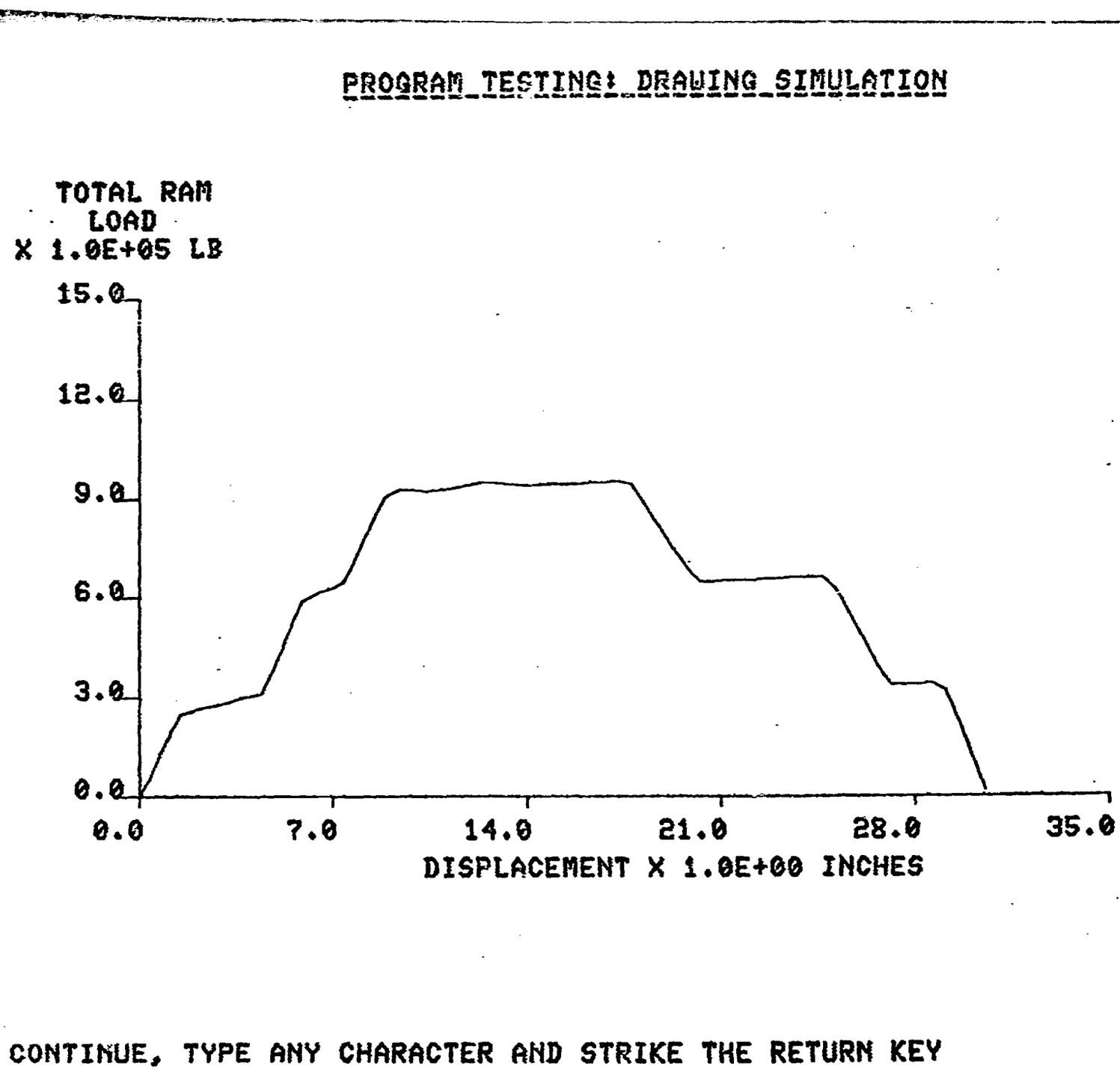

Figure B-4. Load-displacement plot on a full screen.

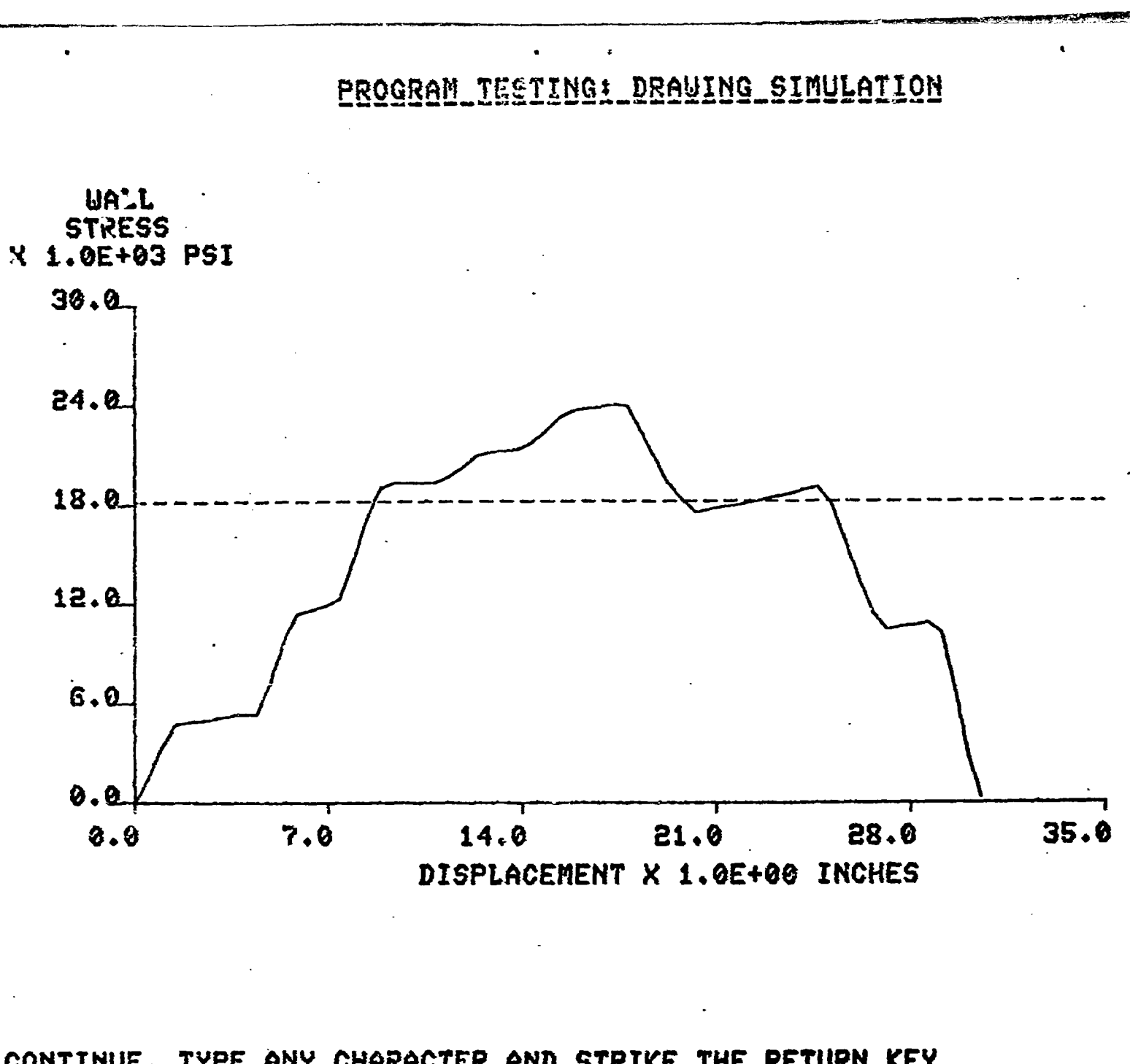

Figure B-5. Wall stress-ram displacement plot on a full screen.

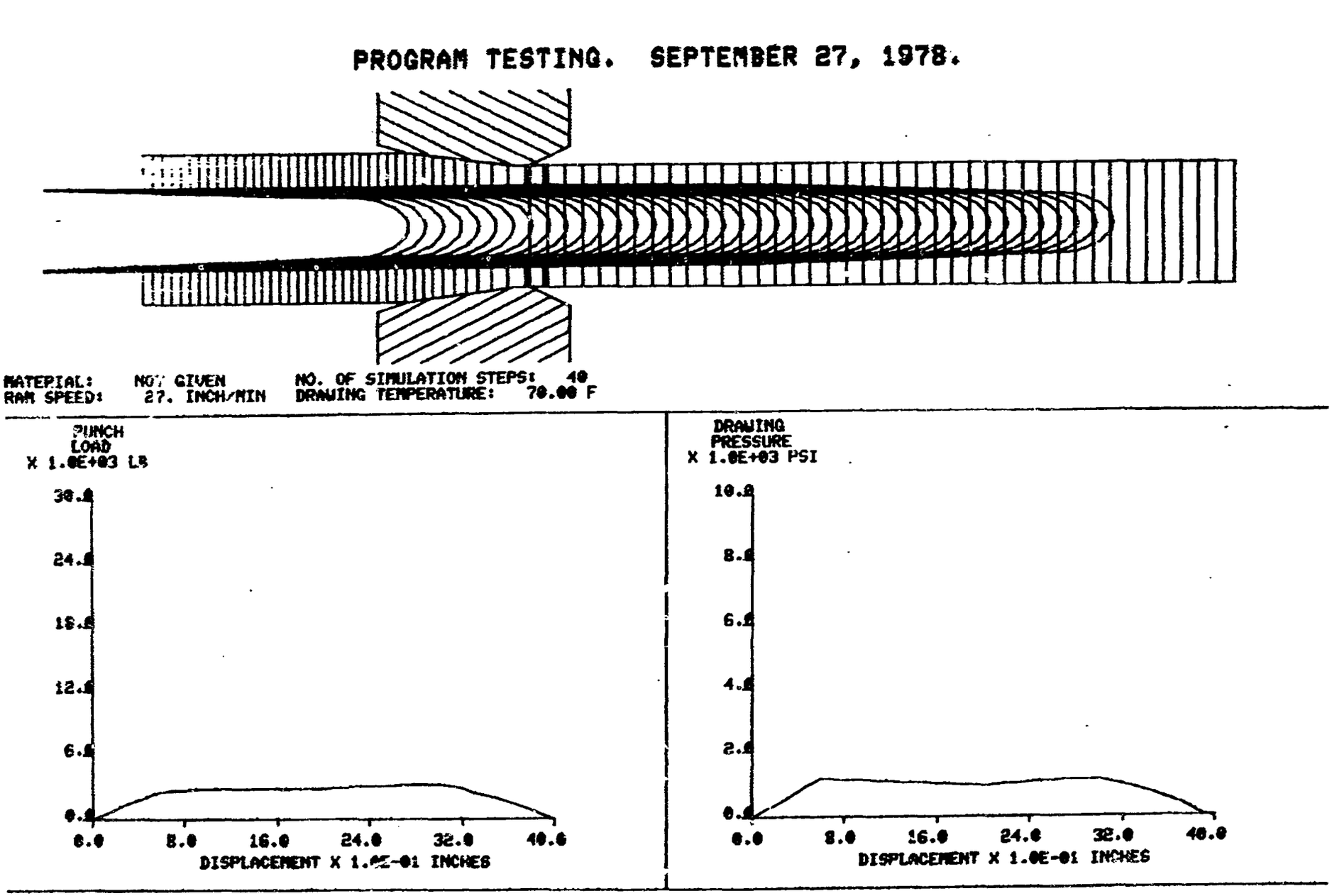

Figure B-6. Simulation of a single die drawing.

APPENDIX C.

DESIGN OF STREAMLINED DIES FOR COLD AND HOT DRAWING

The general practice in industry is to use dies of conical shape for drawing of shells. Conical die shape has the advantage of being easy to manufacture. The bore of the conical shaped die can be machined without, ordinarily, any copying attachments on the boring machine by setting the required angle. However, an analysis of stresses acting along the drawn (ironed) wall shows that the chances of punch through are higher in the case of shells drawn through conical shaped dies than the shells drawn through streamlined dies. The object of this task was, therefore, to design dies with double curvature and dies whose inner contour is described by a higher degree polynomial-referred henceforth as double curvature dies and polynomial dies. The set task was carried out by optimizing the force requirements using the computer program CDVEL developed earlier (ref. 1). The processes considered for optimization were cold drawing of 4.2-in. M335 shell and hot drawing of 155 mm M107 shell.

Dies for Cold Drawing of M335 Shell

Figure C-1 shows the die configuration for the first drawing die used in the final double draw. The die entry angle has been chosen as 5 degrees to accommodate for the double curvature. It is, however, to be noted that this angle could be increased without affecting the performance of the die. The die has been designed in such a way to ensure proper blending of the top curvature, namely the curvature with 40 mm radius, with the straight conical portion of the entry angle of 5 degrees. This condition has been ensured for all the die designs described in this appendix. If it is desired that the die entry angle be changed, sufficient care has to be taken to blend the increased (or decreased) taper with the top curvature.

Figures C-2 and C-3 show the die configuration for (i) a double curvature profile and (ii) a polynomial profile curvature. These two dies were designed for combined reduction of the first and the second draws of the final double draw. Since the ratio of the wall stress to the flow stress in the product was between 0.9 and 0.94, it was felt that the two stages of the final double draw can be combined in a single pass.

The curvature for the polynomial profile between the linear distances of 20 mm and 36 mm along the thickness of the die, with the 20 mm point as the

All dimensions in mm. (Dimensions in brackets are in inches.)

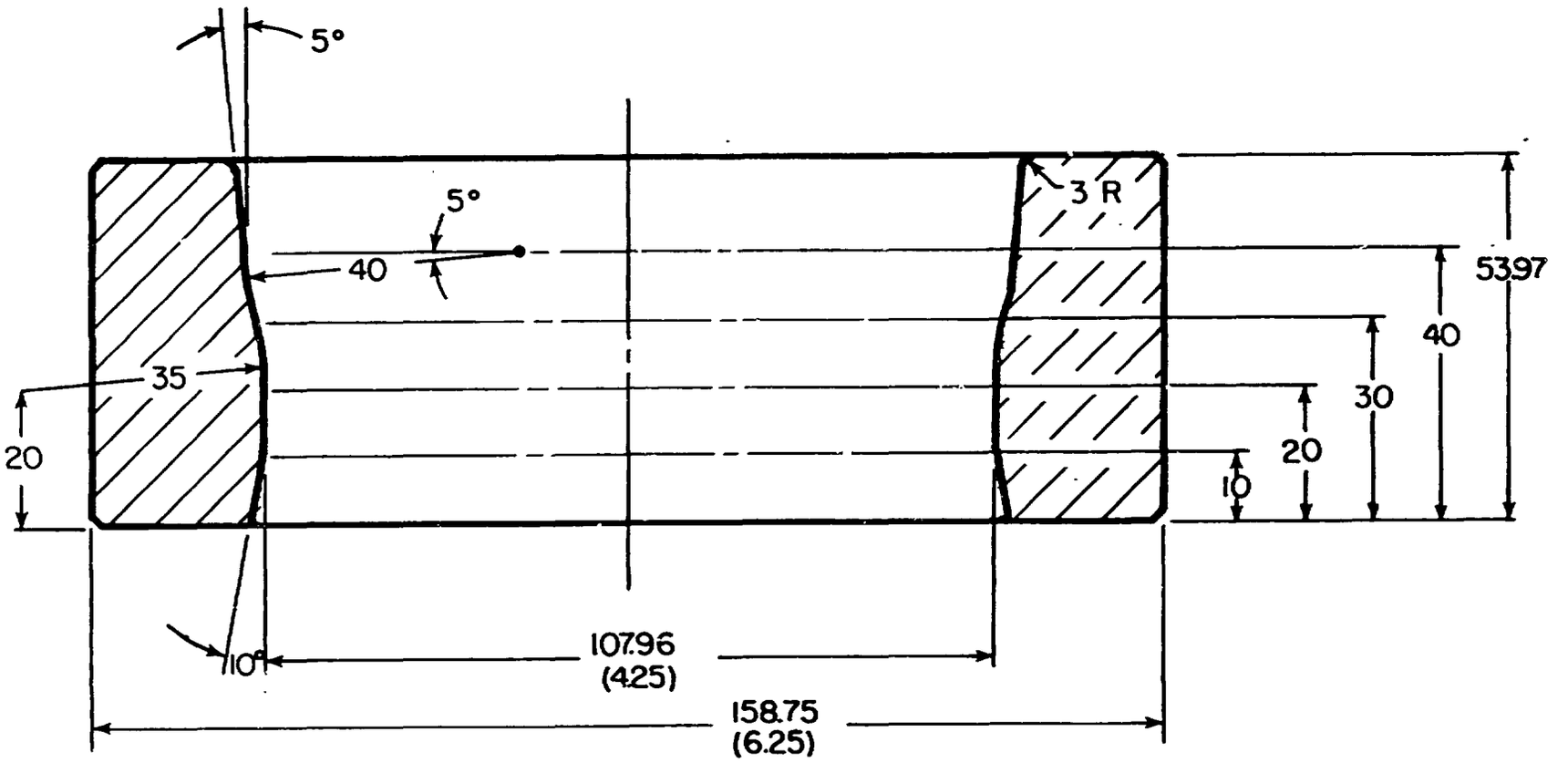

Figure C-1. Double curvature die shape of 107 mm, M335 shell (first ring, final double draw).

datum and the value of 'Z' measured positive from this point in the vertical direction, is described by:

$$r = 56.64 - 0.1226.10^{-2} (21.2 - Z)^3 + 0.437.10^{-4} (21.2 - Z)^4 \text{ (mm)} \qquad \text{(C-1)}$$

Dies for Hot Drawing of M107 Shell

Billet temperature for hot drawing was assumed to be 1100° C for the optimization process. The die designs with the double curvature profile for the three stages of hot drawing are shown in figures C-4 to C-6. For all these cases, the height of the die was maintained at 62.5 mm (2.5 in.). A compound entry angle (10 degrees and 5 degrees) has been used in this design. Die design also ensures proper blending of all transition points. Height of the die can be reduced in the top portion, if necessary, without affecting the performance of the dies. The outer diameter of the dies was maintained at 186.6 mm for all the three stages and this dimension also corresponds to the die outer diameter used currently for the hot drawing operation.

Dies with polynomial profile were also designed for the first and the second draw operations. As the reduction for the third stage is small, the design for this stage with the polynomial curve was not carried out. Figures C-7 and C-8 show the die configurations with polynomial profile for the first and the second draw respectively.

The polynomial profile for the first hot drawing operation shown in figure C-7 is described by the following equation between the linear distances 17 mm and 41.5 mm, with the Z direction being positive in the vertical direction with the reference point (Z=0) at 17 mm;

$$r = 90.17 - 1.382.10^{-3} (24.5 - Z)^3 + 4.23.10^{-5} (24.5 - Z)^4 \text{ (mm)} \qquad \text{(C-2)}$$

Similarly, for the polynomial die profile of the second hot draw operation shown in figure C-8, the die profile between the linear distances of 17 mm and 36.1 mm, with the Z direction being positive in the vertical direction and the point corresponding to 17 mm as the reference (Z=0), is described by:

$$r = 85.09 - 1.458.10^{-3} (19.1 - Z)^3 + 5.726.10^{-5} (19.1 - Z)^4 \text{ (mm)} \qquad \text{(C-3)}$$

The possibility of combining one or more of stages of hot drawing was also tried out by using the computer program CDVEL. Results revealed changes

All dimensions in mm. (Dimensions in brackets are in inches.)

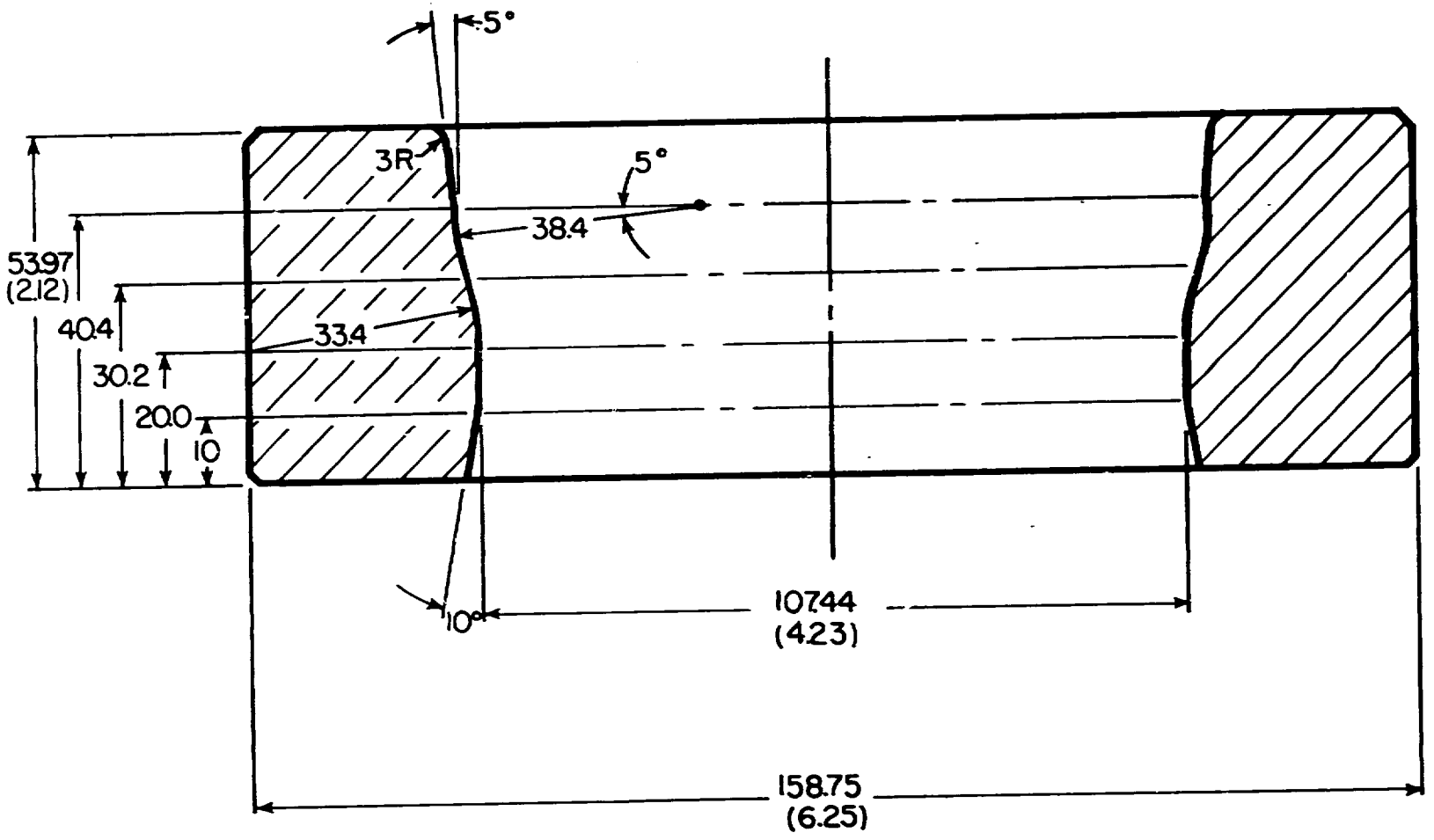

Figure C-2. Double curvature profile for cold drawing of M335 shell (combined first and second draw - final double draw).

All dimensions in mm. (Dimensions in brackets are in inches.)

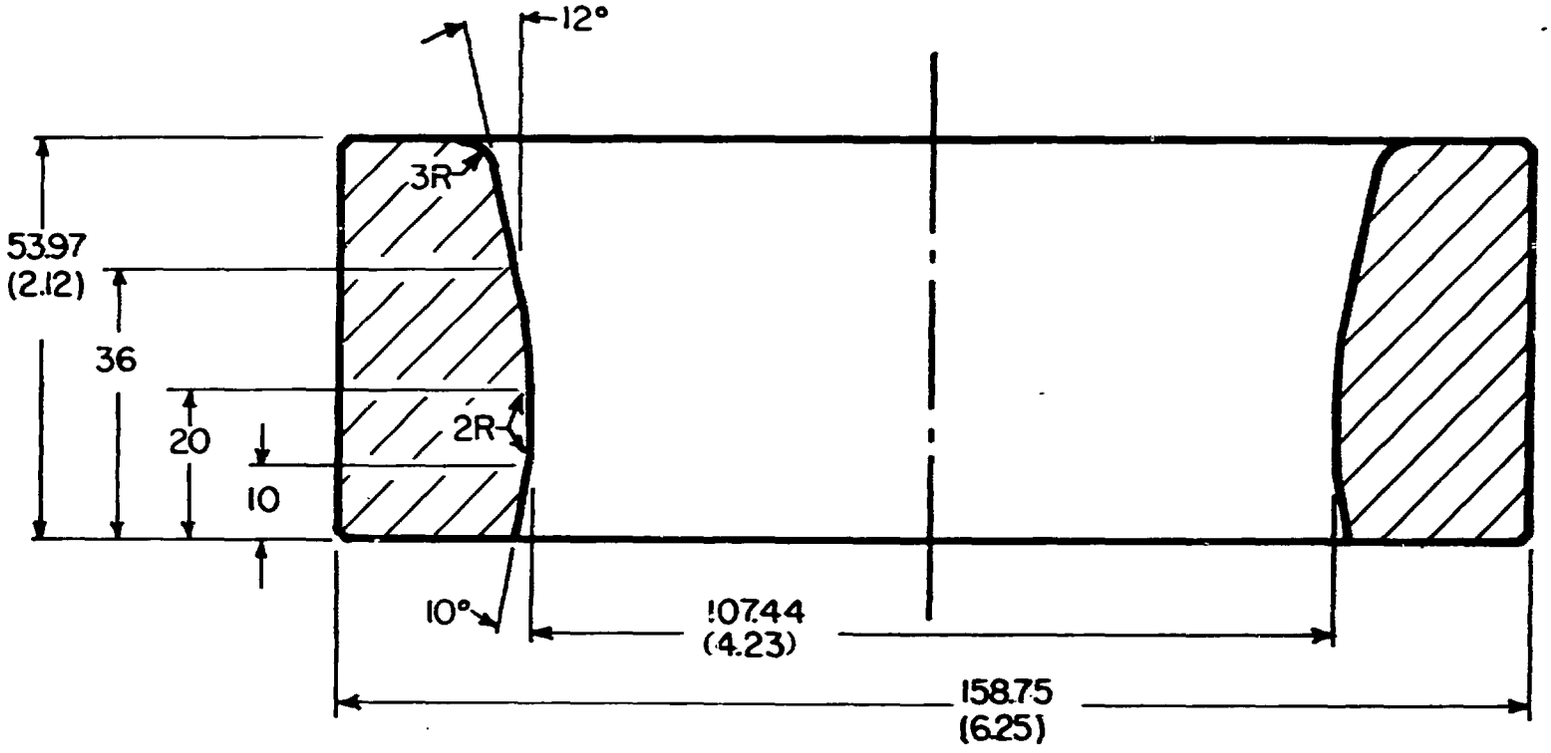

Figure C-3. Polynomial profile for cold drawing of M335 shell (combined first and second draw - final double draw).

All dimensions are in mm. (Dimensions in brackets are in inches.)

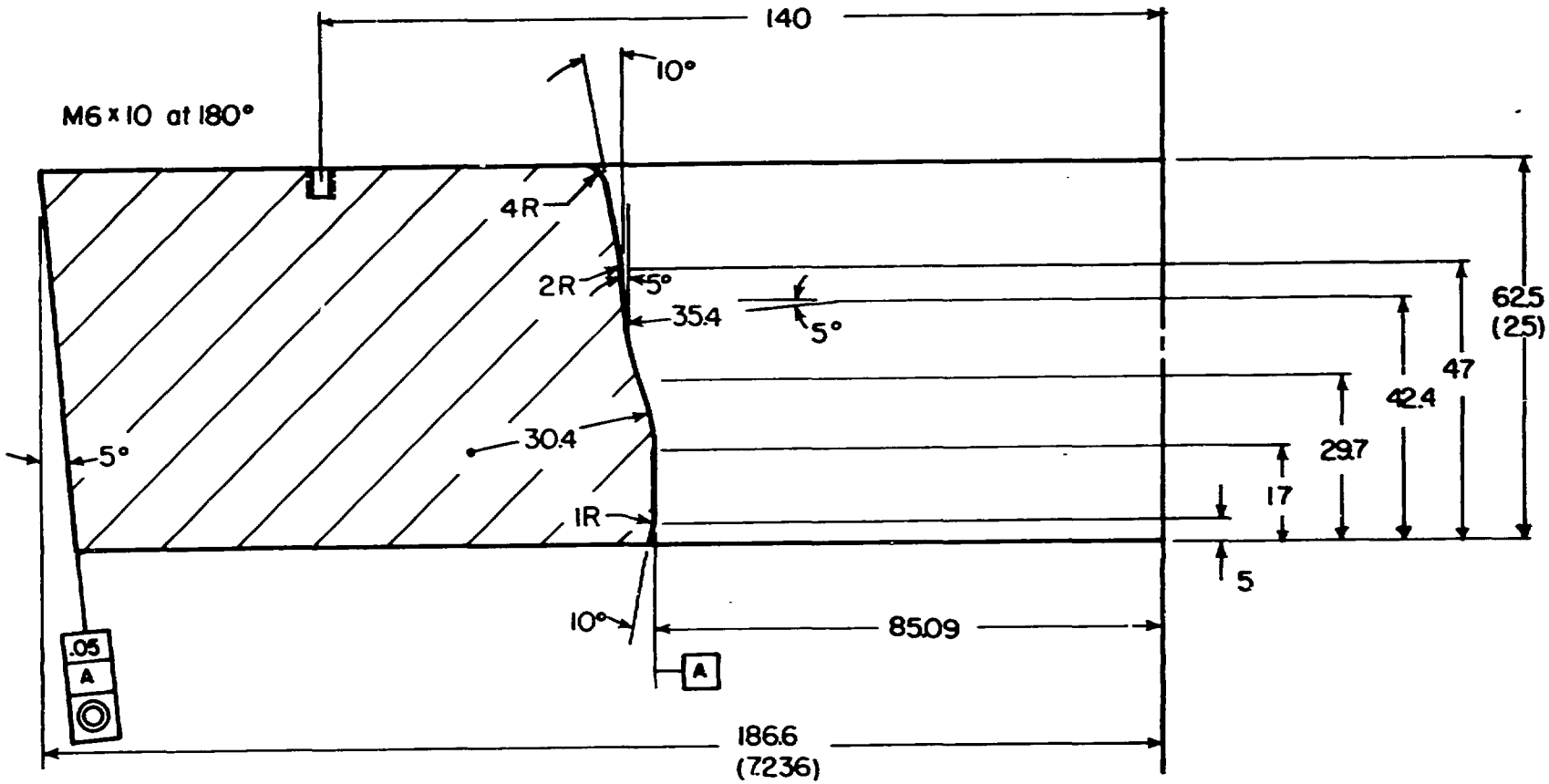

Figure C-4. Double curvature die shape for hot drawing of M107 shell (first draw operation).

All dimensions are in mm. (Dimensions in brackets are in inches.)

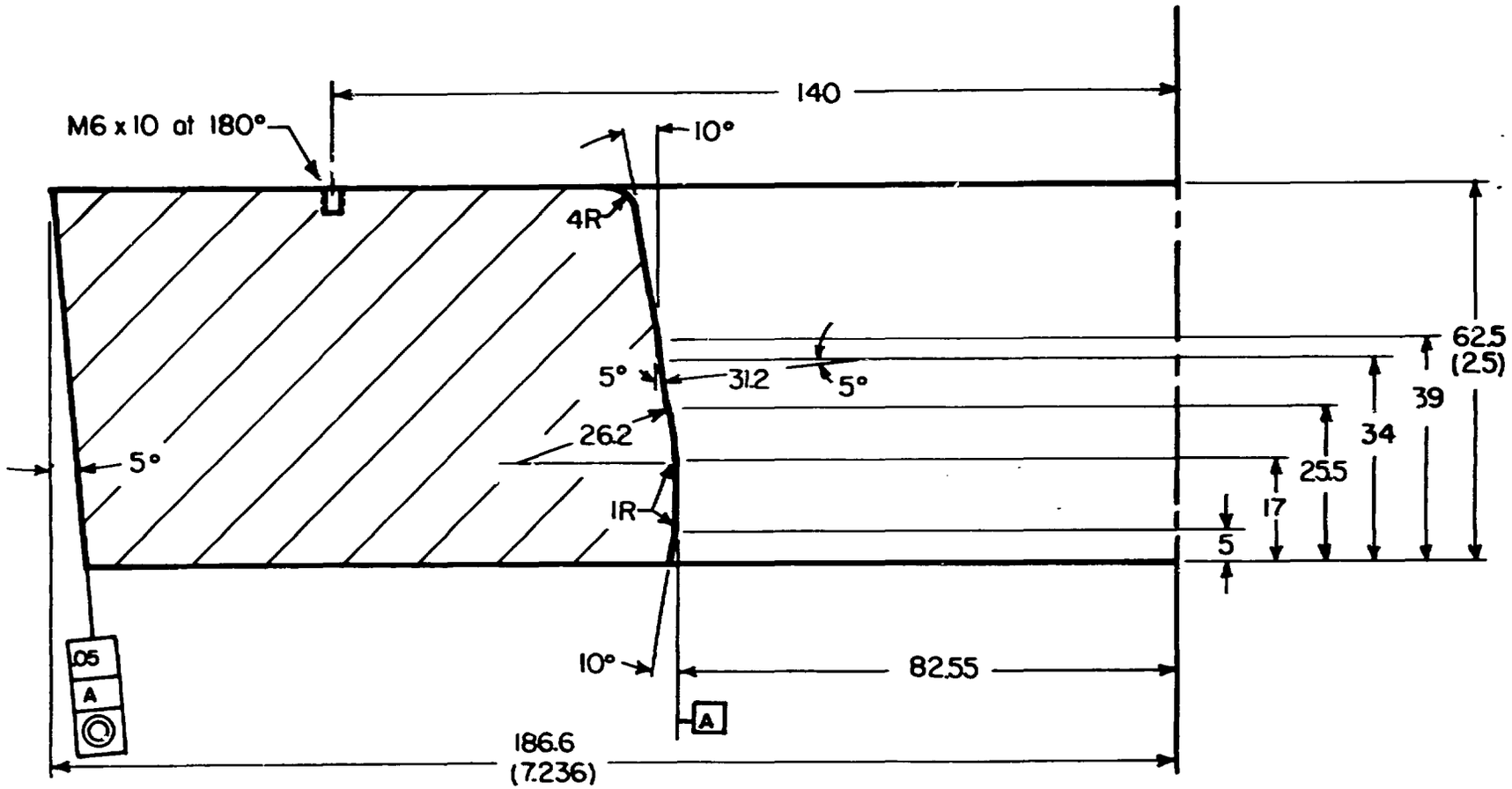

Figure C-5. Double curvature die shape for hot drawing of M107 shell (single draw operation).

All dimensions are in mm. (Dimensions in brackets are in inches.)

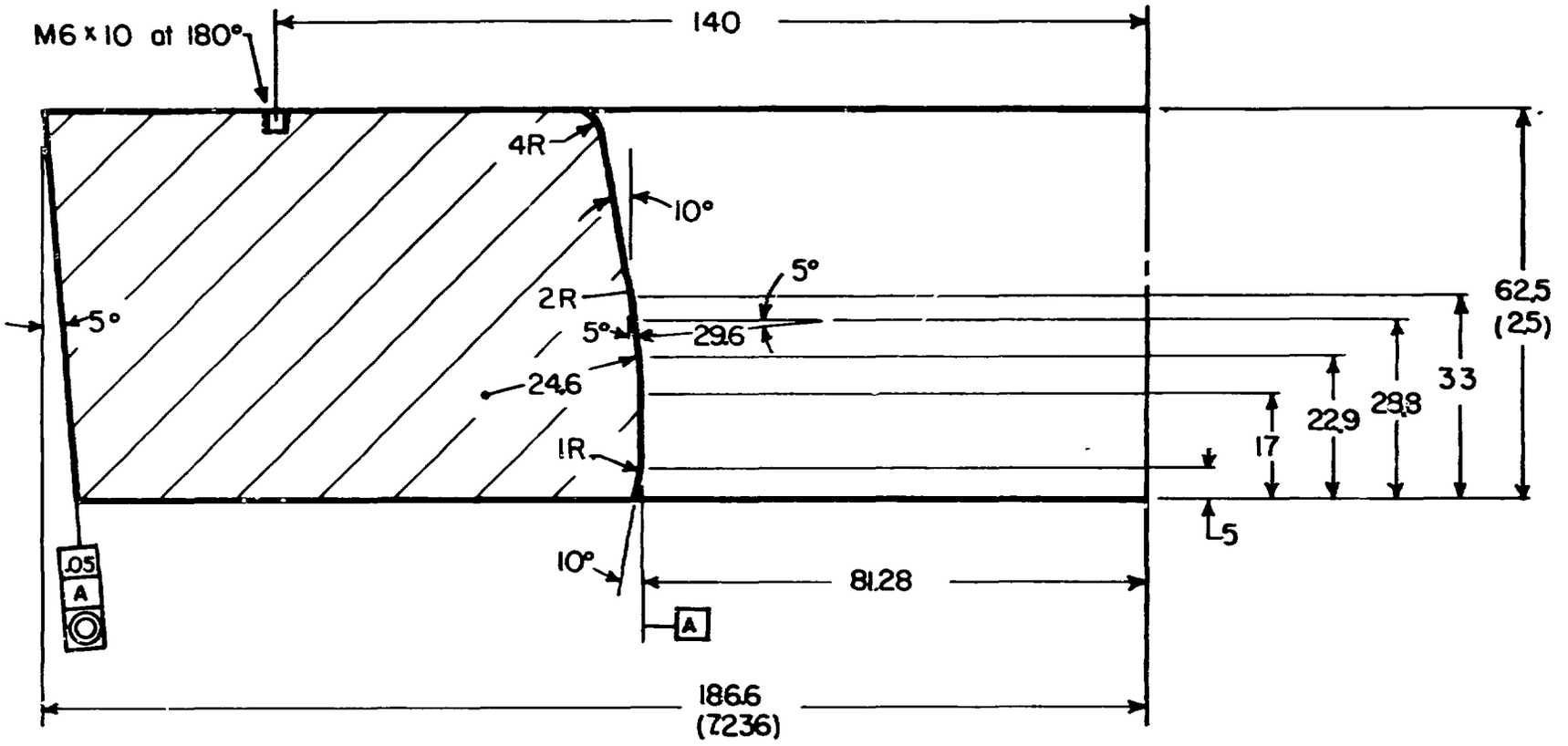

Figure C-6. Double curvature die shape for hot drawing of M107 shell (final draw operation).

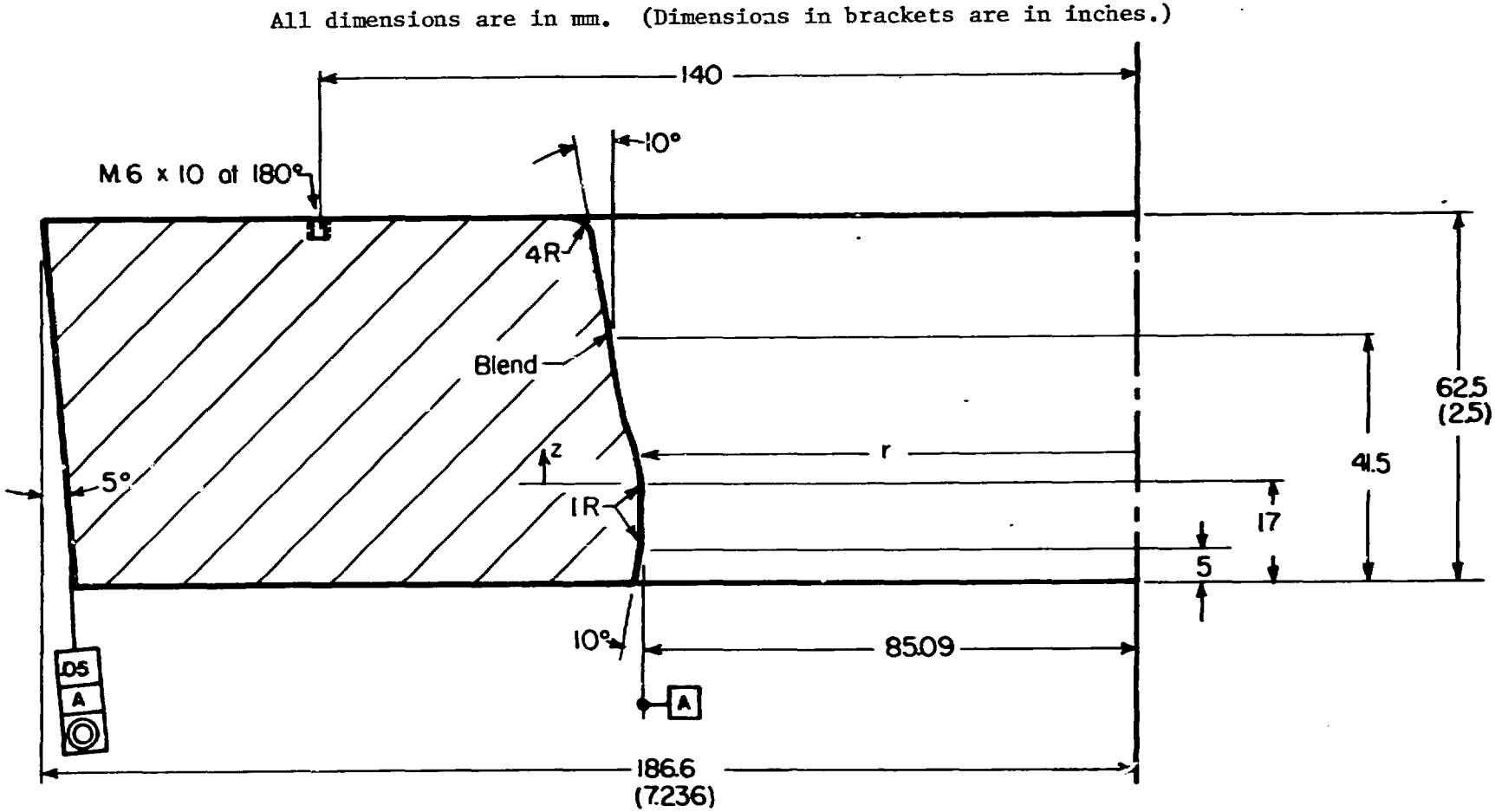

Figure C-7. Polynomial die shape for hot drawing of M107 shell (first draw operation).

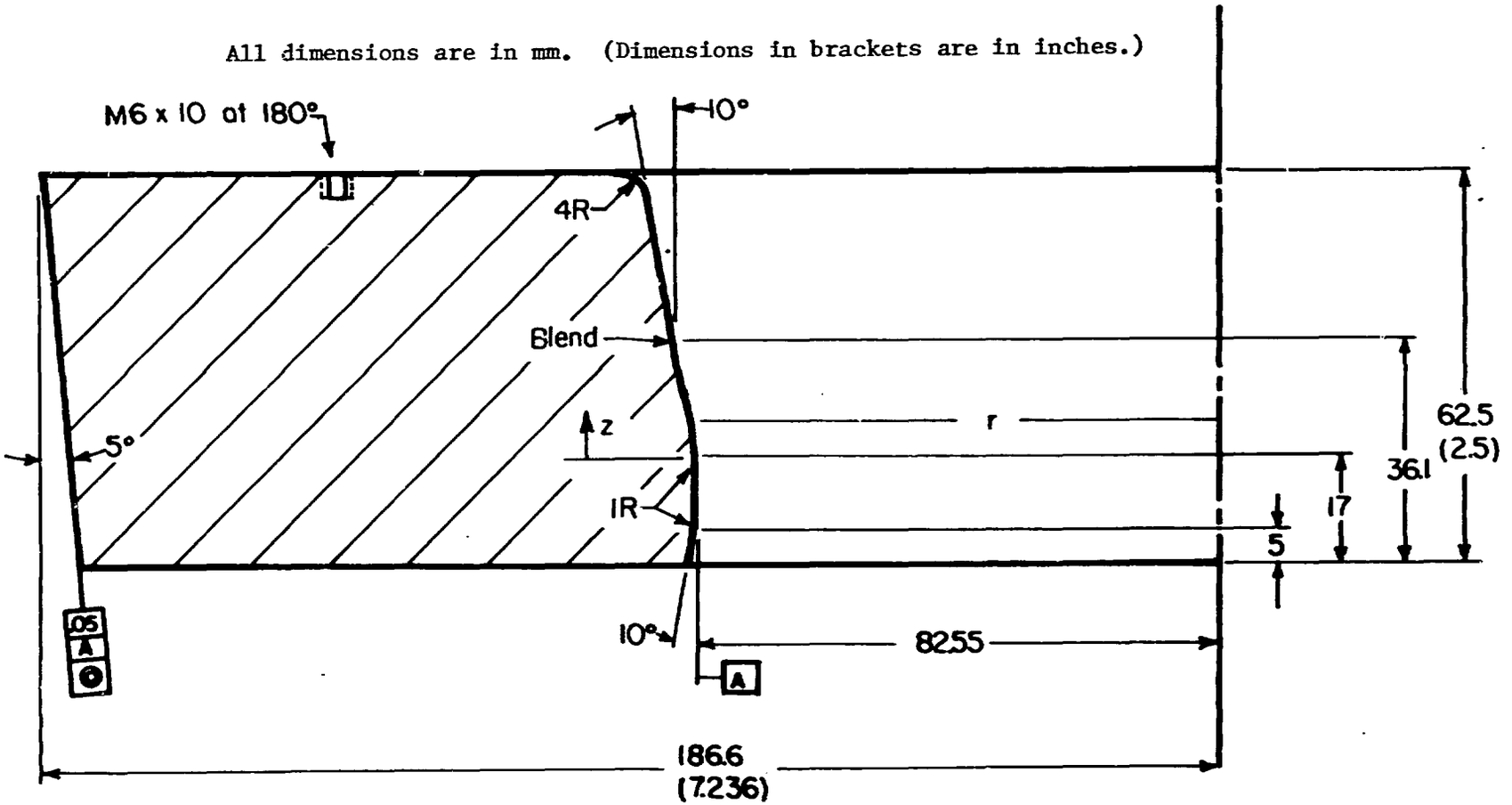

Figure C-8. Polynomial die shape for hot drawing of M107 shell (second draw operation).

of punch through are enhanced when the stages 1 and 2 or 2 and 3 are combined to be done in one pass. Hence, further optimization work was not carried out.

The input data used for the design of dies for both cold and hot drawing and the force requirements for the dies designed (shown in figures C-1 to C-8) are tabulated in Tables C-1 and C-2.

Manufacture of Templates

Drawings of templates of all the dies shown in figures C-1 to C-8 are shown in figures C-9 to C-16. It was decided to use only the double curvature profile dies on the production run initially. Hence, five templates (figures C-9, C-10, C-12, C-13, and C-14) - two for cold drawing and three for hot drawing - were manufactured using a CNC Milling machine at Battelle's Columbus Laboratories.

Plates of 114.3 mm (4.5 in.) x 114.3 mm (4.5 in.) x 3.18 mm (0.25 in.) were used for cold drawing process, and plates of 114.3 mm (4.5 in.) x 114.3 mm (4.5 in.) x 6.35 mm (0.25 in.) were used for the hot drawing process. Schematic representation of the machining process can be seen in figure C-17. The origin of reference (0,0,0) was taken at a point where the die land ends and at a distance away from this point equal to the final radius of the part to be drawn depending on the drawing stage under consideration. It was also ensured before the start of the machining operation that the two edges, namely the reference edge and the edge to be machined, are parallel. The template was clamped on the bed of the machine and a 6.35 mm (0.25 in.) cutter was used to machine the template contour. Initial cuts were rough and a finishing cut was done on all templates to obtain a smooth surface. The computer program was, however, written for the final dimensions of the template only, and the intermediate machining cuts were obtained by a manual setting on the machine using some known offsets and by using the same program. The NC-programs used for the five templates are given in figures C-18 to C-22. These programs are also available on tapes and hence templates to this shape can be manufactured at any time.

Table C-1. Dimensions of billet/interstages/final product.

Dimensions of the Billet/ Interstages/Finished Product	Cold Drawing			Hot Drawing		
	Figure References	mm	in.	Figure References	mm	in.
Outside radius of the billet before first draw	C-1, C-2, C-3	56.64	2.230	C-4, C-7	90.17	3.55
Outside radius of the shell after first draw	C-1	53.98	2.125	C-4/C-5 C-7/C-8	85.09	3.35
Outer radius of the shell after second draw				C-5/C-6 C-8	82.55	3.25
Outer radius of the shell after finish draw	C-2, C-3	53.78	2.117	C-6	81.28	3.20
Inner radius of the shell after finish draw	C-2, C-3	48.59	1.913	C-6	61.60	2.425

Table C-2. Input variables and force requirements for various die designs.

Force Requirements	Cold Drawing	Hot Drawing
Process Variables		
Initial temperature of the billet, C (F)	20 (68)	1100 (2012)
Axial velocity of punch, mm/s (in/s)	100 (4)	465 (18.3)
Friction shear factor at shell-die interface	0.05	0.80
Friction shear factor at shell-punch interface	0.05	0.75
Double Curvature Die		
First Stage, kN (t)	1330 (30.8)	1843 (42.7)
Second Stage, kN (t)		983 (22.8)
Third Stage, kN (t)		557 (12.9)
Combined Draw (first and second stage)	1494 (34.6)	
Polynomial Profile Die		
First Stage kN (t)		1780 (41.2)
Second Stage kN (t)		947 (21.9)
Combined Draw (first and second stage) kN (t)	1472 (34.1)	

All dimensions in mm. (Dimensions in brackets are in inches.)

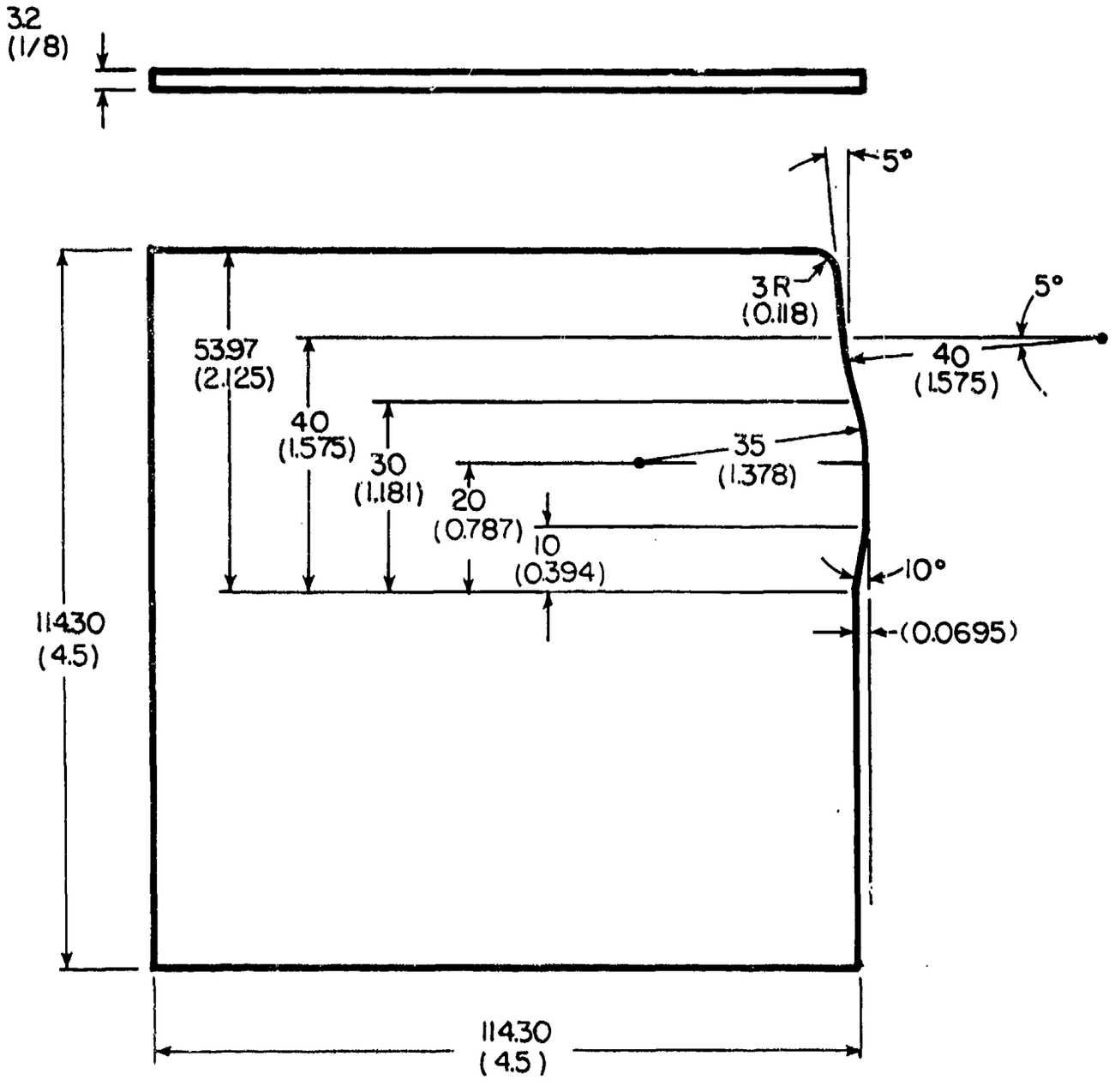

Figure C-9. Sketch of template for cold drawing with double curvature die (first stage, final double draw).

All dimensions are in mm. (Dimensions in brackets are in inches.)

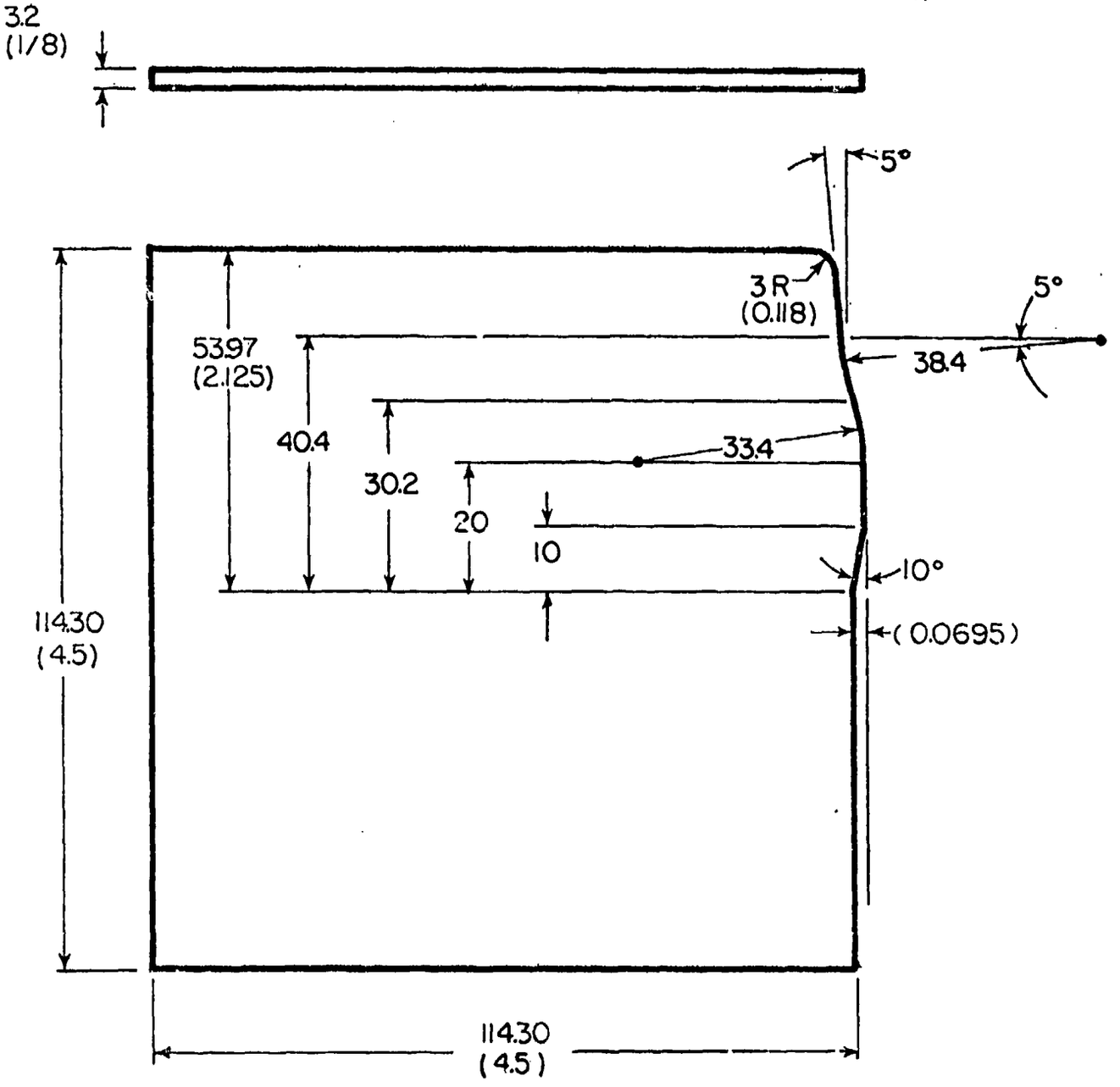

Figure C-10. Sketch of template for cold drawing with double curvature die (combined final double draw).

All dimensions are in mm. (Dimensions in brackets are in inches.)

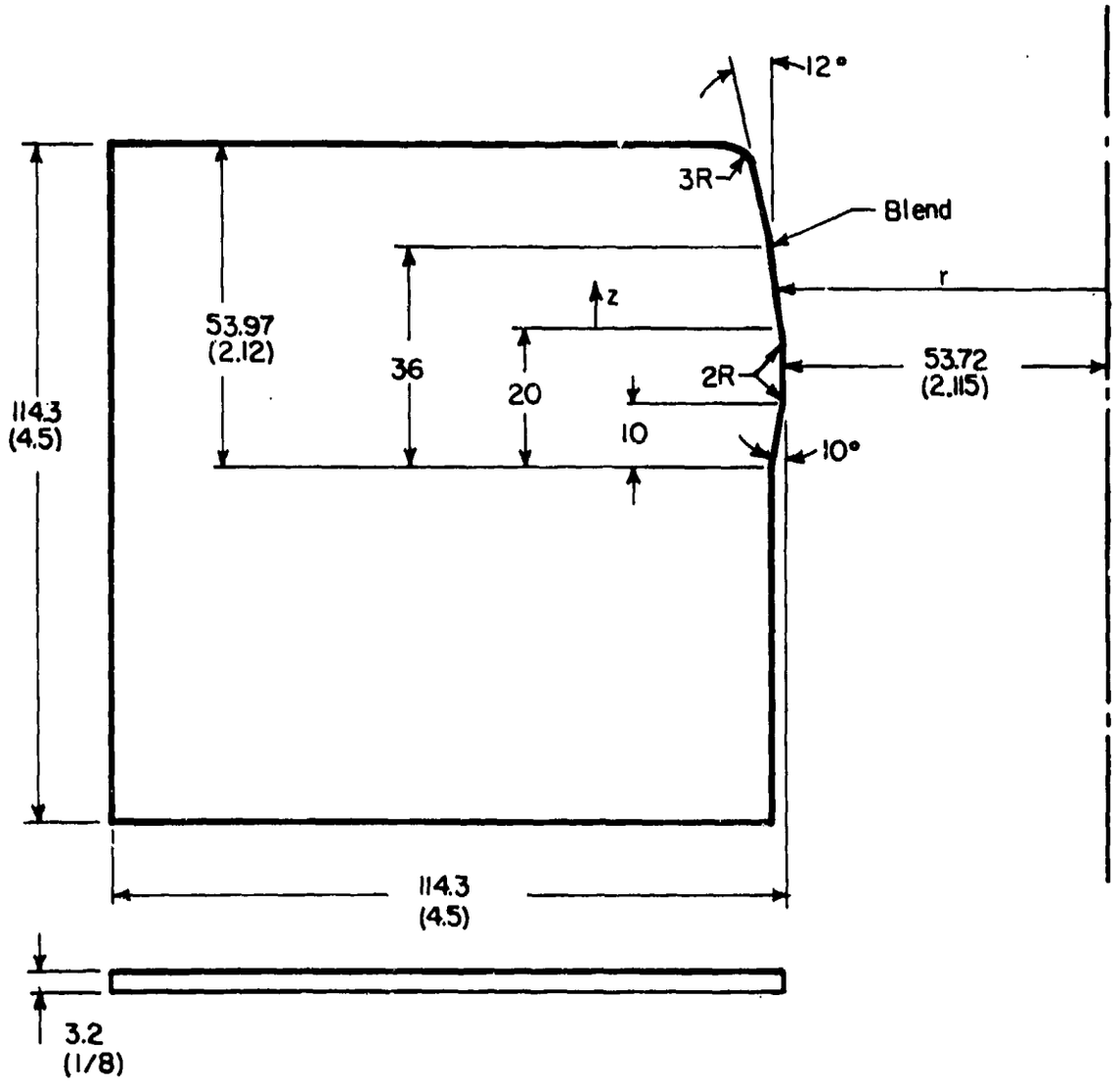

Figure C-11. Sketch of template for cold drawing with polynomial profile curve die (combined final draw) - r = f(Z) described in equation (1).

All dimensions are in mm. (Dimensions in brackets are in inches.)

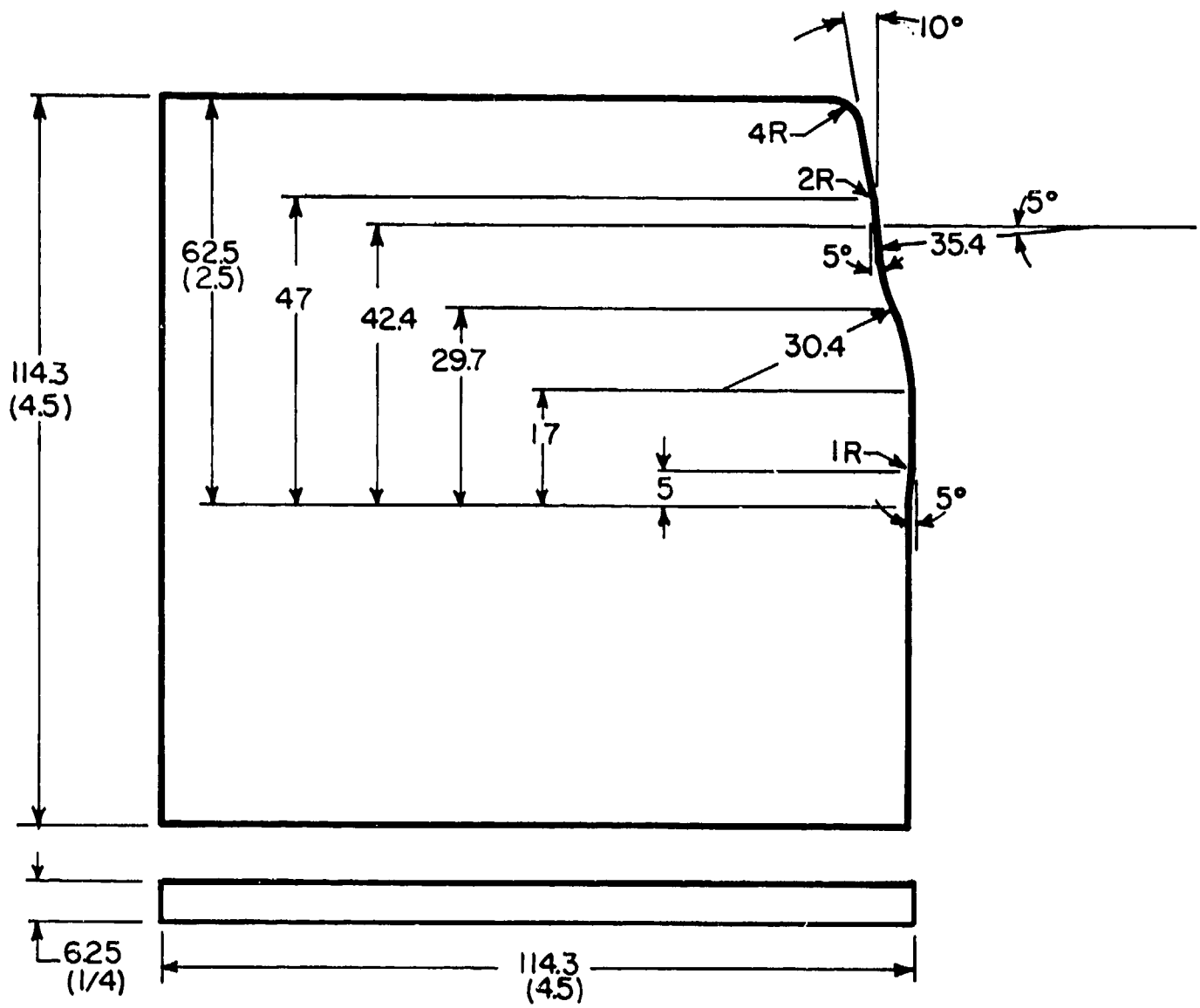

Figure C-12. Sketch of template for hot drawing with double curvature die (first stage).

All dimensions are in mm. (Dimensions in brackets are in inches.)

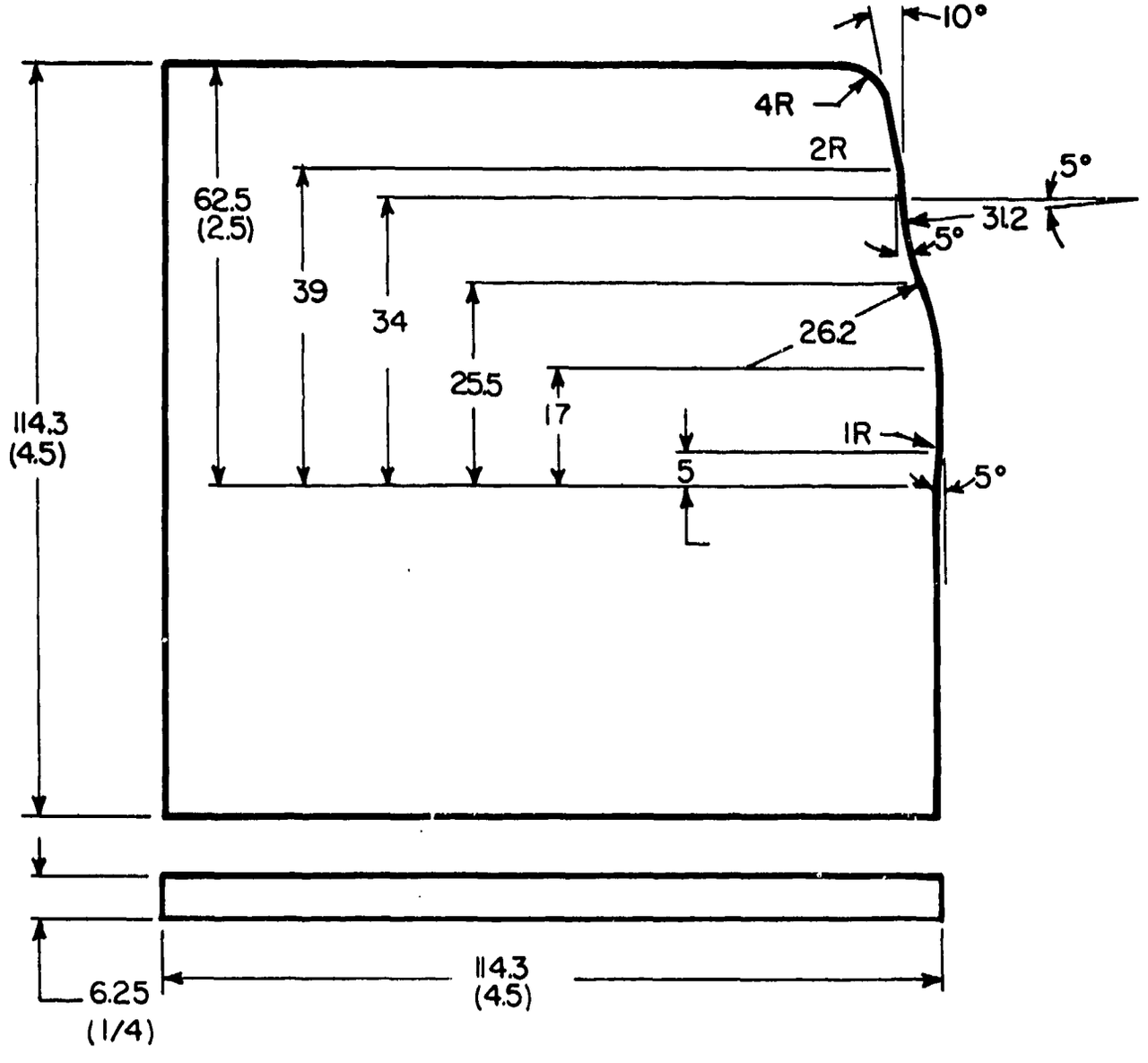

Figure C-13. Sketch of template for hot drawing with double curvature die (second stage).

All dimensions are in mm. (Dimensions in brackets are in inches.)

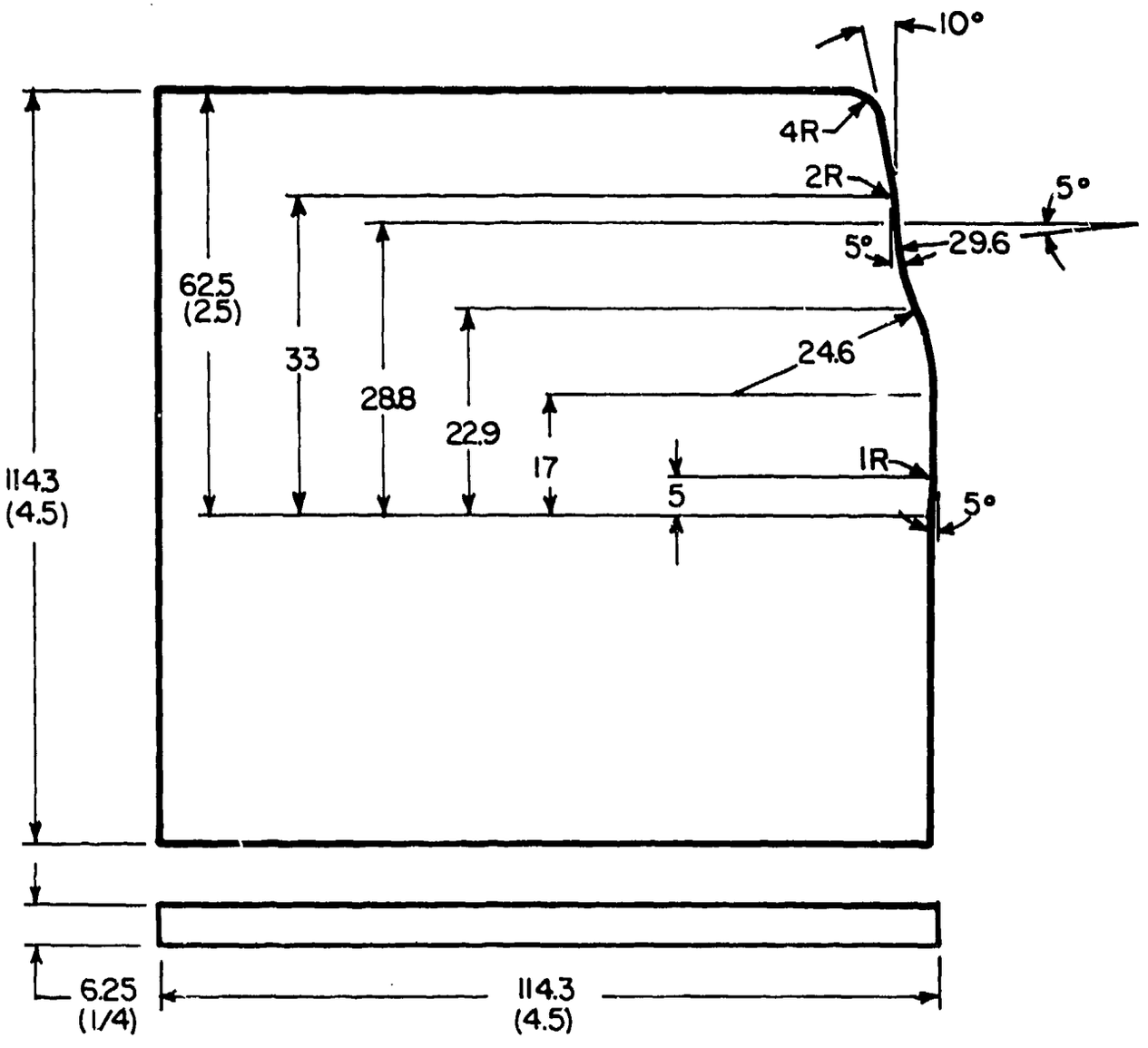

Figure C-14. Sketch of template for hot drawing with double curvature die (final draw).

All dimensions in mm. (Dimensions in brackets are in inches.)

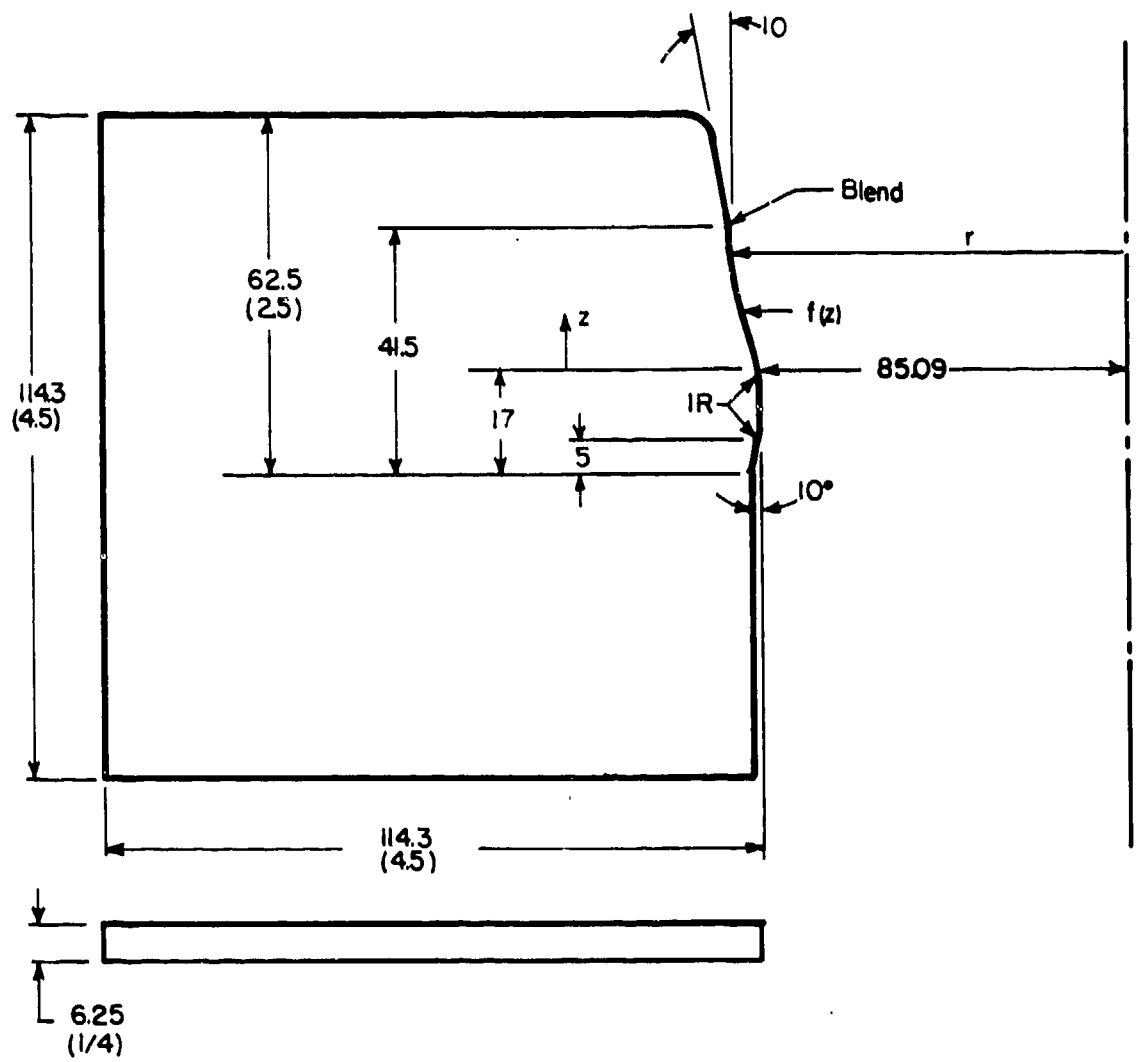

Figure C-15. Sketch of template for hot drawing with polynomial profile die (first stage) - r = f(Z) described in equation C-2.

All dimensions are in mm. (Dimensions in brackets are in inches.)

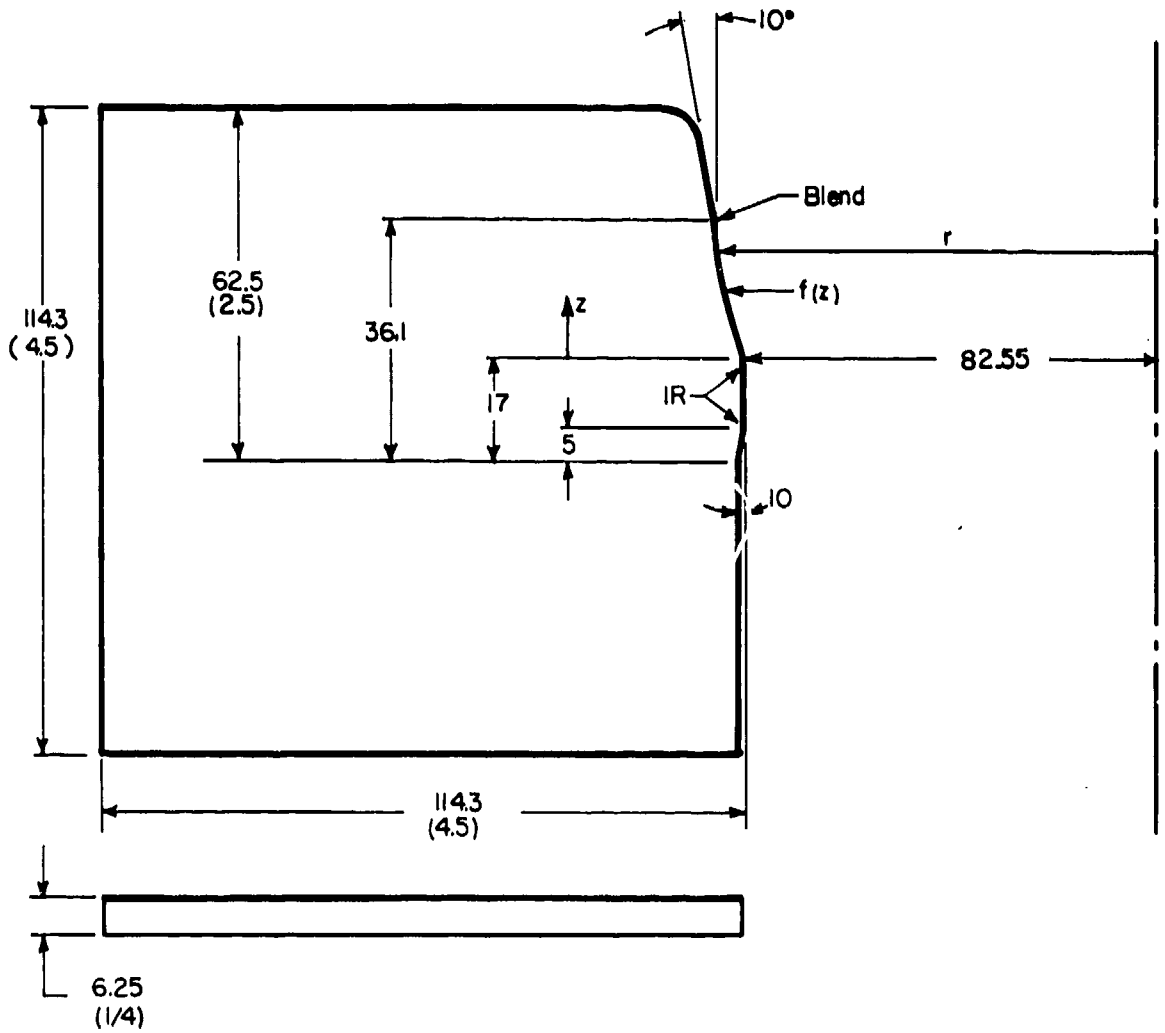

Figure C-16. Sketch of template for hot drawing with polynomial profile die (second stage) - r = f(Z) described in equation C-3.

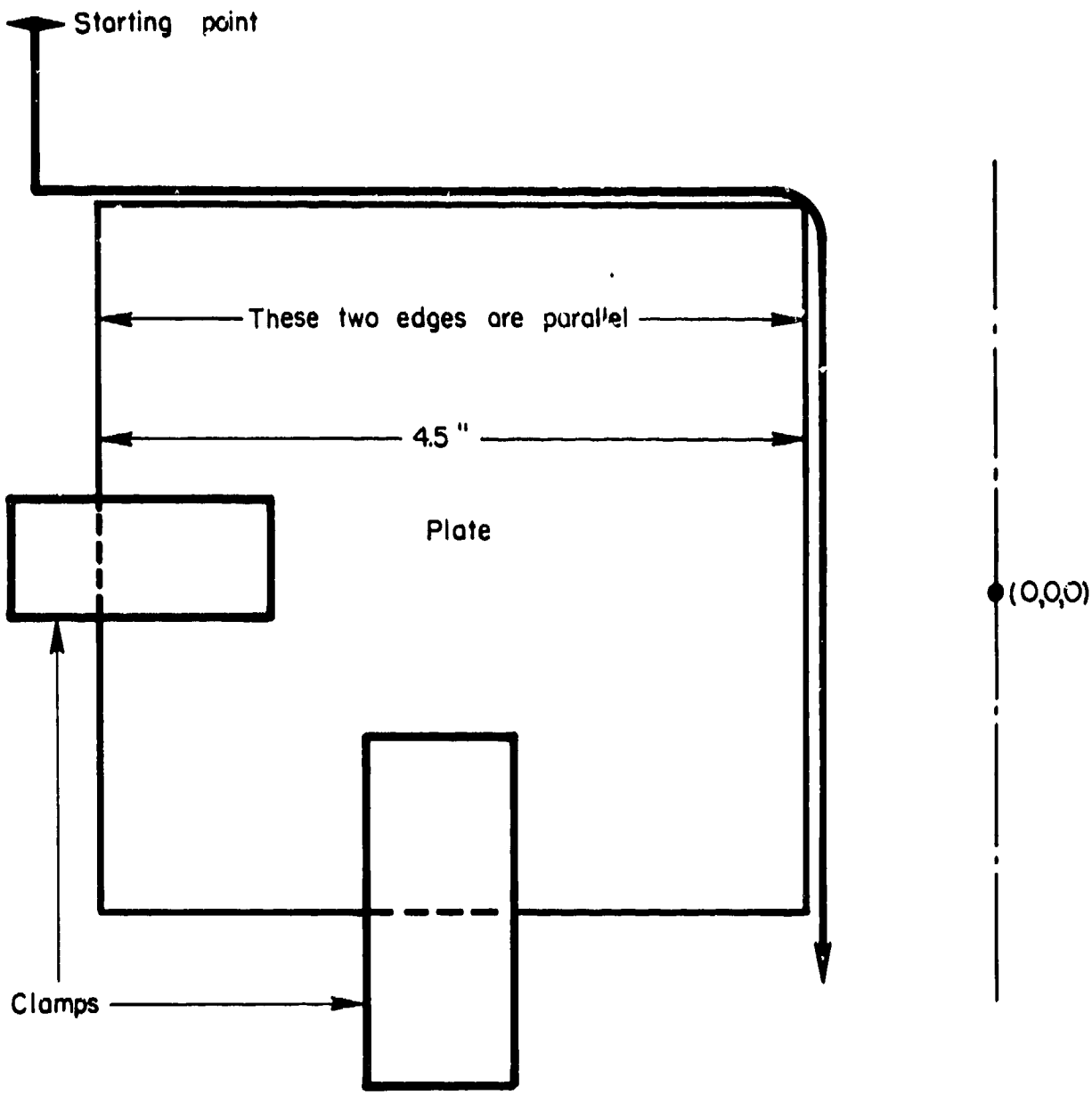

Figure C-17. Schematic sketch for computerized numerical control (CNC) machining of templates for cold and hot drawing operations.

```
C-12K BCLCNC '76

03.10 S NC=(TE-TB)*RC/RS
03.11 S NC=FABS(NC)
03.12 S NC=FITR(NC)+1
03.20 S TH=TB ; S DT=(TE-TB)/(NC-1)
03.30 FOR IC=1,NC ; DO 4
03.40 RETURN

04.10 S XX=XC+RC*FCOS(TH)
04.20 S YY=YC+RC*FSIN(TH)
04.30 P CUT(XX,YY,ZZ)
04.40 S TH=TH+DT
04.50 RETURN

05.01 CUT TEMPLATE FOR RAGHU
05.05 P IAS(0,0,0)
05.06 P SFR(30)
05.07 P PSW()
05.10 S X1=-7125 ; S Y1=2825 ; S CR=125
05.15 S Z1=700 ; S TF=3.14159/180
05.16 P CUT(0,0,Z1)
05.17 P CUT(X1,Y1,Z1)
05.18 P PSW(
05.20 P IRS(X1,Y1,Z1)
05.21 P SFR(5)
05.24 P CUT(-7125,2250,Z1)
05.25 P CUT(-7125,2250,0)
05.30 P CUT(-2386,2250,0)
05.35 S RC=118+CR ; S TB=90*TF ; S TE=5*TF
05.40 S RS=25 ; S XC=-2386 ; S YC=2007
05.45 D 3
05.50 P CUT(-2103,1450,0)
05.55 S RC=1575-CR ; S TB=185*TF ; S TE=194.49*TF
05.60 S RS=25 ; S XC=-658 ; S YC=1575
05.65 D 3
05.70 S RC=1378+CR ; S TB=16.61*TF ; S TE=0*TF
05.73 S RS=25 ; S XC=-3503 ; S YC=787
05.75 D 3
05.80 P CUT(-2001,394,0)
05.85 P CUT(-2070,0,0)
05.90 P CUT(-2070,-2375,0)
05.92 P CUT(-2070,-2375,Z1)
05.95 P SFR(30)
05.96 P CUT(X1,Y1,Z1)
05.99 Q
*>
```

Figure C-18. NC-Program for machining the template for cold drawing die with double curvature profile (first stage - final double draw).

```
C-12K BCLCNC '76

03.10 S NC=(TE-TB)*RC/RS
03.11 S NC=FABS(NC)
03.12 S NC=FITR(NC)+1
03.20 S TH=TB ; S DT=(TE-TB)/(NC-1)
03.30 FOR IC=1,NC ; DO 4
03.40 RETURN

04.10 S XX=XC+RC*FCOS(TH)
04.20 S YY=YC+RC*FSIN(TH)
04.30 P CUT(XX,YY,ZZ)
04.40 S TH=TH+DT
04.50 RETURN

05.01 CUT TEMPLATE FOR RAGHU
05.05 P IAS(0,0,0)
05.06 P SFR(30)
05.07 P PSW()
05.10 S X1=-7125 ; S Y1=2825 ; S CR=125
05.15 S Z1=700 ; S TF=3.14159/180
05.16 P CUT(0,0,Z1)
05.17 P CUT(X1,Y1,Z1)
05.18 P PSW()
05.20 P IRS(X1,Y1,Z1)
05.21 P SFR(5)
05.24 P CUT(-7125,2250,Z1)
05.25 P CUT(-7125,2250,0)
05.30 P CUT(-2391,2250,0)
05.35 S RC=118+CR ; S TB=90*TF ; S TE=5*TF
05.40 S RS=25 ; S XC=-2391 ; S YC=2007
05.45 D 3
05.50 P CUT(-2099,1470,0)
05.55 S RC=1512-CR ; S TB=185*TF ; S TE=195.42*TF
05.60 S RS=25 ; S XC=-717 ; S YC=1591
05.65 D 3
05.70 S RC=1315+CR ; S TB=17.3*TF ; S TE=0*TF
05.73 S RS=25 ; S XC=-3430 ; S YC=798
05.75 D 3
05.80 P CUT(-1990,394,0)
05.85 P CUT(-2060,0,0)
05.90 P CUT(-2060,-2375,0)
05.92 P CUT(-2060,-2375,Z1)
05.95 P SFR(30)
05.96 P CUT(X1,Y1,Z1)
05.99 Q
*>
```

Figure C-19. NC-Program for machining the template for cold drawing die with double curvature profile (combined first and second stages - final double draw).

```
C-12K BCLCNC '76

03.10 S NC=(TE-TB)*RC/RS
03.11 S NC=FABS(NC)
03.12 S NC=FITR(NC)+1
03.20 S TH=TB ; S DT=(TE-TB)/(NC-1)
03.30 FOR IC=1,NC ; DO 4
03.40 RETURN

04.10 S XX=XC+RC*FCOS(TH)
04.20 S YY=YC+RC*FSIN(TH)
04.30 P CUT(XX,YY,ZZ)
04.40 S TH=TH+DT
04.50 RETURN

05.01 CUT HOT IRONING TEMPLATE FOR RAGHU
05.02 P IAS(0,0,0)
05.03 P SFR(30)
05.04 P PSW()
05.05 S X1=-8350 ; S Y1=3200 ; S CR=125
05.06 S Z1=700 ; S TF=3.14159/180
05.08 P CUT(0,0,Z1)
05.10 P CUT(X1,Y1,Z1)
05.12 P PSW()
05.14 P IRS(X1,Y1,Z1)
05.16 P CUT(X1,2625,Z1)
05.18 P SFR(5)
05.20 P CUT(X1,2625,0)
05.22 P CUT(-3822,2625,0)
05.24 S RC=158+CR ; S TB=90*TF ; S TE=10*TF
05.26 S RS=25 ; S XC=-3822 ; S YC=2342
05.28 D 3
05.30 P CUT(-3451,1872,0)
05.32 S RC=0+CR ; S TB=10*TF ; S TE=5*TF
05.34 S RS=5 ; S XC=-3574 ; S YC=1850
05.36 D 3
05.38 P CUT(-3422,1558,0)
05.40 S RC=1394-CR ; S TB=185*TF ; S TE=201.02*TF
05.42 S RS=25 ; S XC=-2158 ; S YC=1669
05.44 D 3
05.46 S RC=1197+CR ; S TB=24.69*TF ; S TE=0*TF
05.48 S RS=25 ; S XC=-4547 ; S YC=669
05.50 D 3
05.52 P CUT(-3225,134,0)
05.54 P CUT(-3249,0,0)
05.56 P CUT(-3249,-2050,0)
05.58 P CUT(-3249,-2050,Z1)
05.60 P SFR(30)
05.62 P CUT(X1,Y1,Z1)
05.64 Q
*>
```

Figure C-20. NC-Program for machining the template for hot drawing die with double curvature profile (first stage).

```
C-12K BCLCNC '76

03.10 S NC=(TE-TB)*RC/RS
03.11 S NC=FABS(NC)
03.12 S NC=FITR(NC)+1
03.20 S TH=TB ; S DT=(TE-TB)/(NC-1)
03.30 FOR IC=1,NC ; DO 4
03.40 RETURN

04.10 S XX=XC+RC*FCOS(TH)
04.20 S YY=YC+RC*FSIN(TH)
04.30 P CUT(XX,YY,ZZ)
04.40 S TH=TH+DT
04.50 RETURN

05.01 CUT HOT IRONING TEMPLATE FOR RAGHU
05.02 P IAS(0,0,0)
05.03 P SFR(30)
05.04 P PSW()
05.05 S X1=-8250 ; S Y1=3200 ; S CR=125
05.06 S Z1=700 ; S TF=3.14159/180
05.08 P CUT(0,0,Z1)
05.10 P CUT(X1,Y1,Z1)
05.12 P PSW()
05.14 P IRS(X1,Y1,Z1)
05.16 P CUT(X1,2625,Z1)
05.18 P SFR(5)
05.20 P CUT(X1,2625,0)
05.22 P CUT(-3678,2625,0)
05.24 S RC=158+CR ; S TB=90*TF ; S TE=10*TF
05.26 S RS=25 ; S XC=-3678 ; S YC=2342
05.28 D 3
05.30 P CUT(-3252,1557,0)
05.32 S RC=0+CR ; S TB=10*TF ; S TE=5*TF
05.34 S RS=5 ; S XC=-3375 ; S YC=1535
05.36 D 3
05.38 P CUT(-3223,1243,0)
05.40 S RC=1228-CR ; S TB=185*TF ; S TE=195.83*TF
05.42 S RS=25 ; S XC=-2125 ; S YC=1339
05.44 D 3
05.46 S RC=1032+CR ; S TB=18.94*TF ; S TE=0*TF
05.48 S RS=25 ; S XC=-4282 ; S YC=669
05.50 D 3
05.52 P CUT(-3125,197,0)
05.54 P CUT(-3160,0,0)
05.56 P CUT(-3160,-2050,0)
05.58 P CUT(-3160,-2050,Z1)
05.60 P SFR(30)
05.62 P CUT(X1,Y1,Z1)
05.64 Q
*<^
```

Figure C-21. NC-Program for machining the template for hot drawing die with double curvature profile (second stage).

```
C-12K BCLCNC '76

03.10 S NC=(TE-TB)*RC/RS
03.11 S NC=FABS(NC)
03.12 S NC=FITR(NC)+1
03.20 S TH=TB ; S DT=(TE-TB)/(NC-1)
03.30 FOR IC=1,NC ; DO 4
03.40 RETURN

04.10 S XX=XC+RC*FCOS(TH)
04.20 S YY=YC+RC*FSIN(TH)
04.30 P CUT(XX,YY,ZZ)
04.40 S TH=TH+DT
04.50 RETURN

05.01 CUT HOT IRONING TEMPLATE FOR RAGHU
05.02 P IAS(0,0,0)
05.03 P SFR(30)
05.04 P PSW()
05.05 S X1=-8200 ; S Y1=3200 ; S CR=125
05.06 S Z1=700 ; S TF=3.14159/180
05.08 P CUT(0,0,Z1)
05.10 P CUT(X1,Y1,Z1)
05.12PP PSW()
05.14 P IRS(X1,Y1,Z1)
05.16 P CUT(X1,2625,Z1)
05.18 P SFR(5)
05.20 P CUT(X1,2625,0)
05.22 P CUT(-3615,2625,0)
05.24 S RC=158+CR ; S TB=90*TF ; S TE=10*TF
05.26 S RS=25 ; S XC=-3615 ; S YC=2342
05.28 D 3
05.30 P CUT(-3147,1321,0)
05.32 S RC=0+CR ; S TB=10*TF ; S TE=5*TF
05.34 S RS=5 ; S XC=-3270 ; S YC=1299
05.36 D 3
05.38 P CUT(-3122,1043,0)
05.40 S RC=1165-CR ; S TB=185*TF ; S TE=191.49*TF
05.42 S RS=25 ; S XC=-2086 ; S YC=1134
05.44 D 3
05.46 S RC=969+CR ; S TB=13.91*TF ; S TE=0*TF
05.48 S RS=25 ; S XC=-4167 ; S YC=669
05.50 D 3
05.52 P CUT(-3075,197,0)
05.54 P CUT(-3110,0,0)
05.56 P CUT(-3110,-2050,0)
05.58 P CUT(-3110,-2050,Z1)
05.60 P SFR(30)
05.62 P CUT(X1,Y1,Z1)
05.64 Q
*_
```

Figure C-22. NC Program for machining the template for hot drawing die with double curvature profile (final stage).

APPENDIX D.

CHAMBERLAIN'S CONCLUSIONS AND RECOMMENDATIONS

4.2-Inch M335 Shell

Summary of Trials

Press data recorded for production and experimental dies are tabulated in Table D-1. Note that production operation was monitored for 6 hours. Twenty-five projectile bodies were chosen at random and were serialized for physical and mechanical properties data recording. On the R&D press with the streamlined dies, 60 projectiles were drawn, 20 through the top die only, and 40 through both dies. Note that the same production lubricant coating was used for draws with conical dies and the R&D press was used for draws with streamlined dies.

Table D-1. Press data for 4.2-inch M335 shell.

PRESS	Press Speed, mm/s (in./min.)	Press Stroke, m(in.)	Draw Length, m(in.)	Ram	
				MPa (psi)	MN (peak tons)
Production Bliss 200T	67.7 (160)	1.067 (42)	0.432 (17)	6.48 (940)	0.729 (82)
R&D Version 600T	88.9 (210)	1.016 (40)	0.432 (17)	2.07 (300)	0.584 (65.7) (Single Die)
				2.34 (340)	0.665 (74.7) (Both Dies)

Die wear normally is insignificant on cold drawing operations, and this proved to be the case in both runs conducted above. There was no measurable die wear. Chart records from the Brush recorder were given to Battelle representatives who witnessed operations. Chamberlain personnel were not involved with calculations associated with these charts.

Temperature Measurements

Temperature recordings on parts exiting from the dies showed a measurable difference. At the start of the run through the streamlined dies part temperature was 57° C (135° F) coming out of the single die, rising to 82° C (180° F) by the 20th body. After 40 bodies had been drawn through the experimental double draw setup, temperature had stabilized between 91° C (195° F) and 93° C (200° F). By comparison, after a similar number of bodies

were processed through production dies the part temperature stabilized at 104.4° C (200° F). This, together with tonnages recorded above, indicates the metal is flowing easier with streamlined dies.

Residual Stresses/Elastic Recovery

An interesting phenomenon occurred while bodies were being sectioned for hardness samples. These longitudinal sections were taken from the midpoint of each can. Since none of the bodies had undergone the production stress relief after the final draw, some stress bowing was expected when the drawn cans were parted. However, we did not expect the variation in the amount of bowing which actually occurred. The section from the Chamberlain production dies bowed almost twice as much as did the section from the Battelle streamlined dies. This, together with temperature and other data discussed previously is a definite indicator that the Battelle die configuration imparts less energy to the shell for a given reduction of area. Residual stress from the Battelle dies obviously is less, but this would not eliminate the requirement for stress relief following the double draw operation, since there is no subsequent heat treatment before finish machining. In the case of parts requiring intermediate machining operations between drawing and heat treat, the decreased wall stresses would be of great help in controlling the tolerancing of these machining operations.

Streamlined Versus Conical Dies

Chamberlain's own general observations of the comparison between the production conical dies and the Battelle streamlined dies favor the latter. There is one variable not assessed--the use of a 1.78 MN (200-ton) production press with the taper entry dies and a 5.34 MN (600-ton) press with the experimental configuration dies. To be absolutely certain that the Battelle configuration can process parts at less tonnage, the 1.78 MN (200-ton) press should be set up with experimental dies.

However, there are sufficient indicators available to make the assumption that the streamlined dies will allow parts to be generated with less tonnage. If this holds true, munitions manufacturers have several attractive options available such as: (1) accomplishing more severe reductions with existing equipment, possibly reducing the number of cold draws to make a part, (2) taking on bigger cold drawing jobs not handled before because of marginal

press tonnage, and (3) putting existing jobs into lighter presses which may be available but were never used on the basis of tonnage available.

105 mm M107 Shell

Summary of Trials

The draw press was monitored for 4 hours while the production dies were being used and another 4 hours while the streamlined dies were being tested. New production dies were inserted at the beginning of the test to allow direct comparison with new contoured dies. Drawn shell bodies were chosen at random to have measurements taken and recorded. No process changes were made other than to change dies.

Table D-2. Press data for 105 mm M107 shell.

Press	Pressing Speed	Draw Stroke
Bliss 400 T Hydraulic	0.406 m/s (960 in./min)	2.438 m (96 inch)
Dies	**Ram Pressure, MPa (psi)**	**Draw Force, MN (tons)**
Conical Draw	5.65-5.93 (820-860)	1.17-1.22 (131-137)
Contoured	5.69-5.93 (825-860)	1.17-1.22 (131-137)

At the end of the 4-hour test period, no die wear was evident in the streamlined dies. It was decided to let the dies remain in the press until they were worn to the point that they no longer produced acceptable parts. There was no discernible temperature difference in shells drawn through the different types of dies.

Comparison of Computer-Predicted and Measured Loads

As was the case with the cold draw experiments, the computer model predicted higher draw forces than were observed during actual draw tests. These differences were attributed to slight differences in the shape and fit

of tooling and forging. First runs of the model for cold draw did not accurately represent punch-part interfacing. In the case of the hot draw computer run, a difference in the mandrel (punch) shape showed as extra draw force. A rerun of the computer program using corrected values for punch and preform dimensions showed much better agreement not only in the magnitude of the punch force, but in the shape of the load-stroke curve. Chamberlain believes the computer model to be extremely accurate based on this. If the predicted force is so dependent on the part-tooling geometry and responds to corrections and changes as readily as has been shown, it will be of great value in the design of dies and punches. This would be a real start toward the development of computer-aided design of projectile tooling.

The difference in the measured press load was not as great for the hot draw as in the production and experimental dies in the cold draw experiments. This is due to the fact that the normal production dies used in hot drawing are very similar to streamlined dies. Cold work dies are a more simple conical shape while the hot work dies are a double conical shape, more nearly like the streamlined dies and, in fact, are a very efficient design. This too, was shown by the computer model in the ram force values for the production dies and streamlined dies. Predicted ram forces for productions dies and streamlined dies were very nearly equal.

Die Wear

Computer-developed dies produced acceptable parts during the monitoring period. It was agreed to draw parts through the dies until they failed and no longer produced acceptable parts. A total of 15,836 shells were drawn before removal of the dies. Engineers at Scranton state that the number is half the normal production run on a set of dies. Dies were removed because excessively deep draw marks appeared on the outside of the shell. This is the normal criterion for die removal. Short die life may not be directly attributable to the streamlined design. While short life is not common, it also is not unheard of. Scranton engineers pointed out the single run on the dies should not be basis for branding the dies as a failure. Hot drawing variables such as excessive heat, low heat, or excessive heavy scaling of parts drawn beyond the direct monitoring period can be contributing factors in the early failure. Another reason for not labeling the dies a total failure is

that they did wear out in a normal manner. Deep draw marks caused by washing of the die surfaces was the reason for removal, as stated above. Again, this is normally the reason for removal. Also, the first and third rings were most severely worn, also a normal occurrence.

A phenomenon termed "die slap", a readily detectable noise during drawing of shells was an item of note during the monitoring period. The noise is heard as shells exit a die and then enter the succeeding die. "Slap" was distinctive during the monitored period using standard dies, but was curiously absent during monitoring of the streamlined dies. The sound is commonplace in normal production runs and can be either aggravated or lessened by the die spacing as determined by shell length. If shells are longer, slap is reduced; shorter shells make a more noticeable sound. Scranton personnel believe the sound is a combination of forward extrusion off the punch and over running of the press as drawing force is immediately decreased as the shell exits the die. There was no decided effort to continue observation of the dies beyond the monitoring period, so it is not known if the streamlined dies remained "quiet". An increase in shell length may well have caused the lack of noise at the beginning of the run.

Conclusions

Scranton engineers agree generally with the assessment that the computer model does, indeed, represent the drawing process. The dramatic differences in cold draw work were as predicted. The less dramatic differences in hot draw experiments were also as predicted, however. As with other computer programs, the drawing model appears to be sensitive to the validity of input information. Perhaps this sensitivity would work to the advantage of model users in optimizing drawing processes. Die/mandrel combinations could be compared to give the lowest energy draw conditions.

Greatest advantage would be gained by those who use the cold draw process. There are fewer variables to contend with:

- Tool wear is not significant so predictions will remain valid throughout the process.
- Lubricant is uniformly applied and because tool wear is minimal, friction will not change the process.

- Heat differentials are not present since working starts at room temperature.
- Parts are cleaner--no scale is present on the parts.

For these reasons the model will yield consistently more reliable draw predictions.

DISTRIBUTION

	Copies
A. Department of Defense	
Director of Defense Research and Engineering Office Attn: Mr. S. Persh Washington, DC 20301	1
Director Defense Advanced Research Projects Agency Attn: Dr. E. C. Van Reuth	1
Dr. C. Lehner	1
Dr. E. Blase 1400 Wilson Boulevard Arlington, VA 22209	1
Defense Documentation Center Attn: TIPDR Cameron Station Alexandria, VA 22314	12
B. Department of the Army	
Assistant Secretary of the Army (R&D) Attn: Deputy for Science and Technology Washington, DC 20310	1
Deputy Chief of Staff for Research Development and Acquisition Department of the Army Attn: DAMA-ARZ-D Washington, DC 20310	1
Commander US Army Material Development Readiness Command Attn: DRCDM-D	1
DRCDM-R	1
DRCDMD-T	1
DRCD-L, Foreign Science & Tech Div	1
DRCDE-E, Edson Gardner	1
DRCDE-I	1
DRCDE-W	1
DRCMT, L. Croan	1
DRCMT, Col N. Vinson	1
DRCDE-DE, E. Lippi 5001 Eisenhower Avenue Alexandria, VA 22333	1

	Copies
Commander Aberdeen Proving Ground Attn: STEAP-TL, Technical Library DRXSY DRXSY-GA Aberdeen Proving Ground, MD 21010	 1 1 1
Director Ballistic Research Laboratory Attn: DRDAR-BLT Aberdeen Proving Ground, MD 21010	 1
Weapons System Concept Team/CSL Attn: DRDAR-ACW Aberdeen Proving Ground, MD 21010	 1
Technical Library Attn: DRDAR-CLJ-L Aberdeen Proving Ground, MD 21010	 1
Technical Library Attn: DRDAR-TSB-S Aberdeen Proving Ground, MD 21005	 1
US Army Materiel Systems Analysis Activity Attn: DRXSY-MP Aberdeen Proving Ground, MD 21005	 1
Commander US Army Electronics Research and Development Command Attn: DRSEL (Tech Lib) Fort Monmouth, NJ 07703	 1
Director US Army Air Mobility Research & Development Lab Ames Research Center Attn: Mr. Paul Yaggy Moffet Field, CA 94035	 1
Commander US Army Air Mobility R&D Labs Attn: SAVDL-ST Fort Eurstis, VA 23604	 1
Commander US Army Material Development & Readiness Command Scientific and Technical Infor Team-Europe Attn: DRXST-STL APO, New York 09710	 1

	Copies
Commander US Army Research and Standardization Group (Europe) Attn: DRXSN-E-RM P.O. Box 65 FPO, New York 04510	1
Commander Rock Island Arsenal Attn: DRXIB-MT Technical Information Div SARRI-ER	1 1 1
Commander US Army Harry Diamond Labs Attn: DRXDO-TIA 2800 Powder Mill Road Adelphi, MD 20783	1
Commander US Army Materials & Mechanics Research Center Attn: DRXMR-X, Dr. E. Wright DRXMR-PT Technical Information Div Watertown, MA 02172	1 1 1
Director US Army Maintenance Management Center Attn: DRXMD-A Lexington, KY 40507	1
Commander US Army Research Office P.O. Box 1221 Attn: Dr. George Mayer, Director Dr. E. Saibel Research Triangle Park, NC 27709	1 1
Commander US Army Natick Research & Development Command Attn: DRXRE, Dr. E. Sieling Technical Information Div Kansas Street Natick, MA 07160	1 1

	Copies
Commander US Army Foreign Science & Tech Center Attn: W. Marley J. Bollendorf 220 7th Street, NE Charlottesville, VA 22901	 1 1
Commander US Army Mobility Equipment Research & Development Command Attn: STSFB-MMM, Mr. W. Baer DRSME-RZT DRDME-MMM Ft. Belvoir, VA 22060	 1 1 1
Commander Ballistic Missile Defense Systems Attn: BNDSC-TS DRDMI-R DRCPM-LCE, B. Crosswhite Technical Library P.O. Box 1500 Huntsville, AL 35809	 1 1 1 1
Commander Rocky Mountain Arsenal Attn: Technical Information Div Denver, CO 80240	 1
Director US Army Industrial Base Engineering Activity Attn: DRXIB-MT Rock Island, IL 61201	 2
Commander U.S. Army Armament Materiel Readiness Command Attn: DRSAR-LEP-L Rock Island, IL 61299	 1
Director US Army Advanced Materials Concept Agency Attn: Technical Information Div 2461 Eisenhower Avenue Alexandria, VA 22314	 1
Commander US Army Tank-Automotive R&D Command Attn: DRDTA-RKA, V. Pagano DRDTA-KP DRDTA-RE, C. Bradley DRDTA-Z, J. Panks DRSTA-E Warren, MI 48090	 1 1 1 1 1

	Copies
Commander US Army Tank-Automotive Materiel Readiness Command Attn: DRSTA-E Warren, MI 48090	1
Commander US Army Aviation Research and Development Command Attn: DRDAV-EXT (Tech Lib) P.O. Box 209 St. Louis, MO 63166	1
Commander US Army Troop Support and Aviation Material Readiness Command Attn: DRSTS 4300 Goodfellow Blvd. St. Louis, MO 63120	1
Director USDARCOM Intern Training Center Attn: DRXMC-ITC-PPE Red River Army Depot Texarkana, TX 75501	1
Commander US Army Armament R&D Command	
Attn: DRDAR-CG, MG B. Lewis	1
DRDAR-TD, Dr. R. Weigle	1
DRDAR-TDR, E. Eichelberger	1
DRDAR-SC, Dr. D. Gyorog	1
DRDAR-LC, Dr. J. Frasier	1
DRDAR-SCM, J. D. Corrie	3
Dr. E. Bloore	1
DRDAR-SCM-P, Mr. I. Betz	1
DRDAR-SCM-P, Mr. F. Lee	10
DRDAR-SCP	1
DRDAR-LCU-M	1
DRDAR-LCU, Mr. Bushey	1
DRDAR-LC	1
DRDAR-PMM	1
DRDAR-PBM-GA, G. O'Brien	1
DRDAR-SCM-M	1
DRDAR-TSS	5
DRDAR-QA	1
DRCPM-CAWS	1
DRCPM-SA	1
DRCPM-ADG	1
DRCPM-NUC	1
DRCPM-AAH 30mm	1
DRCPM-TMA Dover, NJ, 07801	1
U.S. Army Armament R&D Command Attn: DRDAR-LCB-TL Watervliet, NY 12189	1

	Copies
Commander Rep, Alabama Army Ammunition Plant Childersburg, AL 35044	1
Commander Rep, Badger Army Ammunition Plant Baraboo, WI 53919	1
Commander Rep, Burlington Army Ammunition Plant Burlington, NJ 08016	1
Commander Rep, Cornhusker Army Ammunition Plant Grand Island, NB 68801	1
Commander Rep, Gateway Army Ammunition Plant St. Louis, MO 63143	1
Commander Rep, Hays Army Ammunition Plant Pittsburgh, PA 15207	1
Commander Holston Army Ammunition Plant Kingsport, TN 37662	1
Commander Indiana Army Ammunition Plant Charlestown, IN 47111	1
Commander Iowa Army Ammunition Plant Burlington, IA 52600	1
Commander Rep, Joliet Army Ammunition Plant Joliet, IL 60436	1
Commander Kansas Army Ammunition Plant Parsons, KS 67357	1
Commander Lake City Army Ammunition Plant Independence, MO 64050	1
Commander Lone Star Army Ammunition Plant Texarkana, TX 75501	1

	Copies
Commander Longhorn Army Ammunition Plant Marshall, TX 75671	1
Commander Louisiana Army Ammunition Plant Shreveport, LA 71102	1
Commander Milan Army Ammunition Plant Milan, TN 38358	1
Commander Newport Army Ammunition Plant Newport, IN 47966	1
Commander Radford Army Ammunition Plant Radford, VA 24141	1
Commander Rep, Ravenna Army Ammunition Plant Ravenna, OH 42266	1
Commander Riverbank Army Ammunition Plant Riverbank, CA 95367	1
Commander Scranton Army Ammunition Plant Scranton, PA 18501	1
Commander Rep, St Louis Army Ammunition Plant St. Louis, MO 63160	1
Commander Rep, Sunflower Army Ammunition Plant Lawrence, KS 66044	1
Commander Twin Cities Army Ammunition Plant New Brighton, MN 55112	1
Commander Volunteer Army Ammunition Plant Attn: SARVO-T Chattanooga, TN 37401	1
Commander Anniston Army Depot Attn: DRXAN-DM Anniston, AL 36201	1

	Copies
Commander Corpus Christi Army Depot Attn: DRXAD-EFT Corpus Christi, TX 78419	1
Commander Fort Wingate Depot Activity Attn: DRXFW-M Gallup, NM 87301	1
Commander Tobyhanna Army Depot Attn: DRXTO-ME-B Tobyhanna, PA 18466	1
Commander Tooele Army Depot Attn: DRXTE-SEN DRXTE-EMD Tooele, UT 84074	1 1
Commander Letterkenny Army Depot Attn: DRXLE-M DRXLE-MM Chambersburg, PA 17201	1 1
Commander Lexington-Blue Grass Army Depot Attn: DRXLX-SE-1 Lexington, KY 40507	1
Commander New Cumberland Army Depot Attn: DRXNC-SM New Cumberland, PA 17070	1
Commander Pueblo Army Depot Attn: DRXPU-ME DRXPU-SE Pueblo, CO 81001	1 1
Commander Red River Army Depot Attn: DRXRR-MM Texarkana, TX 75501	
Commander Sacramento Army Depot Attn: DRXSA-MME-LB Sacramento, CA 95813	1

	Copies
Commander Seneca Army Depot Attn: DRXSE-SE Romulus, NY 14541	1
Commander Sharpe Army Depot Attn: DRXSH-SO DRXSH-M Lathrop, CA 95330	1 1
Commander Sierra Army Depot Attn: DRXSI-DQ Herlong, CA 96113	1

C. Department of the Navy

Chief Bureau of Ships Department of the Navy Attn: Code 343 Washington, DC	1
Chief Bureau of Aeronautics Department of the Navy Attn: Technical Information Div Washington, DC	1
Chief Bureau of Weapons Department of the Navy Attn: Technical Information Div Washington, DC 20025	1
Commander Naval Air Development Center Johnsville, Aero Materials Dept Attn: Mr. Forrest Williams Warminister, PA 18974	1
Commander Naval Air Systems Command Department of the Navy Attn: AIR 5203, Mr. R. Schmidt AIR 604 Washington, DC 20360	1

	Copies
Officer in Charge US Navy Material Industrial Research Office Attn: Code 227 Philadelphia, PA 19112	1
Commander Naval Ships Systems Command Department of the Navy Attn: Code 03423 Washington, DC 20023	1
Commander US Naval Weapons Laboratory Attn: Technical Information Div Dahlgren, VA 22448	1
Commander US Naval Engineering Experimental Station Attn: WCTRL-2, Materials Lab Annapolis, MD 21402	1
Commander US Naval Ordnance Laboratory Attn: Code WM Silver Spring, MD 20910	1
D. Department of the Air Force	
Director Air Force Materials Laboratory Attn: AFML, Technical Library LTE LTM LTN Wright-Patterson AFB Dayton, OH 45433	1 1 1 1
Director US Naval Research Laboratory Attn: Mr. W. S. Pellini, Code 6300, Metallurgy Div Mr. W. J. Ferguson Mr. J. Baker Dr. H. C. Posey Dr. F. Rosenthall Mr. C. Sanday Washington, DC 20375	1 1 1 1 1 1

	Copies
Director Naval Ships Research & Development Center Attn: Mr. Abner R. Willmer, Chief of Metals Research	1
D. W. Taylor	1
Code 042, Tech Lib	1
Bethesda, MD 20084	
Director Air Force Armament Laboratory Attn: AFATL/DLOSL	1
ADTC/DLJW	1
Eglin AFB, FL 32542	
Director Air Force Weapons Laboratory Attn: Technical Information Div	1
Kirtland AFB, NM 87118	
Director Air Force Materials Laboratory Wright-Patterson AFB Attn: AFML/LLD, Dr. T. M. F. Ronald	1
AFML, Tech Library	1
Dayton, OH 45433	
Commander Aeronautical System Div Wright-Patterson Air Force Base Attn: Technical Information Div	1
Dayton, OH 45433	
Commander Air Research & Development Command Andrews Air Force Base Attn: RDRAA	1
Washington, DC 20025	

E. Other Federal Agencies

Director National Academy of Science Attn: Materials Advisory Board	1
2101 Constitution Avenue, N.W. Washington, DC 20418	
Director National Aeronautics & Space Administration Attn: Code RPM	1
Federal Building #10 Washington, DC 20546	

	Copies
Director National Aeronautics & Space Administration Attn: Code RPM Federal Building #10 Washington, DC 20546	1

F. Private Organizations

Battelle Memorial Institute Attn: Metals & Ceramic Information Center Dr. T. Leontis 505 King Avenue Columbus, OH 43201	1 1
Materials Research Laboratory, Inc. Attn: Dr. E. J. Ripling 1 Science Road Glenwood, IL 60425	1